Effect on Pavement Wear of Increased Mass Limits for Heavy Vehicles – Stage 3

G. Arnold, B. Steven, D. Alabaster & A. Fussell

An important note for the reader

This report is the final stage of a project commissioned by Transfund New Zealand before 2004, and is published by Land Transport New Zealand.

Land Transport New Zealand is a Crown entity established under the Land Transport New Zealand Amendment Act 2004. The objective of Land Transport New Zealand is to allocate resources in a way that contributes to an integrated, safe, responsive and sustainable land transport system. Each year, Land Transport New Zealand invests a portion of its funds on research that contributes to this objective.

While this report is believed to be correct at the time of its preparation, Land Transport New Zealand, and its employees and agents involved in its preparation and publication, cannot accept any liability for its contents or for any consequences arising from its use. People using the contents of the document, whether directly or indirectly, should apply and rely on their own skill and judgement. They should not rely on its contents in isolation from other sources of advice and information. If necessary, they should seek appropriate legal or other expert advice in relation to their own circumstances, and to the use of this report.

The material contained in this report is the output of research and should not be construed in any way as policy adopted by Land Transport New Zealand but may be used in the formulation of future policy.

Contents

List of Figures

List of Tables

Executive summary

Introduction

The road transport industries in New Zealand and Australia have been lobbying for increases in the allowable mass limits for heavy vehicles on the basis of increased efficiency and benefits to the economy. Some of the proposals for increased mass limits involve increased axle load limits, which would clearly lead to additional pavement wear. Road controlling authorities (RCAs), while sharing the industry's aims for increased efficiencies in the road transport system, are concerned that any additional pavement wear generated by higher axle loads is paid for so that the standard of the road network can be maintained. New Zealand has a mass-distance Road User Charging (RUC) regime, where the users pay for the road wear they generate, and therefore there is a need to accurately predict road wear from various levels of loading.

Accelerated Pavement Test

In this study, co-funded by Austroads and Transfund New Zealand and conducted in 2002, an accelerated pavement test was undertaken at the Canterbury Accelerated Pavement Testing Indoor Facility (CAPTIF) in Christchurch, New Zealand, to compare the effect of mass on pavement wear for five different sections of pavement which are more typical of those found in New Zealand and Australia. The two 'vehicles' at CAPTIF, known as SLAVEs (Simulated Loading and Vehicle Emulators), were configured with identical suspensions but with different axle loads: one to 40 kN to simulate the current 80 kN axle load limit, and the other to 60 kN to simulate a possible increase to a 120 kN axle load limit. The two SLAVEs trafficked parallel independent wheelpaths so that the relative wear generated by the two could be compared.

Construction of Pavement

The pavement constructed at CAPTIF was in five segments comprising three different basecourse materials. Three basecourses were placed in thick highway strength pavements (320 mm) and two higher quality materials were placed in thinner pavements (250 mm).

Testing the Pavement

Testing the pavement consisted of applying a set number of loading cycles, collecting sets of measurements, and then repeating the cycle. Testing proceeded until 1,000,000 load cycles had been applied.

Analysis

Vertical surface deformation (VSD) was used as the main measure of pavement wear. It is directly related to rutting and the variability in VSD leads to increased roughness. Results from previous CAPTIF tests have shown it to be correlated to dynamic loading and to the variability in pavement structure. Both roughness and rutting are key measures used by RCAs to determine the need for pavement maintenance. By comparing the rate of progression of VSD under the two loading regimes (40 kN and 60 kN), the impact of mass

increases on pavement wear were determined and the impact on road maintenance costs estimated.

Various equations of either power or linear-type functions were fitted to the measured VSD data. Common coefficients were found for some equations in that only the axle load and pavement type need to be known to predict VSD with load cycles. These equations were applied to an imaginary road network to predict the impact in terms of rehabilitation requirements should the axle load be increased from 40 kN to 60 kN.

Conclusions

From these measurements a number of important findings were deduced:

• VSD (vertical surface deformation), which is a fundamental form of pavement wear that results in both rutting and increased surface roughness, again proved to be the most useful measure for monitoring pavement wear at CAPTIF.

• The 60 kN wheel load resulted in VSD values nearly twice those obtained with the 40 kN wheel load in all the pavement segments.

• Segment E, in which a lower quality aggregate (complying with the former TNZ M/5 specification) was used, failed at 87,000 load cycles under the 60 kN load and at 250,000 load cycles under the 40 kN load.

• A conventional power law relationship was fitted to describe the differences in VSD between the two levels of loading for each of the five pavement segments, and the exponent for the power law ranged between 2 to 4 for Segments A, B, C and D.

• The value of the exponent depended on the pavement type and the value of VSD taken to be the end-of-pavement life.

• Reviewing the progression of VSD with load cycles shows that the pavement underwent two distinct phases of VSD. An initial period of rapid change was observed, here called compaction, followed by a period with a constant (linear) rate of change called wear. Least squares regression can be used to fit a straight line to the linear part of the VSD versus load cycles curve. The intercept of this line with the y-axis then gives the compaction component, and the slope gives the wear component.

• The compaction–wear linear relationship was modified to include a multiplier for the pavement type and the ratio of axle load to the reference load of 40 kN. This relationship with common coefficients could be fitted to all the VSD data from this research. In Stage 1 where a 50 kN axle load was compared to the 40 kN load, this relationship has the advantage of being able to predict VSD for other pavement types and axle loads.

• A power law model (called the Kinder–Lay (1988) model) and a linear model with a blending function that models the initial progression of VSD in the compaction stage (of the Wolff & Visser (1994) model) were also fitted to the VSD data, using both best fit coefficients (where the coefficients were changed for each pavement segment) and common coefficients across the whole dataset.

- All equations used to predict VSD fitted the data fairly well. Probably the power law model (of Kinder & Lay) gave the best fit but its use in extrapolating the results may not be appropriate as it predicts an ever-decreasing rate of change in VSD with increasing load cycles.

Many different equations were determined that predicted VSD for a known pavement type and axle load. A selection of them were applied to an imaginary network to predict deterioration in terms of VSD, and thus to predict the rehabilitation requirements each year should the traffic change from 100,000 passes per year for a 40 kN axle to 100,000 passes per year of a 60 kN axle. It was assumed that the imaginary network consisted of 40 road sections and that, with the 40 kN axles, only one section would require rehabilitation per year. A summary of the analysis follows.

- All equations predicted that 5 to 10 sections would need rehabilitation in the first year. After this, the linear-type equations (compaction–wear and Wolff & Visser) predicted that, on average, around 2 sections per year would need rehabilitation. The base power model, which was a power model fitted to each load, predicted on average 3.6 sections per year would require rehabilitation. Note that this must be tempered with the fact that the 60 kN axle would carry considerably more freight per axle pass.

- The power exponent that relates damage (number of rehabilitations per year) to the ratio of axle load to reference load of 40 kN raised to this power exponent, ranged from 1.7 to 1.9 for the linear model, and was 3.2 for the base power model.

- The large number of pavement sections requiring rehabilitation in the first year after the new 60 kN axle loads were introduced, all required rehabilitation again at the same time (from 8 years to 22 years depending on the model used).

- Removing the first year rehabilitation requirements made very little difference to the power law exponent, and thus this negates the need for a one-off payment to be included in the RUC for new vehicles operating at the higher mass limits.

- The average number of rehabilitations required each year predicted by the base power model (3.6 per year) was significantly higher than the other models (2.0 per year). The base power model was the best match to the measured data. However, this large difference in results is partly related to the way the VSD results are extrapolated beyond the measured data. The base power model predicts an ever-decreasing rate of change in VSD while the linear type models predicts a constant increase.

- For Segment E constructed with low strength rounded aggregates that failed within 250,000 load cycles, exponent values as high as 6 were calculated as the test progressed. However, the rapid nature of the final failure reduced the exponent to 2.6 at the end of testing. This result illustrates that weaker sections in the road network which are adequate at present could fail quickly with the introduction of higher mass limits.

- When applying the equations used in this study to predict the damage caused by other tyre types and pressures not used here, then an adjustment is required to the axle load. This adjustment can be calculated from the measured strain value where the adjusted axle load is the axle load with the standard tyres and pressure used in the CAPTIF test that causes the same strain. The result is an increase in axle load for Super Single tyres with a slight increase or decrease in axle load, depending on the tyre pressure.

- The result of this accelerated pavement test principally provides an indication of the performance of a relatively strong pavement, on a strong dry subgrade, in ideal dry environmental conditions. The behaviour of weaker or saturated subgrades has not been investigated, nor have the effects on older and/or poorly maintained surfaces where moisture may be entering the base.

Recommendations

- Further validation is required of the models proposed to predict VSD with load cycles based on pavement type and axle load.

- Equations that predict VSD with load cycles are based on measured data up to 1,000,000 load cycles. The pavement had not reached the terminal functional condition and to be sure of the correct equation form (either a power or linear function), a test that reaches terminal condition is required for both the reference axle load of 40 kN and that of 60 kN.

- Analysis of the pavement types tested in this Stage 3 is required to determine how the results affect current pavement design practices. For example, in this test some of the thinner pavement segments had a similar life to the thicker pavement segments.

- On the existing pavement, strain measurements should be undertaken for a range of tyre pressures and loads other than those tested. These data will help decide how to interpolate the results for other tyre types, pressures and loads.

- From these results of a rather simple deterioration study, the compaction–wear model and other linear type models should be used cautiously, particularly when predicting the relative damage to the pavement caused by an increase in axle loads.

- Some of the models developed that predict VSD have a multiplier depending on the pavement type. So that these models can be applied to other pavement types, a relationship needs to be developed with a common pavement parameter like the structural number (SNP) and/or FWD measurements.

Abstract

To improve the efficiency of the road transport industry, a range of mass limit increases for heavy vehicles has been proposed. Some of the options for mass increases include increasing the axle load limit, which would inevitably lead to increased road wear. New Zealand has a mass-distance Road User Charging (RUC) regime where the users pay for the road wear they generate, and therefore there is a need to accurately reflect the wear.

Stage 3 of this study, carried out in 2002, aimed to accurately predict road wear from various levels of loading, an accelerated loading test was undertaken at the Canterbury Accelerated Pavement Testing Indoor Facility (CAPTIF) to compare the wear generated by different levels of loading. The pavement consisted of five different segments that were subjected to 1,000,000 load cycles in two parallel wheelpaths. The axle load on one wheelpath was 8.2 tonnes while the load on the other was 12 tonnes. As a result various models for predicting VSD (Vertical Surface Deformation) have been developed. Some of these models require knowing only the axle load and pavement type to predict VSD.

Applying VSD models to an imaginary network showed a significant amount of rehabilitation is required in the first year after an increase in axle load. The base power model predicted the highest damage compared with the other linear type models.

1.   Introduction

1.1   Background

The road transport freight industry in New Zealand understandably wishes to increase its efficiency. One of the ways to do this is through increases in the mass limits allowed for heavy vehicles. This in turn can result in economic benefits to the whole country provided the impact of the changes in mass limits are accurately known and considered in assigning the new limits, and in determining appropriate road user charges (RUC). One of the impacts concerning road controlling authorities (RCA) is the effect on increasing mass limits on the life of their pavements or how much more pavement rehabilitation and maintenance will be required.

In response to the industry's requests for larger and heavier vehicles, Transit New Zealand (Transit) undertook, between 1999-2001, a study to assess the economic and safety impacts of increasing mass limits. This study investigated two scenarios:

- Scenario A, where heavier vehicles subject to the same dimensional limits as those currently in place would be permitted to operate across the entire network;

- Scenario B, where longer and heavier vehicles would be permitted to operate only a selected set of key routes.

Within these two scenarios several axle mass limit options, as shown in Table 1.1, were considered.

Table 1.1   Axle mass limit options in Transit Heavy Vehicle Limits project.

Option	Allowable weights (tonnes)			
	steer axle	single axle	tandem axle	triaxle
Present	6.0	8.2	15	18
1	6.0	8.2	15	19
2	6.0	8.2	15	20
3	6.0	8.8	16	20

Transit's evaluation of these proposed changes in mass limits included research into their impacts on safety, road geometry, economics, and on pavements and bridges. In determining the pavement wear impact of these changes in mass limits, existing theories for the relationship between vehicle loads and pavement wear were applied. The most widely used existing theory for determining the effect of mass limit increases on pavement life is the fourth power law. This is used to determine the pavement loading as a number of Equivalent Standard Axles (ESAs). The formula for converting an actual axle load to ESA is:

$$ESA = \left[\frac{Actual\ axle\ load}{Reference\ axle\ load} \right]^{4}$$

This fourth power relationship between axle loads and pavement life has never been validated on New Zealand's thin-surfaced unbound granular pavements. Power values between 1 and 8 have been suggested by different researchers throughout the world for different pavement structures and failure mechanisms (Cebon 1999, Kinder & Lay 1988, Pidwerbesky 1996). The AUSTROADS Pavement Design Guide (1992), which is the basis of New Zealand design practice, uses a power of 4 for unbound basecourse performance and a power of 7.14 for subgrade performance.

The use of a fourth power relationship predicts that the 7.3% increase in allowable loading for a single axle, as per option 3 (Table 1.1), will result in a 33% increase in pavement wear, and consequently an RCA can expect a 33% increase in the length of pavement rehabilitation required per year. The actual situation is not as extreme as this because, in the first place, not all vehicles will change to the higher limits, and second the higher axle load limits will result in higher payloads and consequently fewer trips for the same freight volume. Nevertheless, this change will represent a significant increase in annual expenditure on roads for an RCA, who need to budget for it. The uncertainty in the validity of the fourth power rule poses difficulties when requesting increases in funding for the next financial year. Justifying an increase in the road user charges (RUC) based on a fourth power rule that has not been validated in New Zealand is expected to be increasingly difficult, particularly as research results from accelerated pavement tests are suggesting different relationships.

The study reported here is Stage 3 of a multi-stage accelerated pavement testing programme. This programme is investigating, by research at Transit New Zealand's Canterbury Accelerated Pavement Test Facility CAPTIF on typical New Zealand pavement designs, the relative effect on pavement life of an increase in axle load from 8.2 tonnes (i.e. 40 kN for a half axle with dual tyres) to 12 tonnes (i.e. 60 kN for a half axle with dual tyres). Results from Stages 1 and 2 (de Pont et al. 2001, 2002) determined the research to be conducted in this Stage 3 and are reported in the following sections.

1.2 Increase in mass limits effect on pavement wear – Stage 1

The previous research project undertaken at CAPTIF was a direct comparison of rutting between a 40 kN (8.2-tonne axle load) dual-tyred half axle (i.e. present load limit) and 50 kN (10-tonne axle load) dual-tyred half axle. CAPTIF is a circular track and the wheelpaths of the two vehicles (i.e. 40 kN and 50 kN) were separated. The pavement was constructed to have three different sections. All sections had the same subgrade but three different good quality basecourses were used, laid in the same depth. The results of Stage 1 are reported in de Pont et al. (2001) and the key findings are summarised here.

The exponent n (e.g. fourth power or otherwise) was determined for all the pavement sections based on the following conventional power law equation:

1.   Introduction

$$\frac{N_{40kN}}{N_{50kN}} = \left[\frac{P_{50kN}}{P_{40kN}}\right]^{n}$$

Equation 1.1

where:

n = the exponent of the power law

N_{50kN} = the load cycles of load P_{50kN} for a given level of wear

N_{40kN} = the load cycles of load P_{40kN} for the same given level of wear as achieved by load P_{50kN} in N_{50kN} load cycles.

Vertical surface deformation (VSD), a similar parameter to rutting, was used as the failure criteria or level of wear. There was a large variation (between 2.8 and 9) in the exponent value required to give the best fit to the conventional power law (Figure 1.1). As the pavement design of the four segments constructed at CAPTIF for Stage 1 was substantially similar in character, the result that the exponents for a power law model should vary so much is surprising. This makes it difficult to predict the appropriate exponent value in advance.
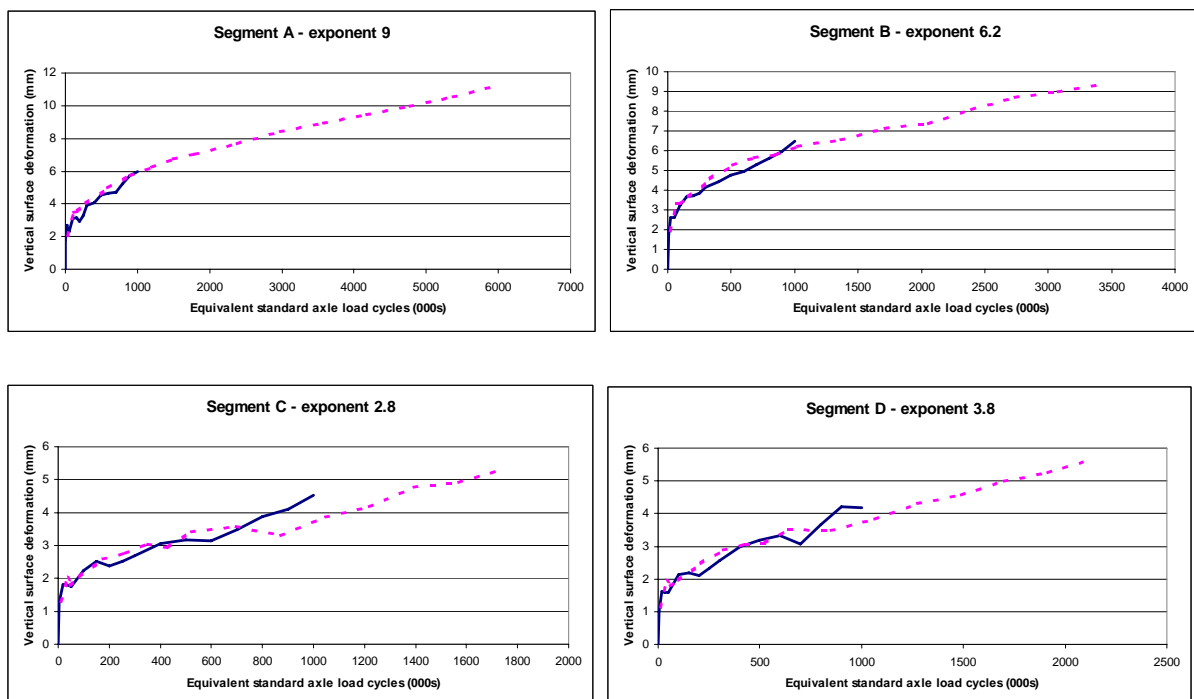
Figure 1.1   Power law fits to VSD for all four segments (de Pont et al. 2001).

The large variation in the power law exponent for each of the pavement segments constructed with different premium quality basecourse aggregates prompted the use of a lower quality regional aggregate in the Stage 3 accelerated pavement test at CAPTIF. Further, a different method for determining the appropriate exponent to relate the damage between the two vehicle loads was proposed. This new method first uses a *compaction–wear* model to describe the progression of VSD.

Reviewing the progression of VSD with load cycles shows that the pavement underwent two distinct phases of VSD. An initial period of rapid change was observed, here called *compaction*, followed by a period with an approximately constant (linear) rate of change, here called *wear*. Least squares regression can be used to fit a straight line to the latter part of the VSD versus load cycles curve. The intercept of this line with the y-axis then gives the compaction component and the slope gives the wear. For each of the four pavement segments, a power law function can be used to relate the compaction and wear between the normally loaded and more heavily loaded wheelpaths. The best-fit exponent values for compaction and wear were quite similar for each pavement segment, and did not vary too much between segments.

The exponent values for the compaction–wear model were between 1 and 3.4 for compaction, and between 1.8 and 3 for wear. (The values for pavement segment C were a little lower than this but repairs to the pavement surface during the test meant that very few data points could be used in this segment.) The implication of this is that, if the axle load limit were to be increased, the underlying wear rate of the compaction–wear model would increase, as indicated by the power law function, with an exponent of between 1.8 and 3.

1.3 Laboratory-predicted v in-service performance of unbound granular pavements

The project, *Relationships between Laboratory Predicted Performance and In-Service Performance of Unbound Granular Pavements Based on Measured Stresses and Strains* was completed in combination with the Stage 1 project, and compared the 50 kN axle with the 40 kN axle. One of the outputs from this project was a pavement model that predicts deformation of the pavement from measured material characteristics in the repeat load triaxial apparatus and computed stresses and strains in the pavement. This model can be used to determine the impacts on pavement wear of various tyre loads, pressure and types used in the load response test.

1.4 Increase in mass limits effect on pavement wear – Stage 2

In the first task of the Stage 2 research (de Pont et al. 2002), stresses and strains were measured within the pavement for a range of tyre types, loads and pressures. During this work an additional 19,000 cycles of loading were applied to the original pavement. The work was performed as part of an AUSTROADS research programme and has been reported in Vuong & Sharp (2001).

In the second task of the Stage 2 research, the mass of the 40 kN vehicle from the Stage 1 research was increased to 50 kN and a further 300,000 load cycles were applied. This was undertaken to examine how the rate of rutting on an existing pavement would change with the application of a heavier load.

The results of this task were included in de Pont et al. (2001) and further analysed in de Pont et al. (2002).

In the third and final task of the Stage 2 research, which the Stage 2 report (de Pont et al. 2002) is predominantly about, the track was rehabilitated, resurfaced with a chipseal, and tested using both the 50 kN and 40 kN simulations. The loads were in separate wheelpaths to provide a direct comparison of loss of surface texture.

1.5 Increase in mass limits effect on pavement wear – Stage 3

For this Stage 3 a new fully instrumented pavement was constructed and tested in a similar process to the Mass Limits Stage 1 project. The responses of three types of aggregate were measured: two premium quality aggregates laid in two thicknesses and loaded with 40 kN (8.2 tonnes) on the outer wheelpath and 60 kN (12 tonnes) on the inner path, and a lower quality basecourse was laid as a thick layer. The basecourse aggregates consisted of one good quality TNZ M/4 type basecourse, a Class I (premium) Australian crushed rock, and one lower quality regional variation basecourse (such as Shell Rock). This was to answer three of the questions that remained from the testing carried out over the previous two years.

The first question is how will low quality materials behave. The testing in Stages 1 and 2 had only considered premium quality materials. The results of the Mass Limits Stage 1 testing indicated that even proven high quality materials give considerably different performance to that assumed in our current design models such as the fourth power law. The preliminary results also suggest that the behaviour is very material-dependent, with power relationships between 2 and 9 observed.

The testing will also determine whether the simple fourth power law type model is actually capable of predicting distress to 60 kN axles. This is particularly important as the Bus Industry is pushing for an increase to 60 kN axle limits to match those used in Europe where most bus chassis are sourced. This test will allow at least a simple direct understanding of the pricing that should be applied to such a proposal, as well as provide a better understanding of how we should convert traffic spectrums to Equivalent Standard Axles (ESAs) for pavement design.

Finally, by testing different thicknesses of pavements an understanding will be obtained of the behaviour on under-strength pavements as well as the strong pavements we have tested to date. Without this additional testing, predicting the likely network needs using the current deterioration models will not be possible. The calibration of such models requires the use of historical data to predict future needs.
The information obtained from the tests is required to accurately

- apply pricing for road wear,

- quantify the benefits of allowing increased axle loads,

- convert traffic spectrums to Equivalent Standard Axles (ESAs) for pavement design,

- calibrate deterioration models such as dTIMS HDM-4[1] models supported by Transfund.

1.6 The Canterbury Accelerated Pavement Testing Indoor Facility (CAPTIF)

CAPTIF is located in Christchurch. The facility consists of a 58-m long (on the centreline) circular track contained within a 1.5-m deep x 4-m wide concrete tank, so that the moisture content of the pavement materials can be controlled and the boundary conditions are known. A centre platform carries the machinery and electronics needed to drive the system. Mounted on this platform is a sliding frame that can move horizontally by 1 m. This radial movement enables the wheelpaths to be varied laterally and can be used to have the two 'vehicles' operating in independent wheelpaths. An elevation view is shown in Figure 1.2.
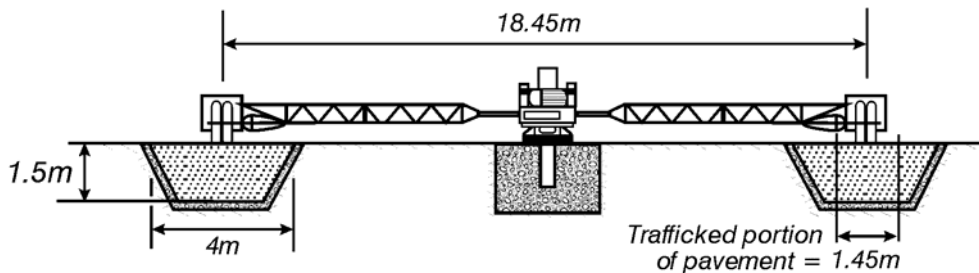
Figure 1.2   Elevation view of CAPTIF.
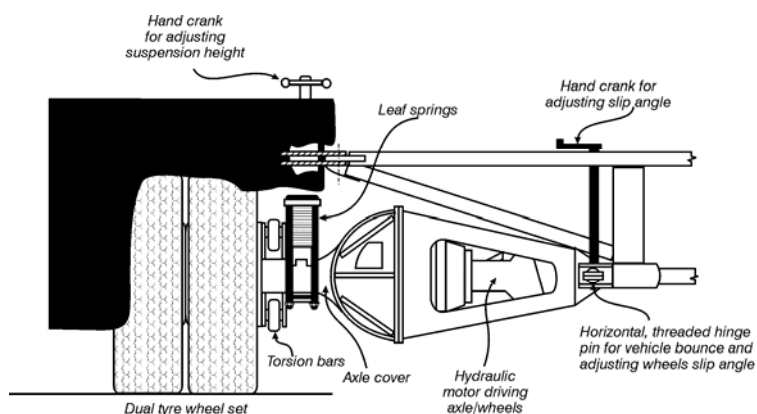
Figure 1.3   The CAPTIF SLAVE unit.

At the ends of this frame, two radial arms connect to the Simulated Loading and Vehicle Emulator (SLAVE) units shown in Figure 1.3. These arms are hinged in the vertical plane so that the SLAVEs can be removed from the track during pavement construction, profile measurement, etc., and in the horizontal plane to allow vehicle bounce.

---

[1]   dTIMS Deighton's Total Infrastructure Management System;
HDM Highway Development & Management

1.   Introduction

CAPTIF is unique among accelerated pavement test facilities in that it was specifically designed to generate realistic dynamic wheel forces. All other accelerated pavement testing facility designs, that we are aware of, attempt to minimise dynamic loading. The SLAVE units at CAPTIF are designed to have sprung and unsprung mass values of similar magnitude to those on actual vehicles and use, as far as possible, standard heavy vehicle suspension components. The net result of this is that the SLAVEs apply dynamic wheel loads to the test pavement that are similar in character and magnitude to those applied by real vehicles. A summary of the characteristics of the SLAVE units is given in Table 1.2. The configuration of each vehicle, with respect to suspensions, wheel loads, tyre types and tyre numbers, can be identical or different, for simultaneous testing of different load characteristics.

Pavement instrumentation which is used at CAPTIF includes: Emu coil transducers for measuring strains in three dimensions in the pavement, h-bar strain gauges for measuring horizontal strains at the bottom of the asphalt layer, and partial depth gauges for measuring the pavement layer deflections. As well temperature probes are used to monitor both the pavement and air temperatures. The vehicle instrumentation consists of accelerometers mounted on both the sprung and unsprung masses of each 'vehicle' and displacement transducers to measure suspension displacements. As the 'vehicles' are a fairly simple quarter vehicle structure, dynamic wheel forces can be calculated by combining the two accelerometer signals weighted by appropriate mass factors.

Other measurement systems used at CAPTIF during testing are: a Falling Weight Deflectometer (FWD), a Loadman falling weight deflectometer, the CAPTIF Deflectometer which is a modified Benkelman beam, a Stationary Laser texture Profilometer (SLP), a transverse profilometer, a DIPStick profiler, and a laser profilometer. The laser profilometer has now effectively replaced the DIPStick for longitudinal profile measurements. For convenience of measurement the track is divided into 58 equally spaced stations which are 1 m apart on the centreline wheelpath.

A more detailed description of the CAPTIF and its systems is given by Pidwerbesky (1995).

Table 1.2   Characteristics of SLAVE units.

Test Wheels	Dual- or single-tyres; standard or wide-base; bias or radial ply; tube or tubeless; maximum overall tyre diameter of 1.06 m
Mass of Each Vehicle	21 kN to 60 kN, in 2.75 kN increments
Suspension	Air bag; multi-leaf steel spring; single or double parabolic
Power drive to wheel	Controlled variable hydraulic power to axle; bi-directional
Transverse movement of wheels	1.0 m centre-to-centre; programmable for any distribution of wheelpaths
Speed	0-50 km/h, programmable, accurate to 1 km/h
Radius of Travel	9.2 m

2.   Objectives

Overall objectives to be achieved in 2003:

- To determine the relative damaging effect on pavement wear and chipseal life compared to the standard load (8.2-tonne dual-tyred single axle) for increases in vehicle loads and tyre pressures, using accelerated testing, load response data, existing accelerated pavement test results, and an appropriate pavement model.

- To determine appropriate road user charges for new heavy vehicle load limits that take into account their effects on both pavement and chipseal life.

- To provide a methodology and pavement model to predict the potential impact on the road network caused by increases in heavy vehicle load limits.

Objectives achieved in 2000/01 (Stages 1 and 2):

- To measure the pavement response (stresses and strains) for a range of tyre types, loads and pressures.

- To determine an appropriate pavement model to predict life.

- To predict pavement life from the pavement response data using an appropriate pavement model.

- To determine the effect on pavement rutting on an already trafficked pavement when the axle loading is increased from 8.2 tonnes to 10 tonnes.

- To determine the relative effect on chipseal life between an 8.2 and a 10-tonne dual-tyred single-axle load.

- To determine further accelerated pavement tests required to achieve the overall objectives of this research project.

Objectives achieved in 2001/02 (relevant to this Stage 3 report):

- To determine the effect on pavement rutting on a new pavement constructed with *premium quality* materials when the axle loading is increased from 8.2 tonnes to 12 tonnes (12 tonnes is the limit proposed by the bus industry).

- To determine the effect on pavement rutting on a new pavement constructed with *marginal* materials when the axle loading is increased from 8.2 tonnes to 12 tonnes.

- To measure the pavement response (stresses and strain) under a 12-tonne axle as the pavement deteriorates.

- Investigate the ability of a simple pavement power model to predict life as pavement loads increase.

- Investigate the validity of a simple power model when considering weak (thin) and strong (thick) pavements.

2.   *Objectives*

- To predict pavement life from the pavement response data using an appropriate pavement model.

- To determine further accelerated pavement tests required to achieve the overall objectives of this research project.

3. Pavement tests

3.1 Pavement design

The objective of the pavement design was to produce the relatively low levels of rutting observed in typical New Zealand and Australian pavements while maintaining a balance between the life of the heavily loaded (60 kN) inner wheelpath and the lightly loaded (40 kN) outer wheelpath.

The Waikari clay subgrade was modelled with a 10th percentile design in-situ CBR of 10, based on test results from previous research in 1999/2000 (de Pont et al. 2001), and used the standard 10 times CBR relationship to obtain the modulus.

The decision to use five segments of different materials and thickness was made as a result of recommendations from previous research and feedback from local authorities to the previous 1999/2000 research at CAPTIF. The 1999/2000 research investigated the relative effects of increasing the mass limits on a single-axle dual tyre from 40 kN to 50 kN on pavements with loading volumes typical of New Zealand highways. Local authorities wanted confirmation that the relationships found would hold for their pavements, which typically would be thinner because they carry lower volumes of traffic. These pavements are generally weaker, both in terms of thickness and the lower quality materials used for them.

The research had also recommended validating the relationships by increasing the load and investigating whether the relationships found would continue to hold. As this was the basis of the current research, the decision was made to use the original pavement design for the highway standard pavements.

The original 1999/2000 pavement was designed in an iterative manner using the Austroads (1992) Pavement design guide. The iterative designs assumed a 700 kPa tyre pressure with a 95.6 mm-tyre radius (i.e. 40 kN load) on the outer wheelpath and a 850 kPa tyre with a 97 mm-tyre radius (i.e. 60 kN load) on the inner wheelpath. The basecourse layer was, from previous experience, modelled with a modulus of 400 MPa using Austroads sub-layering.

The iterative analysis suggested the outer (40 kN or 8.2 tonne) wheelpath would require a 250-mm deep basecourse to withstand the design 1,000,000 wheel passes, and a depth of 290 mm for the outer wheelpath assuming the Austroads subgrade strain criterion. Using the fourth power law to convert the 60 kN (10 tonne) wheel to an equivalent number of standard axles, rather than modelling directly, suggested that the outer wheelpath would need to be 270 mm deep.

The final design using 275 mm basecourse resulted in a pavement that, in the outer wheelpath, would theoretically fail by reaching a rutting level of 25 mm at 2,900,000 wheel passes and, in the inner wheelpath, at 600,000 wheel passes, assuming the

Austroads subgrade strain criterion and directly modelling the tyres. Using the fourth power law suggested that the inner wheelpath would fail at 1,200,000 wheel passes.

Experience with the 1999/2000 pavement design and relationships derived for increases in mass limits suggested that the pavement design would be adequate for testing the 60 kN load.

For the weaker 'local authority' pavements a full thickness was used for the lower quality materials and thinner test sections were built with the premium materials.

The final pavement design of 225 mm of basecourse for the thinner sections was expected to effectively fail in the order of 100,000 cycles. If required the thinner test sections would be rehabilitated and the pavement test would be continued on the thicker sections.

3.2   Layout of test pavement

The pavement was constructed in five primary segments:

- Segment A extended from station 00 to station 11;

- Segment B from 11 to 22;

- Segment C from 23 to 34;

- Segment D from 34 to 44; and

- Segment E from 45 to 56.

A 3-m transition zone was allowed between materials, and a 1-m transition ramp was made at subgrade level between the segments of differing thickness. Within each segment on the track centreline 3 primary sites were set aside for intensive monitoring and 7 secondary sites for less intensive monitoring. A plan showing the layout of the different segments is shown in Figure 3.1. An elevation showing the cross section of the pavement design, location of the two wheelpaths, and the in-situ instrumentation is shown in Figure 3.2.

3.3   Pavement materials

Three different pavement materials were selected for the test segments. The first two were used in the 1999/2000 research and are materials typically used in pavement construction in New Zealand. The third material is a local road material, for use on pavements where the design life loading does not exceed 1,000,000 ESAs.

Material A (Sections A & B)

Australian Class 2 premium crushed rock (Montrose Class 2) is a 20-mm maximum size, Class 2 wet-mix crushed rock. The source rock is classified as rhyolite, acid igneous from the Boral quarry at Montrose, Victoria, Australia. The material is angular, rough, hard, blue-grey rock containing some dolomite siltstone and some blue-grey sand.
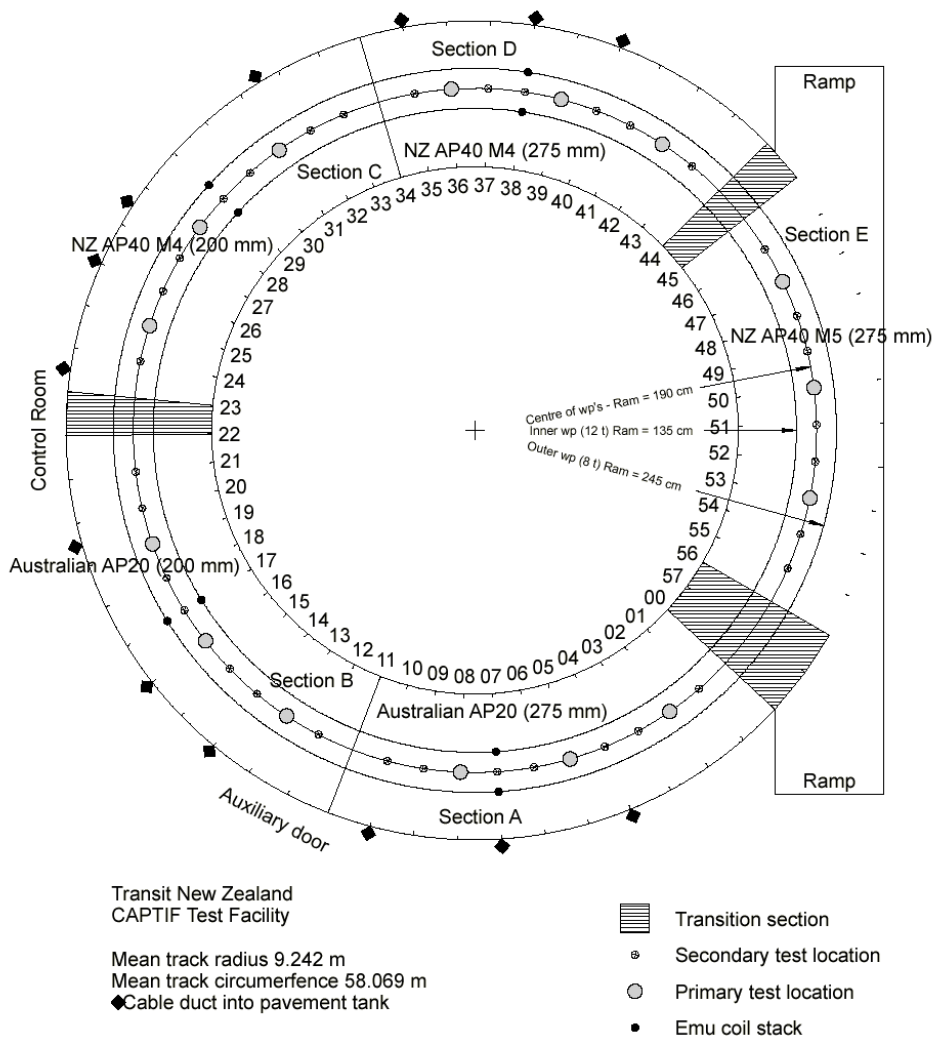
Figure 3.1   Plan showing the layout of the test segments, and positions of stations.
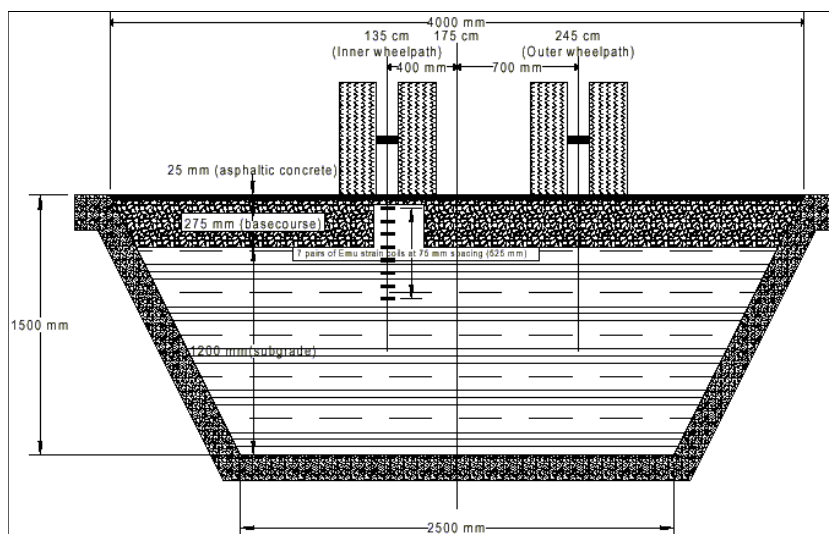
Figure 3.2   Pavement cross-section and wheelpath locations.

Material B (Sections C & D)

New Zealand premium aggregate (complying with TNZ M/4) is a 40-mm maximum sized, AP40 crushed alluvial greywacke gravel. The source is Springston Formation greywacke alluvial gravel, extracted at Pound Road, Canterbury, New Zealand. The material is angular, hard, light bluish-grey, sandy medium gravel with minor silt.

Material C (Section E)

Christchurch, New Zealand uncrushed river gravel (complying with TNZ M/4, Table 3.1). This is a 40-mm maximum sized, AP40, uncrushed alluvial gravel, locally known as TNZ M/5. The source is Springston Formation greywacke gravel, extracted at Coutts Island, Canterbury, New Zealand. The material is rounded, hard, light bluish-grey, sandy medium gravel with a trace of silt.

Laboratory characterisation

The basecourse materials were characterised by the following tests undertaken on samples from stockpiles at CAPTIF:

- Particle Size Distribution (PSD) tests to NZS 4407:1991 Methods of sampling and testing road aggregates (Part 2.4.6.2.1 Sampling road aggregates, Test 3.1 Water content of aggregate, Test 3.8.1 Wet Sieving Test, Test 3.14 Broken Face Test).

- Vibrating Hammer Maximum Dry Density (MDD) tests to determine the compaction and Optimum Moisture Content (OMC) targets to NZ 4402: 1986 Methods of testing soils for civil engineering purposes (Test 4.1.3 NZ vibrating hammer compaction test).

- Repeated Load Triaxial (RLT) Tests to AS 1289.6.8.1-1995 (SA 1995) to determine the resilient modulus of each material.

The results of the tests are listed in Appendix A, and Table 3.1 summarises the maximum dry density, sand equivalent, optimum moisture content, plastic limit and liquid limit for each material.

Table 3.1   Laboratory characterisation test results for the basecourse aggregates used in the test segments.

Material	Maximum Dry Density (t/m³)	Optimum Moisture Content (%)	Sand Equi-valent	Plastic Limit	Cone Pen. Limit	Plasticity Index
Montrose Class 2	2.26	6.0	31	18	22	4
TNZ M/4	2.25	6.0	31	NP	20	NP
TNZ M/5	2.38	4.2	53	NP	19	NP

NP – non plastic

4.   Pavement construction

4.1   Subgrade construction

The existing pavement was excavated and 300 mm of the subgrade was removed. The surface of the remaining Waikari clay subgrade was ripped to a depth of 150 mm by a backhoe digger equipped with a ripper tooth, and then rotary-hoed to a fine tilth by a small tractor. The tractor then used a levelling blade to smooth off the surface and it was rolled with three passes of a Wacker pivot-steer trench roller, while monitoring compaction with a nuclear density gauge. Photos of the construction are in Appendix B.

The clay for the subgrade was placed in lifts, each not exceeding 150 mm using the following procedure:

- a pad was constructed at design level for the tractor and blade to sit on;

- material was brought in from the stockpile by a loader travelling over the previously compacted surface;

- the load was dropped on the front of the pad then dragged back over the edge while the tractor, with its low pressure tyres, smoothed any irregularities;

- levels were monitored by laser level and digital staff throughout back-filling with an allowance for compaction;

- material samples from the lift were checked for water content using a microwave oven and digital scales;

- water was added as necessary using a sprinkler system and flow meter and mixed in with a rotary hoe;

- after waiting overnight for the water content to stabilise, the tractor smoothed off the surface with its blade and three passes were made with the trench roller.

The final lift of the subgrade was overfilled by 25 mm, its water content adjusted, then the subgrade was lightly rolled. A larger tractor, fitted with a laser-controlled blade, cut back the surface to the design level with an allowance for compaction. The surface was rolled with three passes of the trench roller on heavy vibration. The strain coils were installed at the appropriate levels during the subgrade construction. The subgrade surface was covered with plastic sheets when not in use to maintain water content at the desired percentage.

The Dynatest pressure cells were placed at the top of the subgrade on the inner wheelpath, between the coil stations in each segment. Transverse profiles of the top of subgrade at every station were recorded as well as spot heights measured with the laser level.

4.2   Basecourse construction

The first lift of the basecourse was placed in a 150-mm deep layer in segments A, D and E, and 75 mm in segments B and C. The strain coils and pressure cells were placed at the required depths.

Seven passes with the Wacker plate compactor were applied and the density was measured. Spot height readings were taken.

Following these measurements, the final basecourse lift was overfilled by 15 mm and lightly compacted with the trench roller. The tractor with the laser-guided blade trimmed the surface back to design level while a 4-tonne steel/rubber combo roller tightened the surface, which was kept damp with light watering.

Water was applied to the basecourse to bring it up to optimum moisture content (OMC), several passes with the combo roller were applied and the densities were measured. More water was added and compaction was completed with a heavy Wacker plate compactor.

The last of the strain coils and pressure cells were placed and the surface disturbances repaired.

4.3   In-pavement instrumentation

The soil strain instrumentation was extended to enable measurement of the four quality-material pavement segments and in both wheelpaths. The soil strain instrumentation is based on a system purchased from the University of Nottingham, known as the Emu Strain System. Strain coils were fabricated at CAPTIF using Nottingham guidelines. Relay boards, triggering systems, and software were developed at the University of Canterbury. The in-pavement Emu coil arrangement can be seen in Figure 4.1.

Data from Dynatest pressure cells, mounted vertically and horizontally, were also read by the same computer that operated the strain coils. The pressure cell readings were triggered in the same manner as the strain readings, i.e. by an infrared beam. The inner wheelpath pressure cell arrangement was that shown in Figure 4.2.
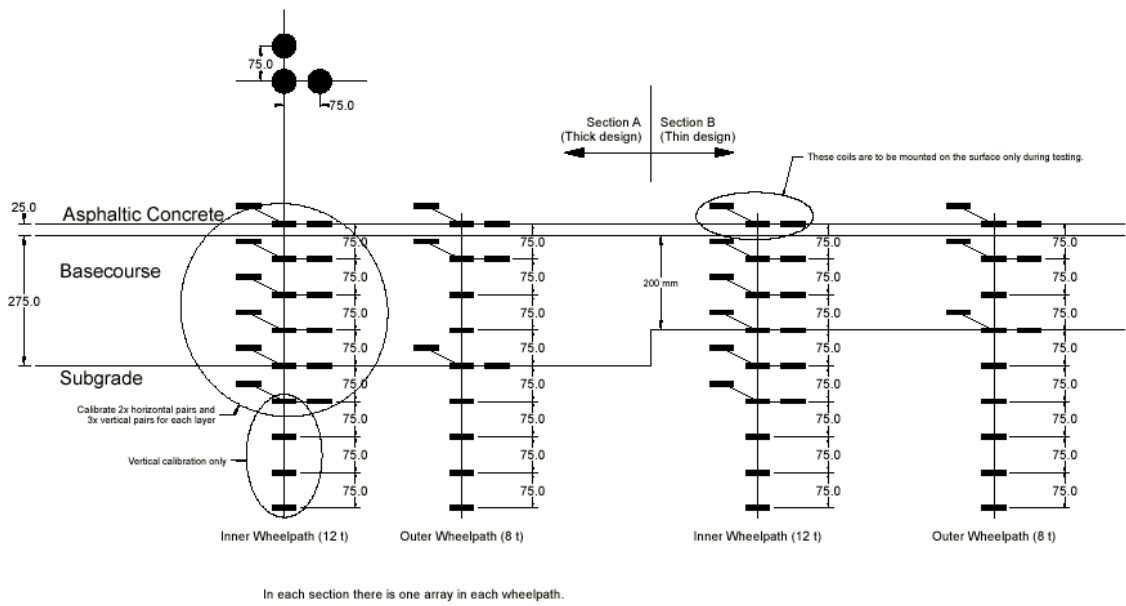
Figure 4.1   Emu coil arrangements for measuring the soil strains in the pavement segments.
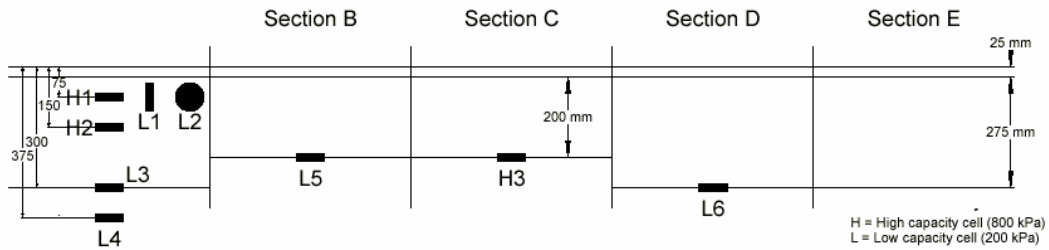
Figure 4.2   Pressure cell arrangements mounted in the wheelpaths.

4.4   Sealing

The basecourse surface was swept with a power broom, heavily tack coated, and 25 mm thick 10-mm asphaltic concrete was placed by an asphaltic concrete paving machine over the entire track. The sealing crew used a footpath roller behind the paving machine. Once the paving machine had completed the circle and left the building, the entire surface was rolled with a 3.5-tonne steel drum roller.

5. Pavement testing during construction

In constructing a pavement at CAPTIF for a comparative study such as this, the aim was to minimise the transverse variability in the pavement structure so that the two SLAVE units are, as much as possible, trafficking identical pavements. Longitudinal variations in the pavement structure are less of a concern but it is difficult to construct a pavement that is very uniform transversely and irregular longitudinally. To test a parameter, such as layer thickness, for uniformity between the two wheelpaths a new variable is constructed, which is the difference between the parameter's value on the inner wheelpath and its value at a position on the same radial line in the outer wheelpath. For a uniform pavement this new 'difference' variable will have a mean equal to zero and a small standard deviation.

5.1 Thickness data

The tables below show the statistics of this 'difference' variable for the layer thicknesses and FWD results. At the 95% confidence level, if the range of the average difference ± 2 × standard error includes zero, then we cannot reject the null hypothesis that there is no difference between the inner and outer wheelpaths.

Table 5.1   Inner and outer wheelpath basecourse layer thickness.

Segment (Station)	Average (mm)		Standard Deviation (mm)		No. of Samples		Difference Statistics (mm)	
	Inner	Outer	Inner	Outer	Inner	Outer	Average	Standard Deviation
A (0-11)	279	286	8.5	6.6	60	60	9	5.2
B (11-22)	218	210	8.0	5.2	60	60	−7	4.9
C (23-34)	215	213	5.0	8.5	60	60	−1	5.9
D (34-44)	291	288	8.2	9.3	54	54	0	4.7
E (45-56)	295	283	2.8	4.3	18	18	−9	3.3

Table 5.2   Inner and outer wheelpath asphalt layer thickness.

Segment (Station)	Average (mm)		Standard Deviation (mm)		No. of Samples		Difference Statistics (mm)	
	Inner	Outer	Inner	Outer	Inner	Outer	Average	Standard Deviation
A (0-11)	43	37	4.2	6.9	60	60	−7	3.6
B (11-22)	36	32	2.1	4.7	60	60	−5	3.7
C (23-34)	36	36	4.5	4.0	60	60	−1	2.4
D (34-44)	30	26	3.8	2.9	54	54	−4	2.4
E (45-56)	27	38	2.5	3.3	18	18	9	0.8

Table 5.3   Inner and outer wheelpath total pavement layer thickness (basecourse and surfacing).

Segment (Station)	Average (mm)		Standard Deviation (mm)		No. of Samples		Difference Statistics (mm)	
	Inner	Outer	Inner	Outer	Inner	Outer	Average	Standard Deviation
A (0-11)	322	323	11	10	60	60	2	4.3
B (11-22)	254	243	9	7	60	60	−11	4.0
C (23-34)	251	249	4	8	60	60	−2	5.7
D (34-44)	321	313	6	8	54	54	−4	3.8
E (45-56)	322	321	3	3	18	18	0	3.0

5.2   Nuclear density / Moisture gauge results

While important in the overall pavement performance, there is no need to consider the transverse variability of the density results obtained during construction, as this will be apparent from the deflection testing results in Section 5.3.

Table 5.4   Subgrade dry density and moisture content.

Segment (Station No.)	Mean Dry Density (t/m3)	Mean Moisture content (%)
Whole Track	1841	8.5

Table 5.5   **Basecourse dry density and moisture content.**

Segment (Station No.)	Mean Dry Density (t/m3)	Mean Moisture content (%)	Relative Dry Density
A-B (0-22)	2166	3.9	96
C-D (23-44)	2163	2.7	96
E (45-56)	2220	2.6	93

5.3   Falling Weight Deflectometer (FWD) results

FWD results for inner and outer wheelpaths during construction are listed in Tables 5.6, 5.7 and 5.8.

Table 5.6   **Inner and outer wheelpath subgrade d0 values.**

Segment (Station)	Average (mm)		Standard Deviation (mm)		No. of Samples		Difference Statistics (mm)	
	Inner	Outer	Inner	Outer	Inner	Outer	Average	Standard Deviation
A (0-11)	1.583	1.583	0.200	0.098	11	11	0.000	0.339
B (11-22)	1.862	1.592	0.503	0.114	11	11	0.269	0.299
C (23-34)	1.723	1.682	0.196	0.185	11	11	0.041	0.342
D (34-44)	1.579	1.464	0.100	0.093	10	10	0.100	0.098
E (45-56)	1.556	1.619	0.167	0.135	12	12	−0.035	0.539

Table 5.7   **Inner and outer wheelpath basecourse d0 values.**

Segment (Station)	Average (mm)		Standard Deviation (mm)		No. of Samples		Difference Statistics (mm)	
	Inner	Outer	Inner	Outer	Inner	Outer	Average	Standard Deviation
A (0-11)	1.047	0.966	0.084	0.080	11	11	0.081	0.017
B (11-22)	1.168	1.203	0.075	0.056	11	11	−0.035	0.224
C (23-34)	1.182	1.130	0.019	0.058	11	11	0.052	0.038
D (34-44)	1.031	1.019	0.027	0.052	10	10	0.013	0.029
E (45-56)	0.993	0.930	0.064	0.036	12	12	0.063	0.041

Table 5.8   Inner and outer wheelpath asphalt d0 values.

Segment (Station)	Average (mm)		Standard Deviation (mm)		No. of Samples		Difference Statistics (mm)	
	Inner	Outer	Inner	Outer	Inner	Outer	Average	Standard Deviation
A (0-11)	0.624	0.648	0.050	0.065	11	11	−0.025	0.121
B (11-22)	0.759	0.796	0.061	0.043	11	11	−0.037	0.184
C (23-34)	0.810	0.866	0.036	0.022	11	11	−0.056	0.106
D (34-44)	0.757	0.828	0.034	0.050	10	10	−0.072	0.142
E (45-56)	0.795	0.815	0.090	0.042	12	12	−0.020	0.134

5.4   Construction Summary

The five test pavements constructed comprised of three different basecourse materials, all three basecourses were placed in thick highway strength pavements (275 mm) and the two higher quality materials were placed in thinner pavements (225 mm). The two high quality materials are a 20-mm maximum sized Australian rhyolite–rhyodacite, acid igneous crushed rock, and a 40-mm maximum sized New Zealand crushed alluvial greywacke gravel. The lower quality material was a 40 mm maximum sized New Zealand uncrushed alluvial greywacke gravel. During construction, the existing Waikari clay subgrade was excavated to a depth of 300 mm, ripped a further 150 mm and re-laid, the basecourse was laid in two layers and Asphaltic Concrete surface was laid by paver. The FWD testing infers that the subgrade has an average in situ CBR of 9.5 % and the basecourse thickness was constructed close to the nominal thicknesses of 225 and 275 mm.

Together with accurate profiles of the pavement layers, a series of tests (Nuclear Density / Moisture Gauge and FWD) were conducted to monitor the test pavements. The FWD tests demonstrate that the inner wheelpath is not statistically stronger than the outer wheelpath. It can be concluded that the pavement has been satisfactorily constructed for the purpose of the research.

6. Vehicle configuration

6.1 Changes in suspension

Running one vehicle at 60 kN for sustained periods required some modifications to SLAVE as larger tyres are required to safely carry the load. At the request of ARRB[2] the suspension for the project in the proposed brief was also altered from 3-leaf parabolic springs to air bags. This required changing the suspension on SLAVE to the air bag system and the reconditioning, modification and adjustment of the shock absorbers to allow use of the air bags at 60 kN.

Bridgestone M840 TCOT (295/80R22.5) tyres had been fitted to allow SLAVE to run safely at 60 kN. These tyres were slightly larger than the Bridgestone M711 11R22.5 tyres normally used at CAPTIF. This required new rims and modification to the SLAVE's chassis to gain the required clearances to the link arms.

The airbag suspension used at CAPTIF was set up for 50 kN loading during the OECD DIVINE project. At that time the valves available for the shock absorbers could only just provide sufficient damping to meet the EC requirements for road friendly suspension. However in the intervening years improvements have been made to the design of shock absorber valves. The existing shock absorbers were removed and new valves installed to increase the amount of damping available. The shock absorbers were tested and then fitted to the suspension.

Finally the suspension as a whole was tested using the EC drop test (Council of the European Communities 1992). The drop test is used in the EC regulations for rating a suspension as road friendly. This test involves running the vehicle at creep speed over a ramp that culminates in an 80-mm drop and measuring the suspension response. Figure 6.1 shows the response of the vehicles to the drop test, and the vehicle parameters and suspension parameters are given in Table 6.1. These values comply with the EC definition of pavement-friendly suspension (natural frequency less than 2Hz and a minimum damping of 20%).

Table 6.1   Suspension parameters from EU drop test.

Vehicle	Vehicle Mass (kN)	Tyre Pressure (kPa)	Natural Frequency (Hz)	Damping (%)
A	60	800	1.5	20
B	40	800	1.6	25

---

[2]   ARRB – ARRB Transport Research Ltd, Vermont South, Victoria, Australia.
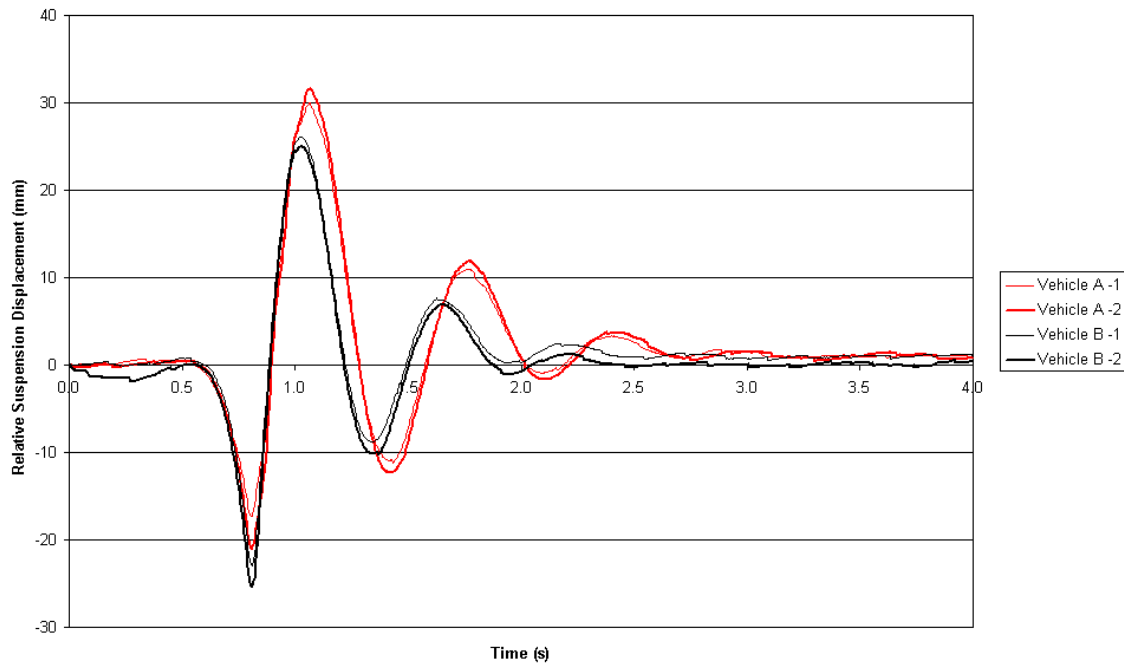
Figure 6.1   Slave response to the 80 mm EC Drop Test.

The pavement was conditioned with 5000 laps of 40 kN loading applied with a uniform loading distribution across the pavement.

6.2   Dynamic load coefficients

At every measurement interval the dynamic wheel forces were measured for both vehicles operating in the test wheelpaths at the test speed of 45 km/h. These dynamic wheel forces measured over the whole track were converted to Dynamic Load Coefficient (DLC) value for each vehicle. The DLC is the standard deviation of the wheel forces divided by the mean. Typically as the pavement roughness increases the DLC of the vehicles increases. In previous tests at CAPTIF (de Pont et al. 1999), DLC has proven to be a clearer indicator of increasing roughness than longitudinal profile measures such as IRI.

To allow dynamic load coefficients to be determined, wheel force profiles were taken on the conditioned surface in the inner and outer wheelpaths. The wheel force profiles are shown in Figures 6.2 and 6.3, while Figure 6.4 shows the change in DLC with increasing load cycles.
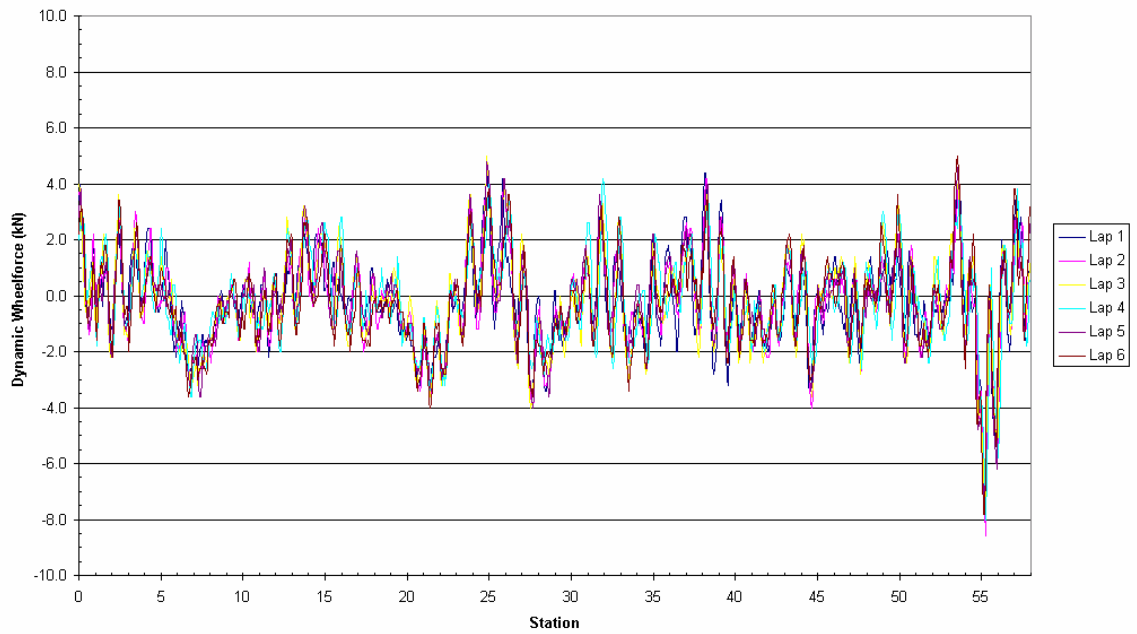
Figure 6.2   Vehicle A (60 kN) and its dynamic wheel force on inner wheelpath (for 6 laps).
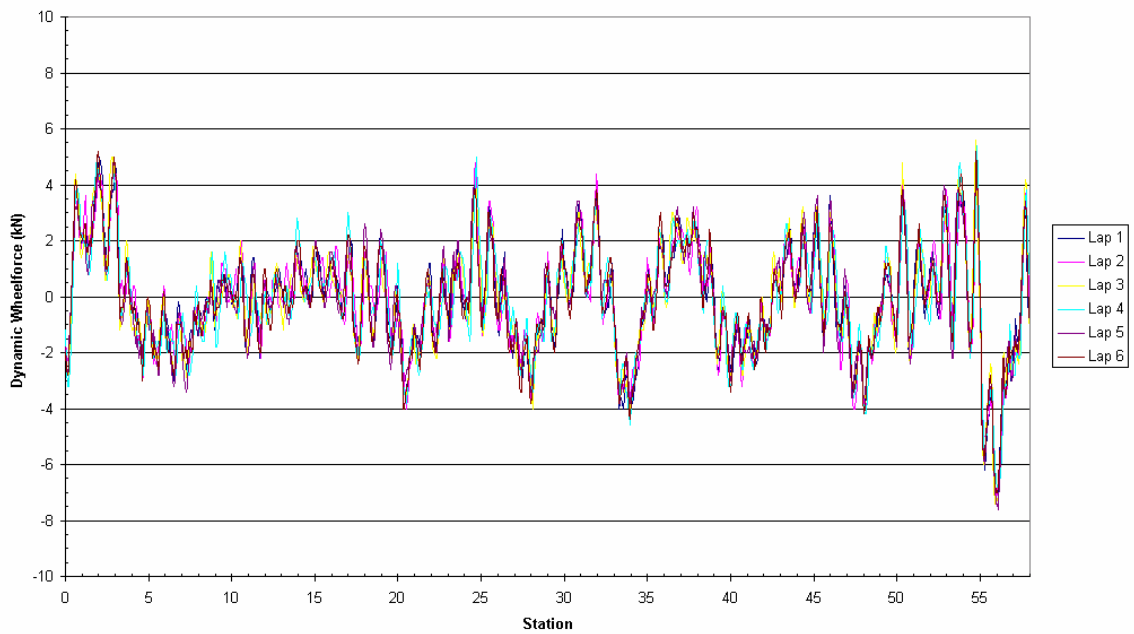
Figure 6.3   Vehicle B (40 kN) and its dynamic wheel force on outer wheelpath (for 6 laps).
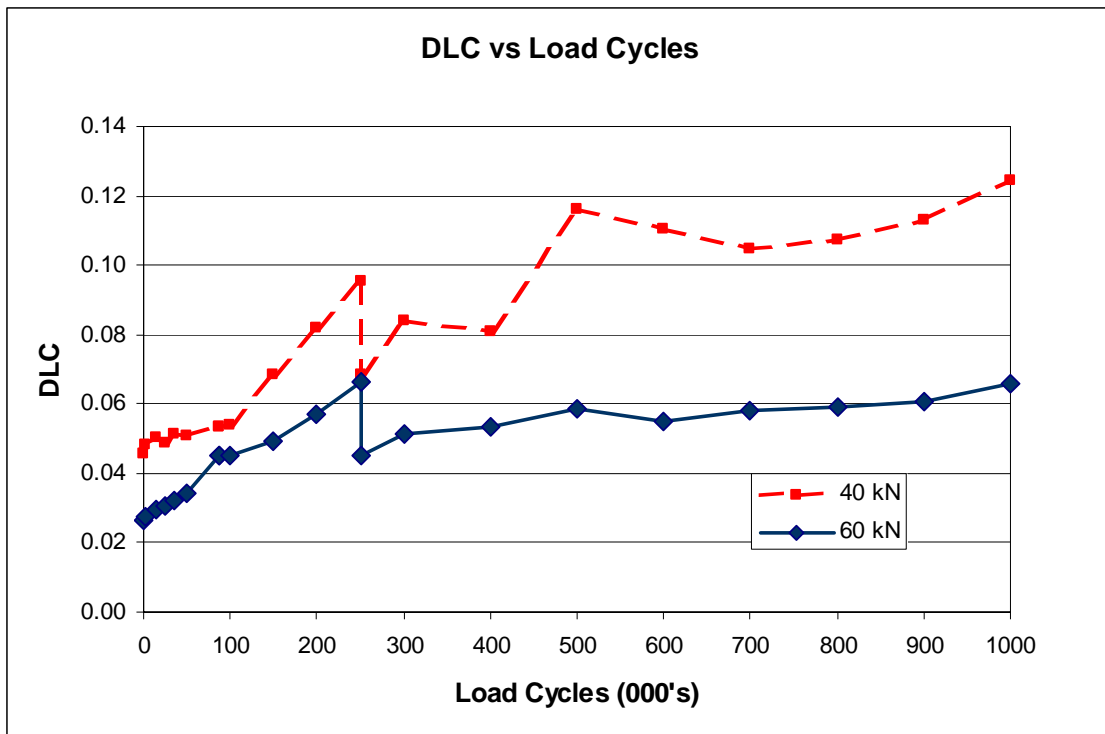
Figure 6.4   Change in DLC with increasing load cycles.

The starting point for the DLC values for each vehicle is different but the rate of change in DLC appears similar. The sudden drop in DLC values is the result of localised repairs to the pavement.

7.   Strain and stress measurements

7.1   Strain measurements

At each measurement interval strain profiles were measured in the instrumented segments (Sections A, B, C and D). A number of points are worthy of note in Figure 7.1. They include:

- As expected the strain under the 60 kN load was highest in all sections.

- The strain measured in the upper subgrade of Section B was higher than Section A; however they performed in a similar manner.

- The strain in the upper subgrade of Section C appears to be lower than the strain in Section D: this is a reversal of what was expected when considering the deflection data from construction. However they performed in a similar manner.

- If the measured strains were to be compared with existing Subgrade Strain Criteria, significantly different performances would have been expected from each section.
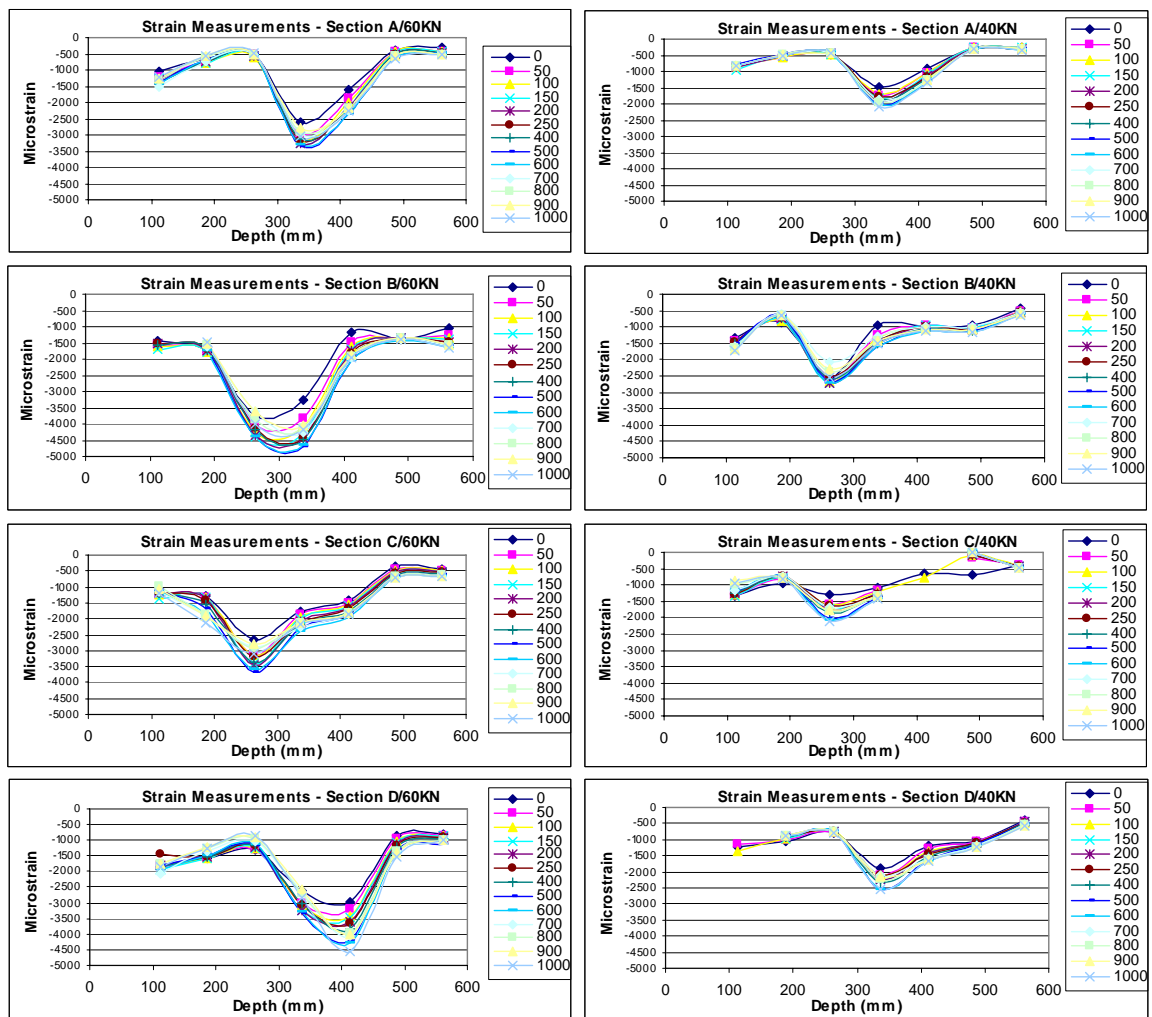
Figure 7.1   Vertical Strain profiles for 60 kN and 40 kN, in Segments A, B, C, D, with increasing depth (from 0–600 mm), for 0 to 1,000,000 load cycles.

37

Figure 7.2 shows the relative increase in strain observed during the project. There appears to be a general strain softening of the subgrade (recorded on gauges below 300 mm in Segments A and D and below 225 mm in Segments B and C), and a hardening of the basecourses.
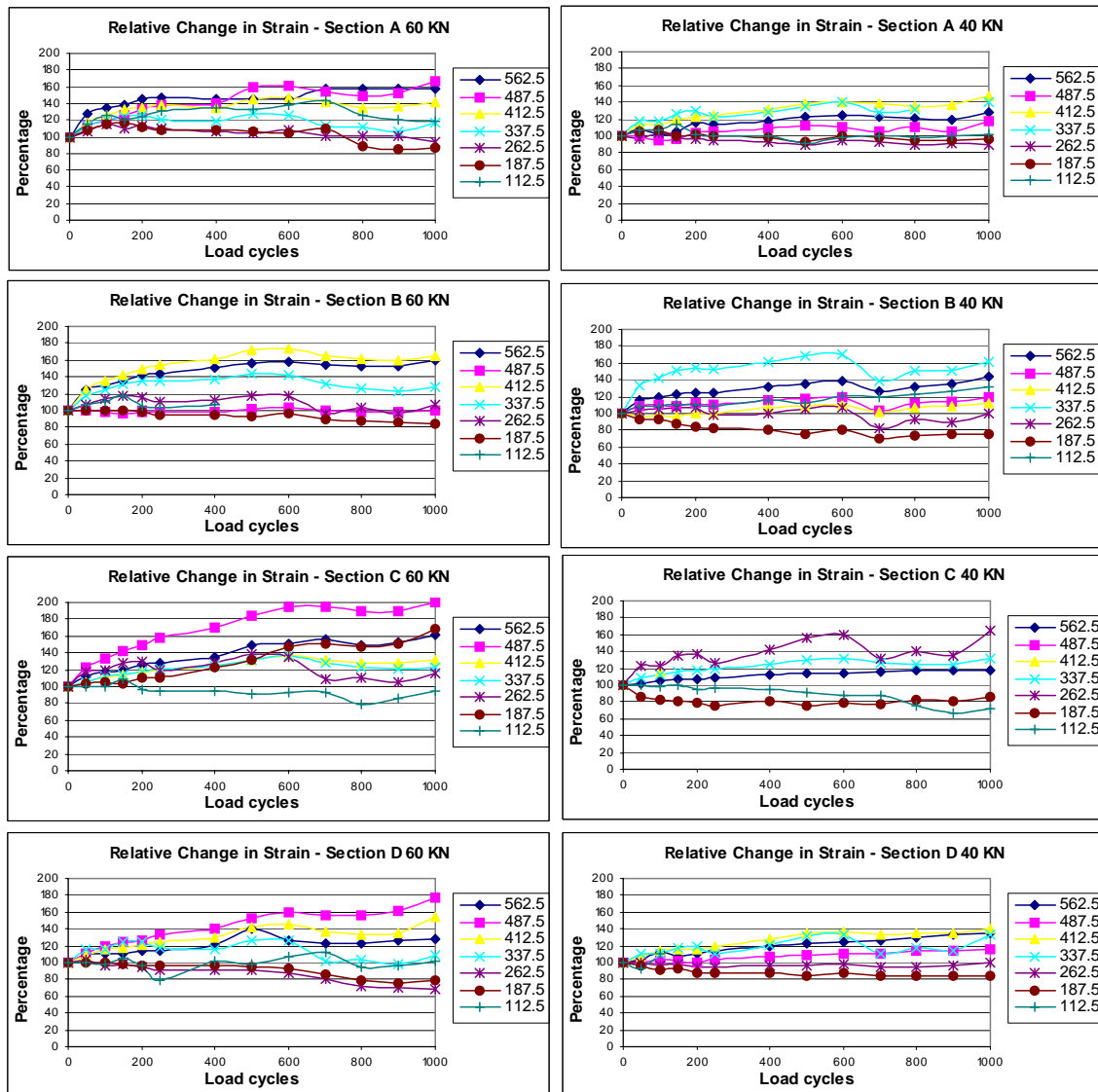
Figure 7.2   Relative increase (%) in vertical strain, for 0 to 1,000,000 load cycles, for Segments A, B, C, D, with increasing depths (mm) in subgrade and basecourse.

An investigation was also made into the feasibility of measuring strains in the upper 75 mm of the pavement. This area has not traditionally been measured due to the metal in tyres and vehicles influencing the measurements. A fixed coil pair (i.e. a pair made of a solid piece of rod) was installed in the pavement to measure influence of the tyre and vehicle. Figure 7.3 shows this influence plotted against the strain profile measured for a floating surface pair. The figure suggests that the influence of the vehicle is insignificant when measuring the peak vertical strain and the bulk of the influence is probably due to the loading plates that sit either end of the tyre. Measurement of strain in the upper 75 mm of the pavement is therefore possible but unacceptable reproducibility was

obtained when making repeat measurements of the floating surface pairs. The cause of the lack of reproducibility is currently being investigated.
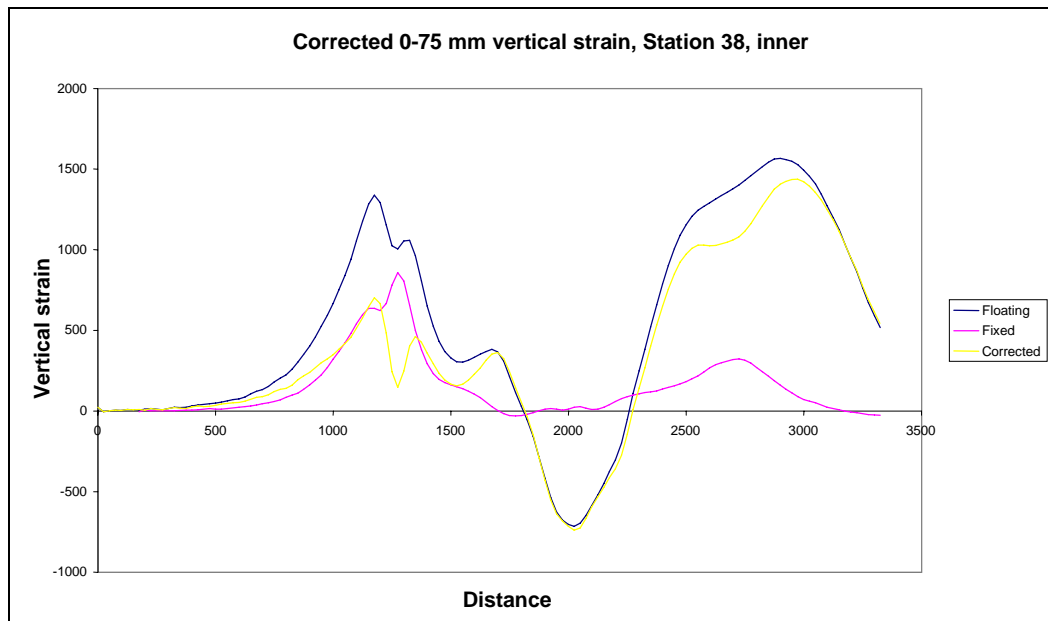
Figure 7.3   Vertical strain at the pavement surface, as the wheel passes over Segment D.

7.2   Stress measurements

At each measurement interval stress profiles with depth were measured in Segment A (Figure 7.4) and the vertical stress at the subgrade–basecourse interface was measured in Segments B, C and D.
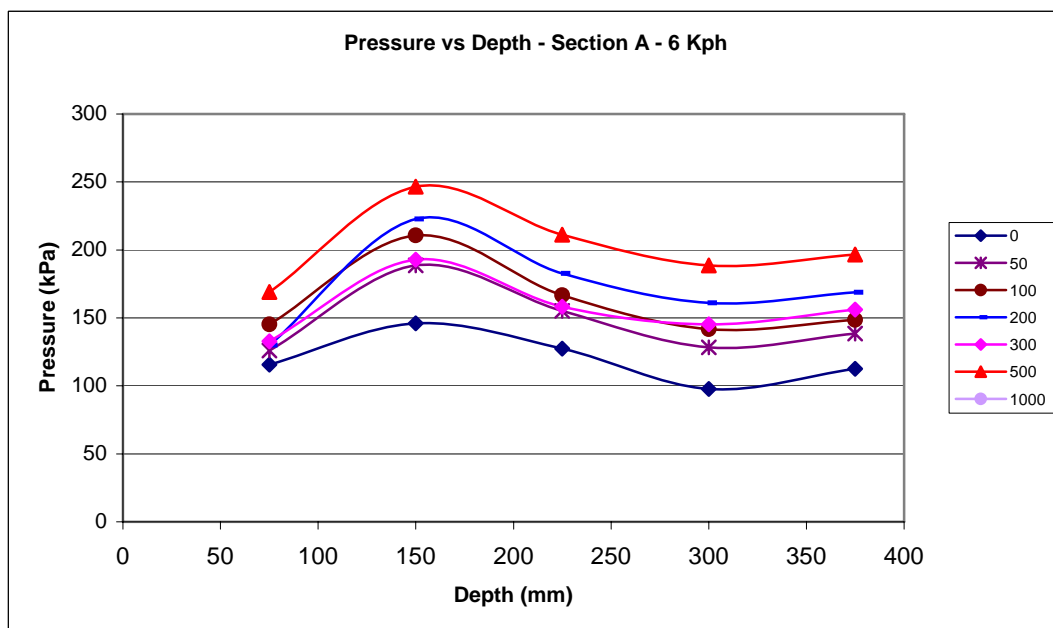
Figure 7.4   Vertical stress profile (in kPa) with increasing depths (to 375 mm), with increasing load cycles (from 0 to 1,000,000), for Segment A.
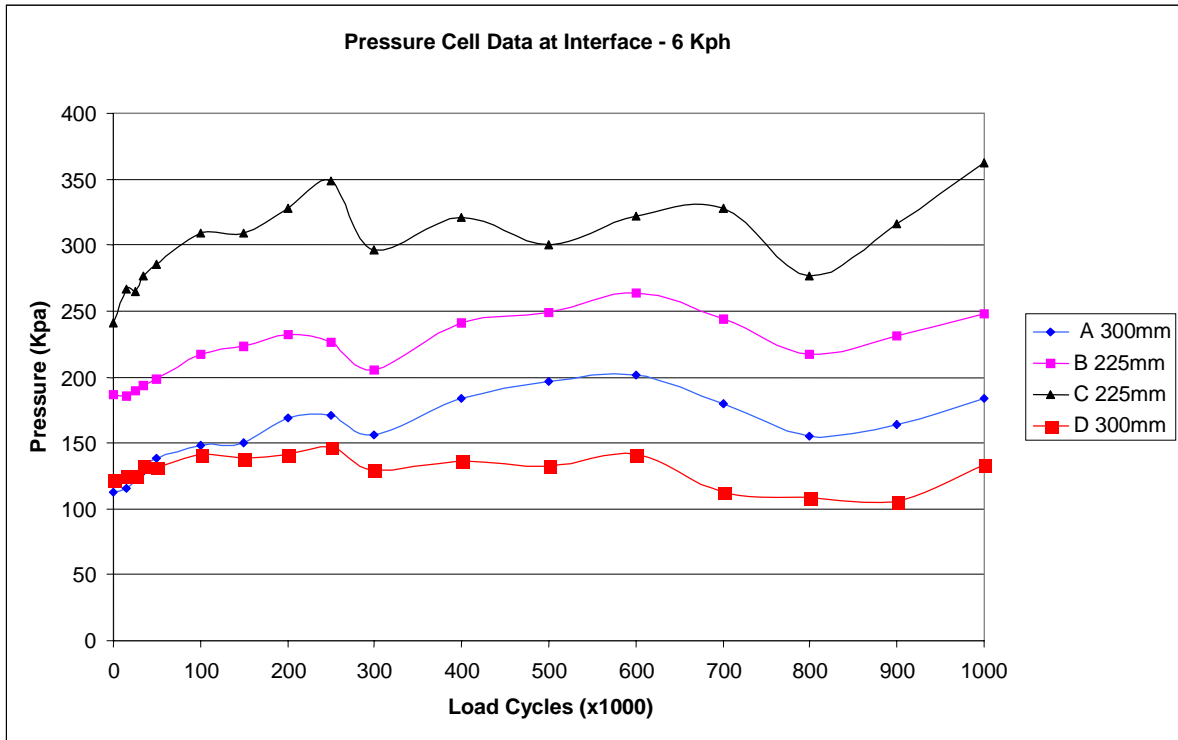
Figure 7.5   Change in vertical stress (in kPa) with increasing load cycles (from 0 to 1,000,000), at the subgrade–basecourse interfaces (at depths in mm), for Segments A, B, C, D.
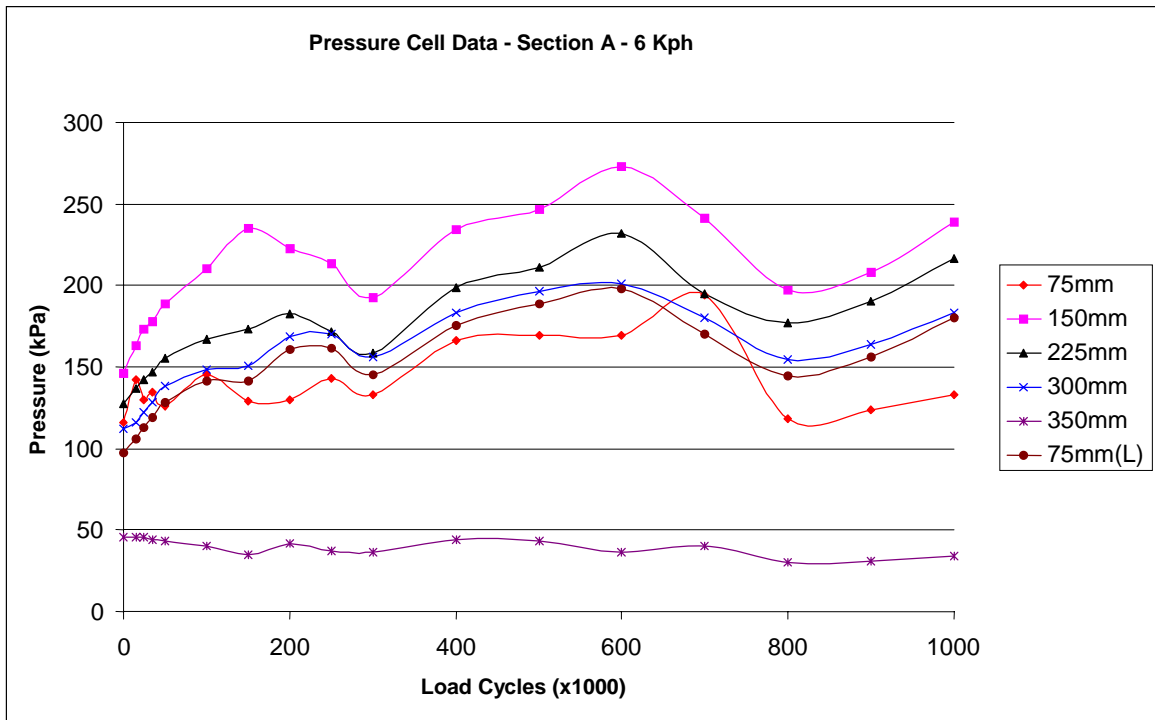
Figure 7.6   Change in vertical stress (in kPa) with increasing load cycles (from 0 to 1,000,000), at different depths (mm), for Segment A.

The stress measurements in Figure 7.4 were very repeatable. However the variation in stress with load cycles shown in Figures 7.5 and 7.6 is difficult to explain. The consistent variation across measurements at each load cycle suggests a measurement error. Transverse measurements of stress were examined to determine if the error was related to positioning of the vehicles, but if this were the case the stresses measured lower in the pavement would have been relatively unaffected, as can be seen in Figure 7.7.
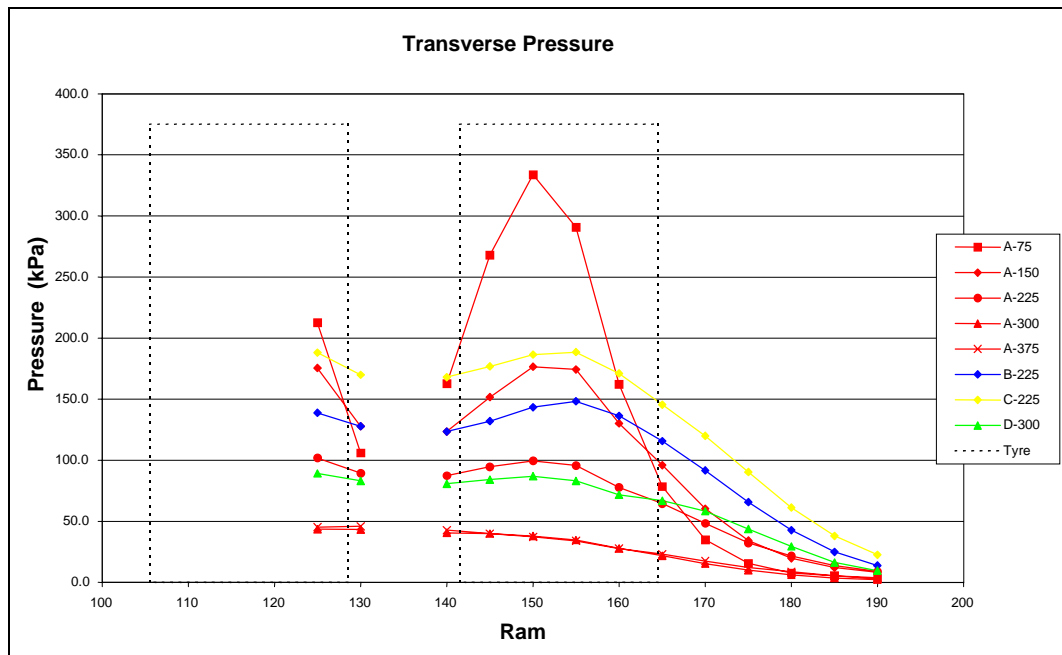
Figure 7.7   Transverse vertical stress distributions for Segments A, B, C and D, at different depths (in mm).

8. Vertical surface deformations and rutting

Vertical Surface Deformation (VSD) is the maximum vertical difference between the measured transverse profile and the original (before trafficking). At each measurement interval the transverse profile of the pavement was recorded at each station. From these measurements, the permanent vertical surface deformation (VSD) was calculated. VSD has proved in past CAPTIF tests (de Pont et al. 1999) to be a fundamental measure of pavement wear which provides useful insights into the pavement performance and behaviour. Both rutting and surface roughness are related to VSD. Rutting is directly related to VSD while roughness is related to the variation in VSD from station to station. VSD has been correlated to both dynamic wheel forces and the variability in pavement structure (de Pont et al. 1999), thus increasing VSD leads to increased roughness. With the transverse profiler at CAPTIF VSD can be measured to a good degree of accuracy and reliability because the measurements are all referenced back to the edges of the concrete tank which are very stable.

Measurements of rutting and roughness do not have the same level of reliability (de Pont et al. 1999). Rutting is determined by calculating or measuring the depth of the rut from a straight edge laid across the wheelpath. Thus the rut depth depends not only on the VSD in the centre of the wheelpath but also that of the highest tangential points inside and outside the wheelpath. The centre point height is influenced by both wheel loads. Roughness is usually given in International Roughness Index (IRI) values, which are calculated from the longitudinal profile using the response of the simulated quarter car.

The dynamic characteristics of the quarter car are such that it responds to surface profile characteristics with wavelengths from 1 m to 30 m (Sayers et al. 1986). To accurately sample the longer wavelength components in this range, it is normally recommended that the section length for IRI calculation is greater than 100 m. As the track at CAPTIF is only 58 m long it does not meet this requirement.

Figure 9.1 shows the progression of VSD for each of the wheelpaths in each pavement segment. Note that Section E, where the lower quality aggregate (Material C) was used, failed early and was consequently replaced with 150 mm of asphalt. The VSD values for Section E after the repair were therefore not considered in the analysis.

9.   Fitting a power law

For all five pavement sections the VSD is greater on the inner wheelpath trafficked with the higher load (60 kN), than on the outer path (40 kN). The conventional approach to comparing the wear generated by two different axle loads is the power law method. This states that the amount of pavement wear caused by one pass of an axle is proportional to some power of its axle load. The most widely used value for this power is four. Thus if a given level of wear is achieved by N_{inner} load cycles of a load P_{inner} or by N_{outer} load cycles of a load P_{outer}, these are related as follows:

Equation 9.1

$$\frac{N_{outer}}{N_{inner}} = \left[\frac{P_{inner}}{P_{outer}}\right]^{n}$$

where   n is the exponent of the power law

For every measured value of VSD and load cycles on the outer wheelpath, the number of load cycles on the inner wheelpath to generate the same VSD can be calculated by interpolation. Alternatively, the number of load cycles on the outer wheelpath that are needed to generate the measured VSDs in the inner wheelpath can be calculated.

In either case, as P_{inner} and P_{outer} are known, the value of the exponent n required to get the power law relationship to hold can be calculated for each VSD value.

Whether the inner or outer wheelpath VSD measurements are used as the reference makes relatively little difference to the results. The results shown (Figure 9.1) are the average of the two methods. For accurate interpolation a smooth curve was fitted through the VSD data, which also reduced the scatter in calculated power laws that are sensitive to the inputs used. These curves are power functions and, with the exception of Segment E that failed early, were found to fit the data fairly well, with the mean difference between measured and calculated mean error ranging from 0.2 to 0.5 mm. However, these exponential functions may not be suitable for extrapolation as it can also be shown that VSD increases linearly with wheel passes after an initial compaction period.

The exponent n in the general power law relationship (Equation 9.1) varied depending on the value of VSD chosen. Results are shown in Figure 9.2 and show a common trend of increasing exponent n with increasing VSD value. Another way of representing the results is to plot the exponent value n, with number of passes of a 60 kN load (Figure 9.3). This may become useful in design to determine the number of ESAs (40 kN) where the number of passes of a 60 kN axle are known. Exponent values ranged from 2 to 4.5 for all the Segments except E. For Segment E, values as high as 6 were calculated during the test but the rapid failure of both inner and outer paths lead to a final exponent of only 2.6. The scale used to plot results was determined to ensure clear differences between Segments A, B, C and D and this often meant the results of Segment E were excluded.
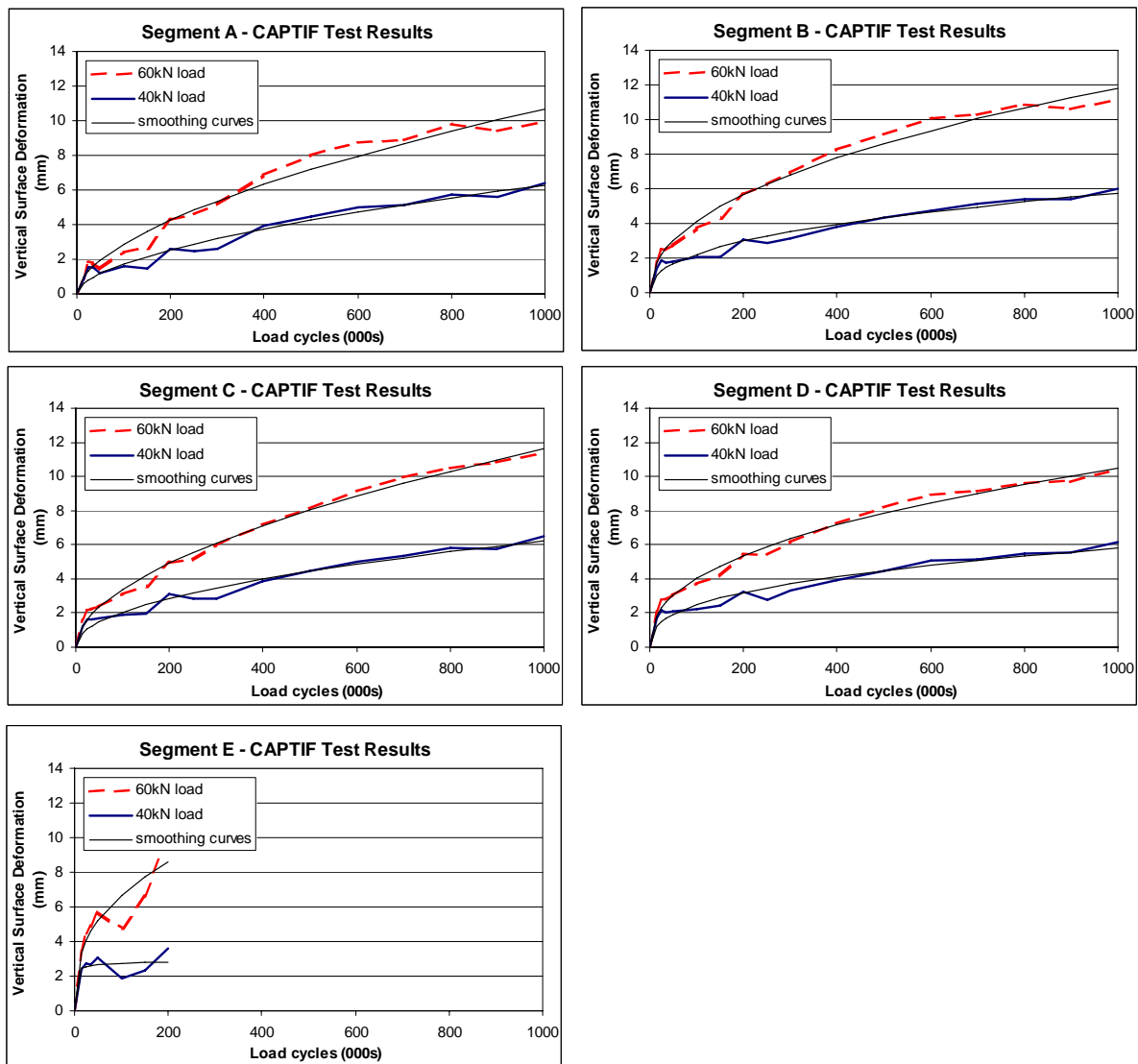
Figure 9.1   CAPTIF VSD (vertical surface deformation) test results with smoothing curves fitted for each pavement segment.

In the first stage of this research VSD versus load passes for 50 kN and 40 kN loads were compared. The power exponents determined in this research varied substantially between each pavement segment where the only difference was the aggregate used. For comparison with results obtained in Stage 3, data from Stage 1 was re-visited to produce charts showing how the exponent changes depending on the value of VSD and number of passes of the 60 kN load. Figures 9.4 and 9.5 show the results.

Power law exponent, *n*, cf VSD

$$\frac{N_{40\,kN}}{N_{60\,kN}} = \left[\frac{60\,kN}{40\,kN}\right]^{n}$$

- — — Segment B
- ⋯⋯ Segment D
- ·—·— Segment C
- ——— Segment A

Vertical surface deformation, VSD, (mm)
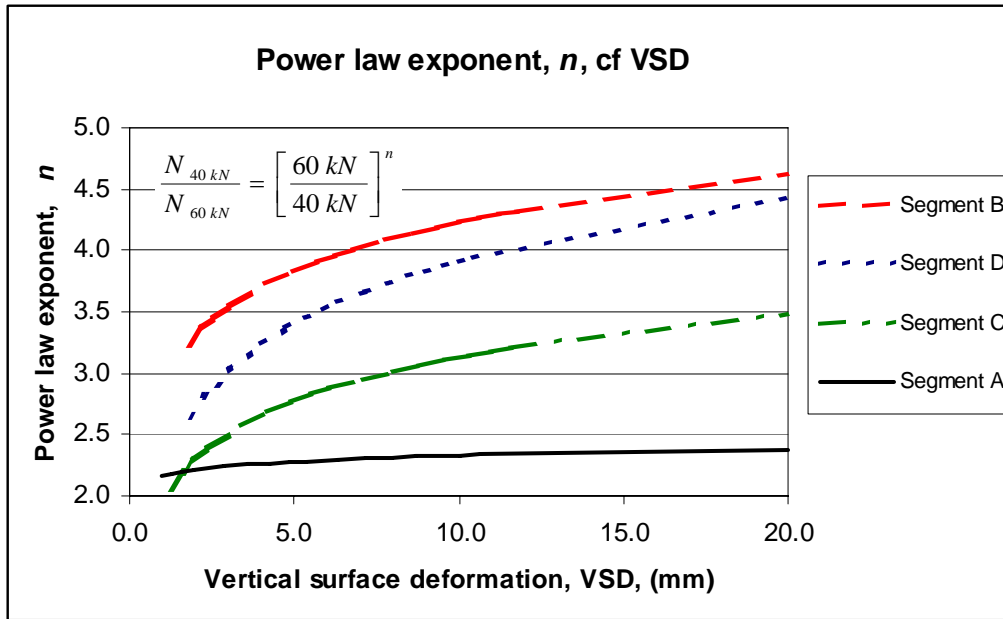
Figure 9.2   Power law exponent*, n,* determined for a range of vertical surface deformation values.

Power law exponent, *n*, cf passes of 60kN load

$$\frac{N_{40\,kN}}{N_{60\,kN}} = \left[\frac{60\,kN}{40\,kN}\right]^{n}$$

- ─ ─ Segment E
- — — Segment B
- ⋯⋯ Segment D
- ·—·— Segment C
- ——— Segment A

Passes of 60kN load (N_{60kN} 000s)
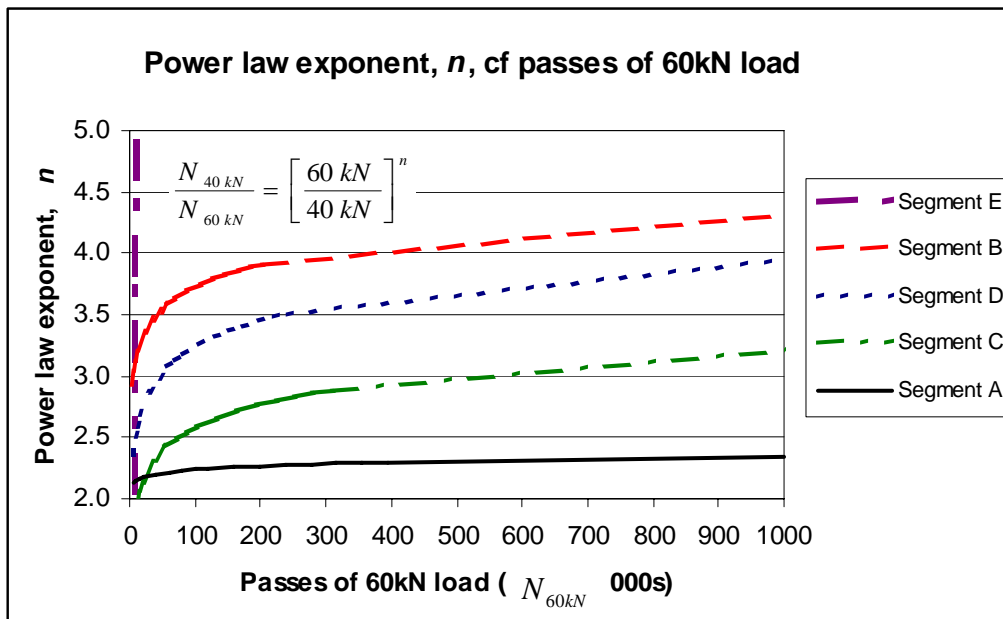
Figure 9.3   Power law exponent, *n*, determined for a range of number of passes of a 60 kN load.
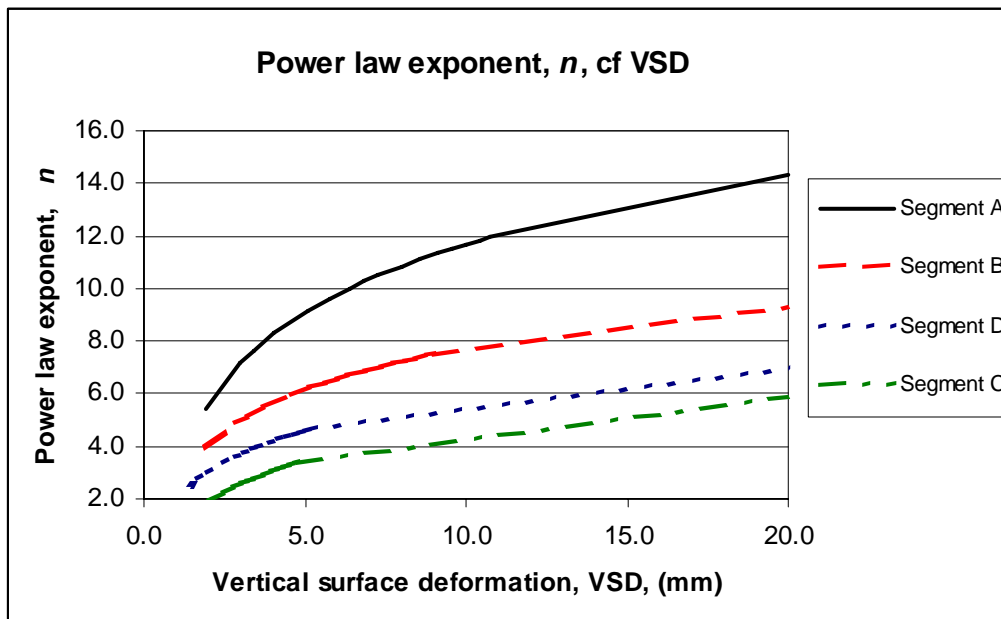
Figure 9.4   Power law exponent, *n*, determined for a range of vertical surface deformation values, from Stage 1 test results, comparing 50 kN with 40 kN axle loads.
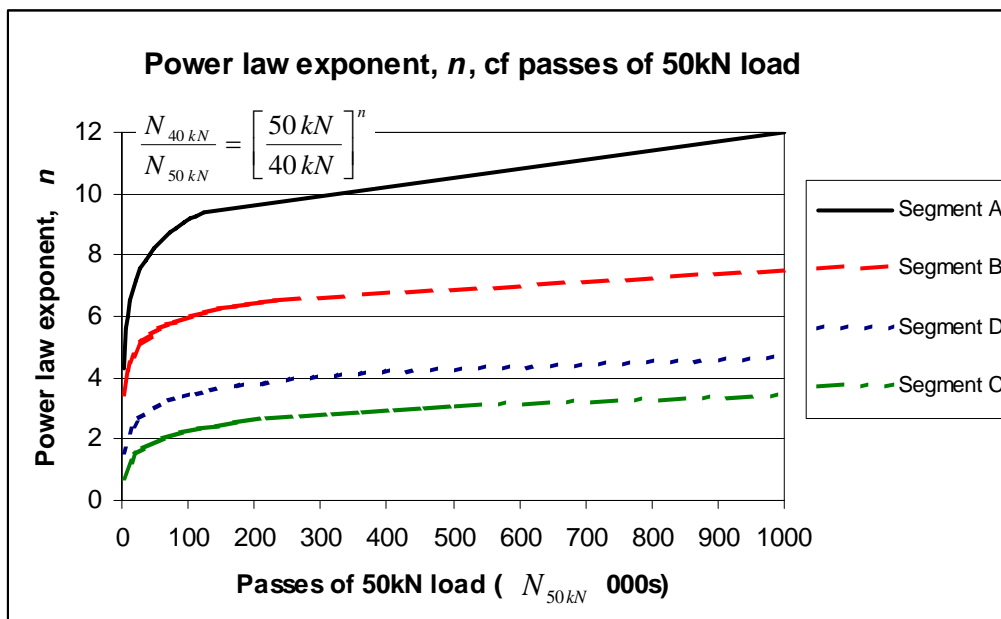
Figure 9.5   Power law exponent, *n,* determined for a range of number of passes of a 50 kN load.
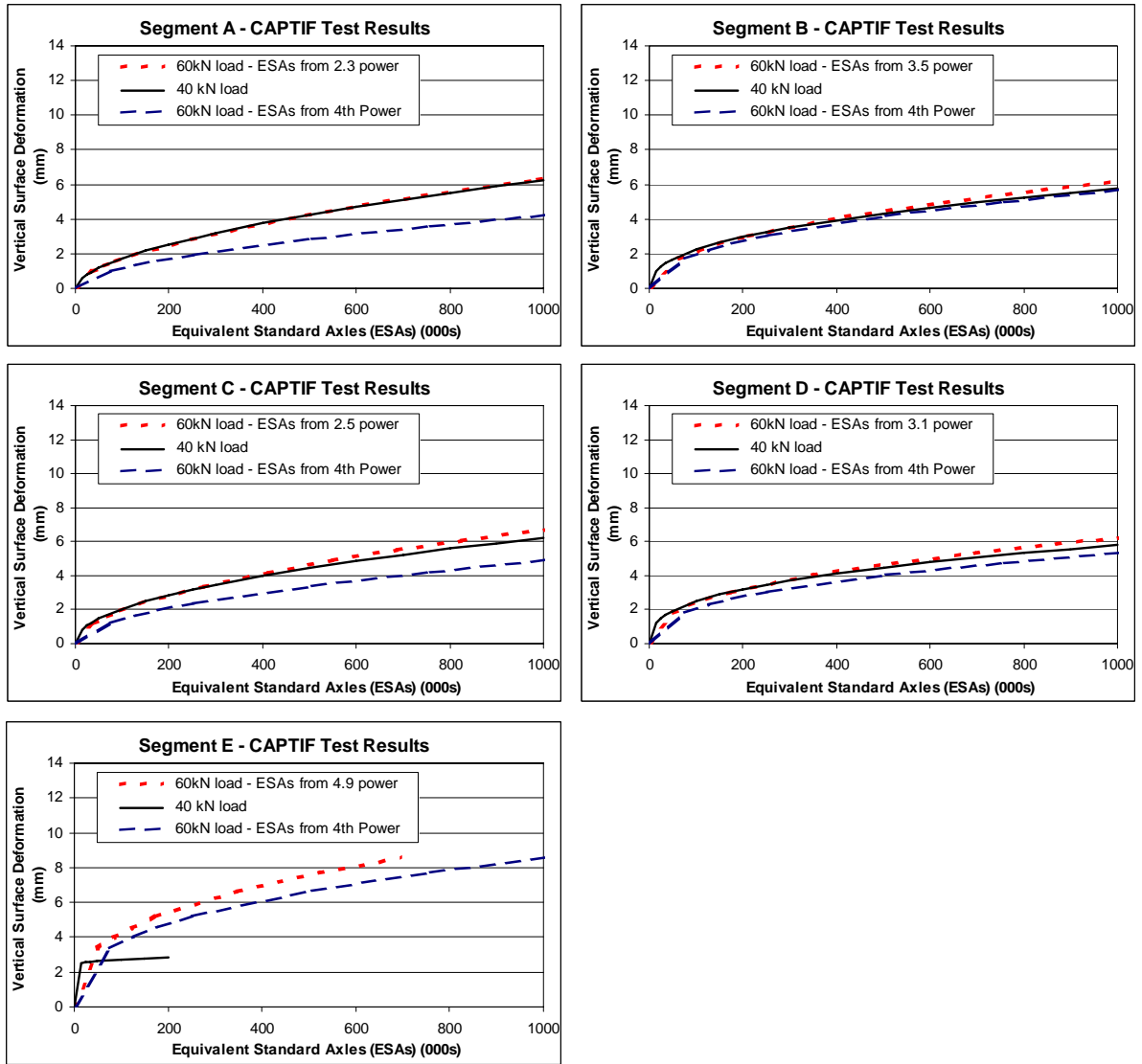
Figure 9.6   Vertical surface deformation (VSD) versus Equivalent Standard Axles (ESAs) calculated using a fourth power exponent and the best-fit power exponent.

The results show that no single exponent value can be used in Equation 9.1 to determine the number of ESAs (i.e. 40 kN axle) for a known number of passes with the 60 kN axle or the 50 kN axle. This result is not surprising as the measured VSD with load passes are not linear for at least the first 200,000 load passes. The fourth power law used in pavement design and road user charges was derived by comparing the number of passes of various loads to reach a terminal or end-of-life condition in the pavement, and not the path to get there. This end-of-pavement-life approach if applied to the CAPTIF dataset would result in the power law exponent values *n* shown in Figure 9.2 for a VSD of 20 mm (i.e. terminal condition). These exponent values still change with pavement type and this influence should be investigated further.

Another approach is to use a best fit exponent *n*, and apply this value in Equation 9.1 to convert the 60 kN load passes to number of ESAs (i.e. 40 kN load). For each pavement segment, ESAs are then plotted versus VSD for both the 40 kN and 60 kN loads. The exponent *n* that gave the best fit for matching the 60 kN and 40 kN VSD data can then be

considered as the appropriate exponent (Figure 9.6) for any number of load cycles. For comparison, the fit obtained with using a fourth power relationship has been shown in the same plots.

Using an appropriate exponent to calculate ESAs for each pavement segment appears to give a reasonable fit to the measured data. Apart from Segment B it is clear that a fourth power is inaccurate. The exponents range from 2.3 to 3.5 (excluding Segment E that failed early) for the pavement tests comparing 60 kN to 40 kN. Using this method the Stage 1 research for tests comparing 50 kN to 40 kN loads found exponent values ranging from 3 to 9 (de Pont et al. 2001).

10.   Deformation modelling

Another method of analysing the VSD results is to fit equations that can be used for predicting pavement deformation for known load cycles, pavement type, and wheel load. These equations can then be used to estimate the additional damage to the road caused by a change in mass limits. Various models, both linear and power, are fitted to the individual VSD results and as a whole. Fitting the models to all the VSD data will reduce the goodness of fit to the individual VSD results. However, the accuracy is still sufficient to enable a single equation to be used for predicting deformation for a range of pavement types. Appendix C shows the use of these equations to predict the rehabilitation requirements for a simple imaginary network to give an example of their possible application.

10.1   Compaction–Wear model

Previous research at CAPTIF in Stage 1 showed a range in power law exponents from 3 to 9. This large variation in exponents was considered to be related to the initial non-linear compaction that occurs, and that this behaviour is influenced by construction and aggregate type. This led to the compaction–wear model that separated the two stages of behaviour. A straight line is fitted to the linear part of the VSD results say after 100,000 cycles. The slope of the line represents the wear rate and the intercept represents the VSD due to compaction. The power law approach can then be used to compare both the intercept and the slope of these lines between the two wheel loads in the outer and inner wheelpath for each segment.

Tables 10.1 and 10.2 show the results of a least squares regression straight line fit to the linear portions of the VSD v load cycles curves for each of the five segments in both wheelpaths. As can be seen from the mean error, these are very good fits and similar to the results found in Stage 1 (de Pont et al. 2001).

Table 10.1   Linear fit parameters for VSD v load cycles on outer wheelpath with 40kN load.

Segment	Intercept–Compaction (mm)	Slope–Wear rate (mm/1000 load cycles)	Mean Error (mm)
A	1.26	0.00542	0.33
B	1.87	0.00433	0.24
C	1.63	0.00504	0.26
D	2.04	0.00429	0.23
E*	0.04	0.01711	0.17

*   Segment E failed before 250,000 load passes (straight line fitted to points from 100,000 to 200,000 only).

Table 10.2   Linear fit parameters for VSD v load cycles on inner wheelpath with 0 kN load.

Segment	Intercept–Compaction (mm)	Slope–Wear rate (mm/1000 load cycles)	Mean Error (mm)
A	2.50	0.00861	0.69
B	4.07	0.00821	0.69
C	2.89	0.00933	0.46
D	3.77	0.00727	0.47
E*	−1.10	0.05560	0.42

*   Segment E failed before 250,000 load passes (straight line fitted to points from 100,000 to 200,000 only).

A power law function can be applied to the compaction and wear components independently. This approach implies relationships of the form:

$$\frac{Intercept\ _{60kN}}{Intercept\ _{40kN}} = \frac{Compaction\ _{60kN}}{Compaction\ _{40kN}} = \left(\frac{Axle\ load\ _{60kN}}{Axle\ load\ _{40kN}}\right)^{a} \qquad \text{Equation 10.1}$$

$$\frac{Slope\ _{60kN}}{Slope\ _{40kN}} = \frac{Wear\ _{60kN}}{Wear\ _{40kN}} = \left(\frac{Axle\ load\ _{60kN}}{Axle\ load\ _{40kN}}\right)^{b} \qquad \text{Equation 10.2}$$

where:

a and b are the exponent values

By taking logarithms, the values of a and b can be calculated for compaction and wear for each of the pavement segments. The results for the exponent values are shown in Table 10.3. It is interesting to note how similar the exponents are for the two components of VSD. The exponents for the different segments, while still not identical, are much more alike than they were in the general power law model, particularly if Segment E is discounted. Segment E failed before 250,000 cycles and, although the results are reported for Segment E, they are not considered when determining overall trends in the results. For comparison the results of exponents calculated for the compaction and wear components in Stage 1 are reported in Table 10.4.

Table 10.3   Exponent values relating compaction and wear between the 40 kN and 60 kN wheelpaths.

Segment	Intercept–Compaction	Slope–Wear rate
A	1.70	1.14
B	1.91	1.58
C	1.41	1.52
D	1.52	1.30
E	–	2.91

Table 10.4   Exponent values relating compaction and wear between the 40 kN and 50 kN wheelpaths from Stage 1 (Table 4.8 in de Pont et al. 2001).

Segment (Stage 1)	Intercept–Compaction	Slope–Wear rate
A	3.40	3.04
B	2.13	1.94
C	0.79	0.99
D	1.06	1.77

This model implies that the compaction is dependent only on the applied wheel load and not on the number of applications of this load (although a number of applications of the load are required to effect the compaction). The wear component is related to both the load and the number of load cycles. A logical extension to this model is that, if after some large number of load cycles the wheel load is increased, the additional compaction associated with the higher wheel load would then take place, as well as the higher rate of wear associated with a higher wheel load. The conventional power law approach does not predict an additional compaction with an increase in wheel load, but it does predict a higher wear rate.

This Compaction–Wear model was expanded in Stage 2 to enable one set of coefficients to cover all pavement segments. This then allows a Compaction–Wear model to be determined based on pavement type only.

The basic form of the Compaction–Wear model is:

$$VSD = C + W \cdot N \qquad \qquad \text{Equation 10.3}$$

where: C is the compaction
           W is the wear rate
           N is the number of applied load cycles

Both C and W were shown to be proportional to a similar power of the applied load, thus the same exponent will be used and then a constant is needed to take account of the differences in the pavement. The full proposed model then can be written as:

$$VSD = K.\left(\frac{P}{40kN}\right)^{a}(C + W.N) \qquad \qquad \text{Equation 10.4}$$

where K is a constant reflecting the differences in VSD propensity
           between the pavement segments
        P is the applied load (kN)
        a is the exponent of the power law for the effect of mass

By comparing the VSD between the 60 kN and 40 kN load wheelpaths, the best fit value for *a* can be determined. Because the compaction–wear model focuses on fitting the linear section of the VSD against the load cycles curve, only the data between 100,000 load cycles and 1,000,000 load cycles were used for estimating *a*. The best-fit value averaging across all four pavement segments (Segment E excluded) is 1.49. The *K* value represents the relative propensity of the different pavement segments to undergo VSD.

It is not possible to determine absolute values of K but, if one of the pavement segments is set as the reference with a K value of unity, the relative K values for the other segments can be determined. Least squares linear regression can then be used to calculate C and W. The results are summarised in Table 10.5.

Table 10.5   Coefficients of a single best-fit Compaction–Wear model for Stage 3 results comparing 60 kN with 40 kN loads.

Segment	K	a	C (mm)	W (mm/1000)	Mean error (mm)
A	1.000	1.49	1.675	0.00431	0.61
B	1.131	1.49	1.675	0.00431	0.56
C	1.089	1.49	1.675	0.00431	0.38
D	1.054	1.49	1.675	0.00431	0.39

Only the K value is specific to the pavement segment. Figure 10.1 shows the VSD against load cycles traces that are predicted by the simple compaction–wear model compared to the measured data for both wheelpaths in all four segments. The simple compaction-wear model assumes that the compaction occurs instantaneously at the commencement of loading and therefore does not match the initial loading cycles well. Apart from this the model predicts the behaviour of all four segments very well.

To test this compaction–wear model with common coefficients further, the dataset in Stage 1 is included. This dataset includes VSD results of a 50 kN load compared with a 40 kN load. An exponent, a, of 1.82 was found by de Pont et al. (2001) for this dataset. Results of combining the data sets are shown in Table 10.6 and Figure 10.2.

Table 10.6   Coefficients of a single best-fit Compaction–wear model for Stages 3 and 1 results combined, comparing 60 kN and 50 kN loads with 40 kN load.

Segment	K	a	C (mm)	W (mm/1000)	Mean error (mm)
Stage 3 (60 kN cf 40 kN)					
A	1.000	1.59	1.803	0.00384	0.70
B	1.136	1.59	1.803	0.00384	0.49
C	1.091	1.59	1.803	0.00384	0.45
D	1.057	1.59	1.803	0.00384	0.39
Stage 1 (50 kN cf 40 kN)					
A	1.369	1.59	1.803	0.00384	0.85
B	1.247	1.59	1.803	0.00384	0.50
C	0.724	1.59	1.803	0.00384	0.41
D	0.744	1.59	1.803	0.00384	0.26
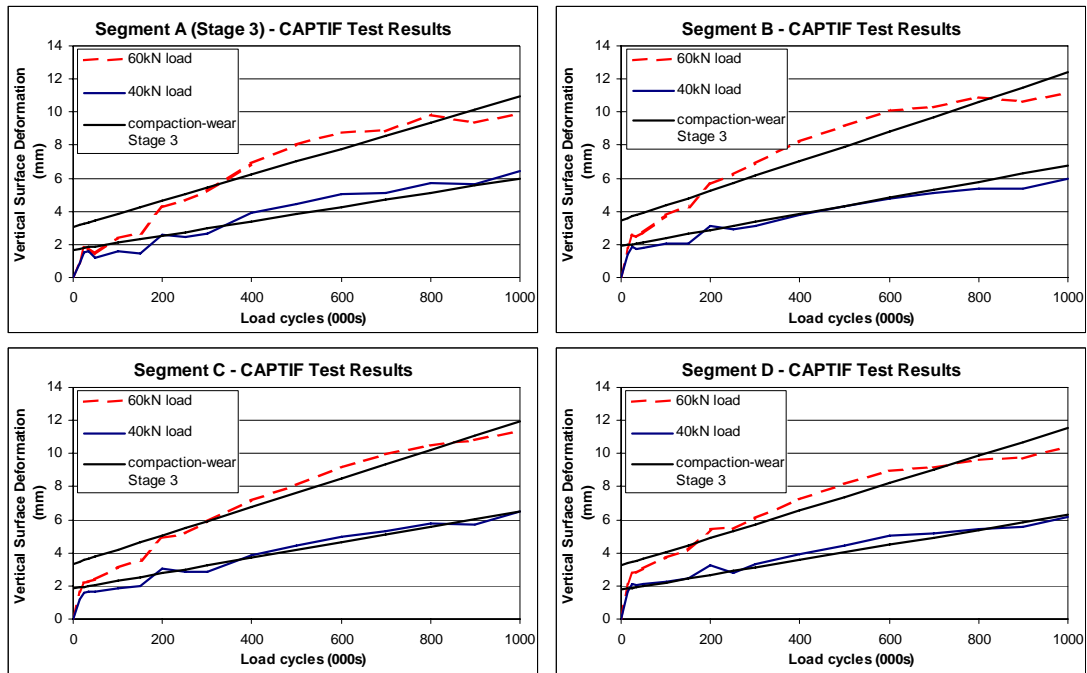
Figure 10.1 Compaction–wear model with common coefficients found with Stage 3 datasets compared with measured values.

As noted in the Stage 1 report (de Pont et al. 2001) a blending function can be used if the model is required to predict the progression of wear at the start of the pavement's life. A simple form of blending can be achieved if C in Equation 10.2 is replaced by *C.N/(N+N_0)* where N_0 is the number of load cycles needed to achieve half the total compaction. It is clear that as *N* becomes much larger than N_0, the term *N/(N+N_0)* approaches 1 and thus the model is the same as it was without the change. Figures 10.3 and 10.4 show the compaction–wear model with blending compared to the measured data where the best fit coefficients (N_0 and other constants change, Table 10.7) are used and with single common coefficients (N_0 = 50,000 load cycles and other constants the same for each pavement, Table 10.8). This simple blending function seems to give a good match to the measured data and has a straightforward physical interpretation.

Table 10.7   Best-fit coefficients of single blended compaction–wear model with Stage 3 dataset. *(K = 1.0; N_o and other constants change)*

Segment	*K*	*n*	*C* (mm)	*W* (mm/1000)	*N_0* (000s)	Mean error (mm)
A	1.0	1.31	10.778	−0.00063	628	0.37
B	1.0	1.71	2.871	0.00325	51	0.36
C	1.0	1.46	1.921	0.00479	24	0.29
D	1.0	1.37	2.425	0.00389	17	0.29

Stage 3, Segments A to D
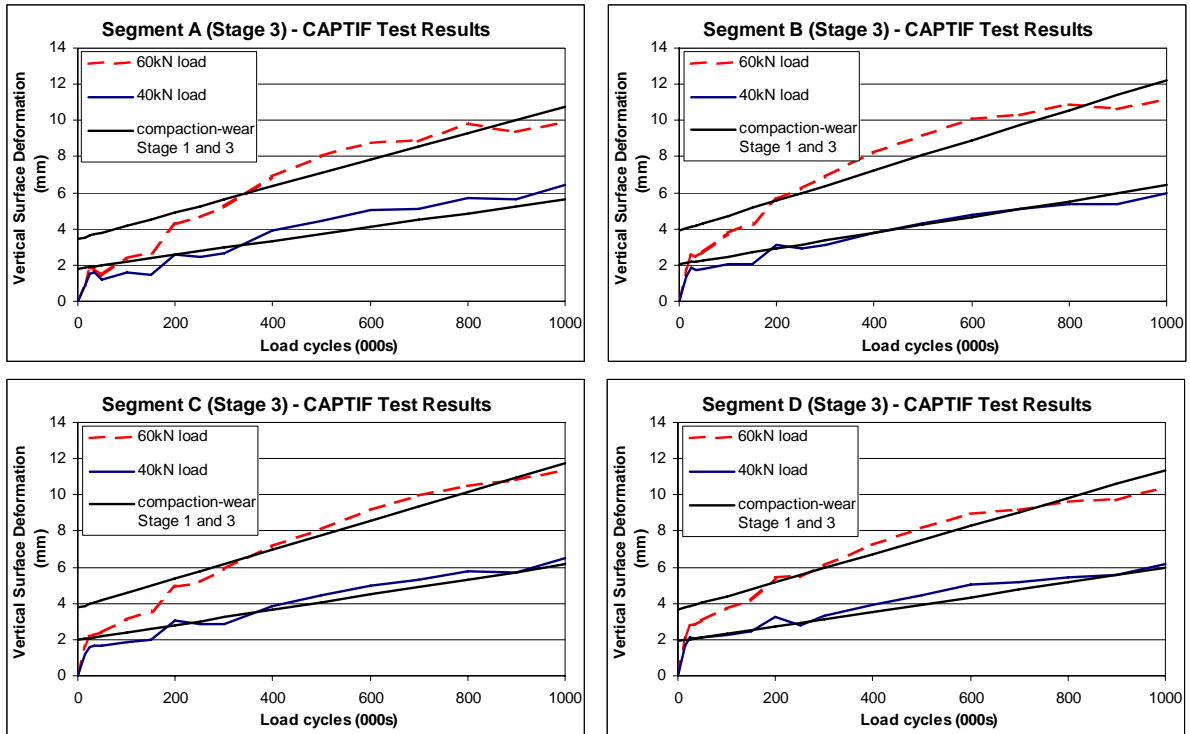
Stage 1, Segments A to D
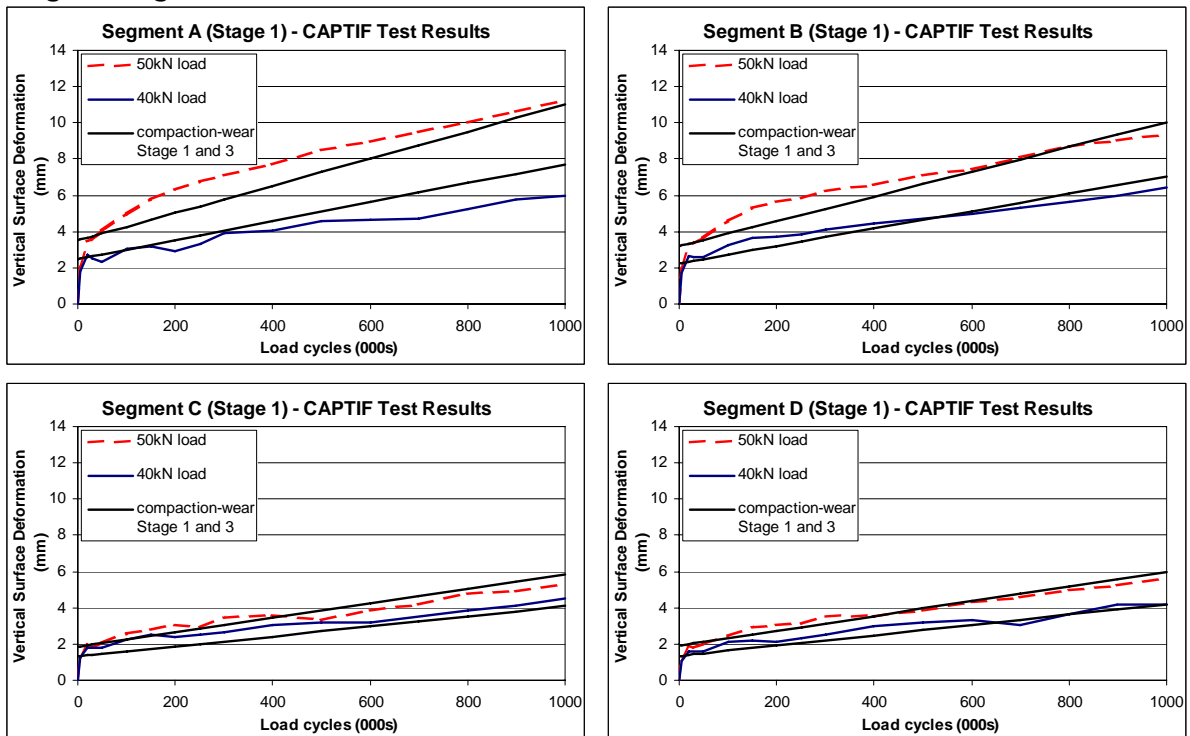
Figure 10.2 Compaction–wear model with common coefficients found with Stage 3 and Stage 1 datasets compared with measured values.

Stage 3, Segments A to D
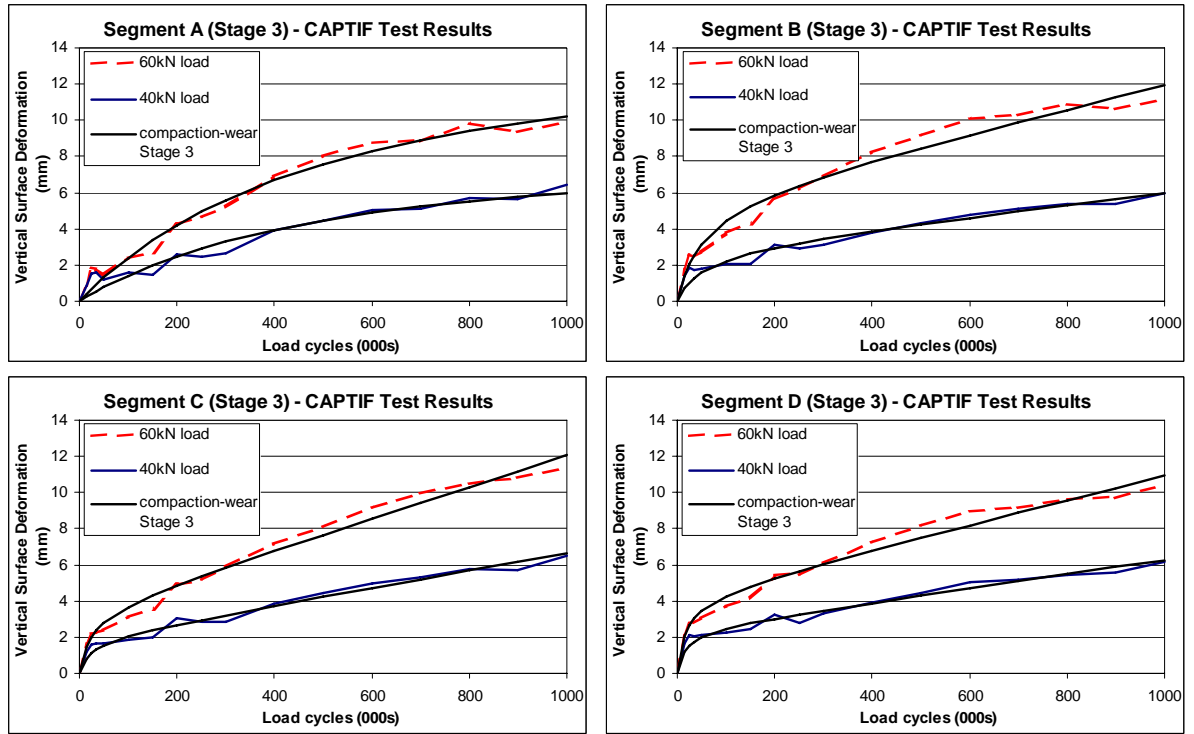
**Figure 10.3	Comparison of single blended compaction–wear model with best fit coefficients found with Stage 3 dataset compared with measured data.**

Stage 3, Segments A to D
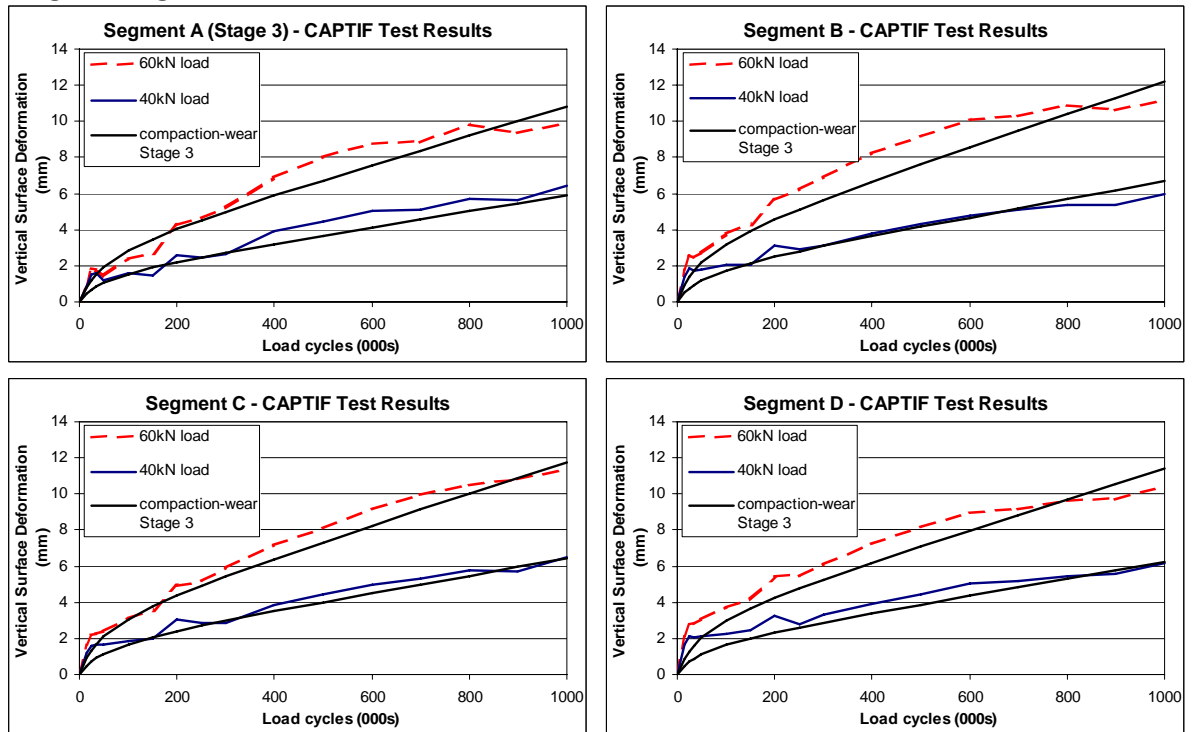
**Figure 10.4	Comparison of single blended compaction–wear model with common coefficients found with Stage 3 dataset compared with measured data.**

Table 10.8 Common coefficients of single blended compaction–wear model with Stage 3 dataset. (N_o, n, C, W in common)

Segment	K	n	C (mm)	W (mm/1000)	N_0 (000s)	Mean error (mm)
A	1.000	1.49	1.675	0.00431	50	0.49
B	1.131	1.49	1.675	0.00431	50	0.65
C	1.089	1.49	1.675	0.00431	50	0.43
D	1.054	1.49	1.675	0.00431	50	0.71

The effect of mass is accounted for by a power law relationship which applies to both the compaction and the wear components in the model. For a single model encompassing all four pavement segments, the best-fit value of the exponent for this power law is 1.49 or in round numbers 1.5. However, as pointed out in the Stage 1 report (de Pont et al. 2001), a sudden increase in mass limits will be expected to result in an increase in compaction which will occur over a relatively short time frame as well as an increase in wear. This will give a step change in the VSD of the pavements which will manifest itself as increased rutting and roughness.

10.2 Kinder-Lay model

Kinder & Lay (1988) developed a model to describe the progression of permanent deformation with loads. This model has the form:

$$VSD = K.C\left(\frac{P}{40kN}\right)^m N^{\frac{m}{a}}$$

<div align="right">Equation 10.5</div>

where K, C, m and α are constants
           P is the axle load in tonnes
           N is the number of load cycles

The Kinder–Lay model (Equation 10.5) provides both an exponent for the effect of mass, and the rate of change of VSD which changes as load cycles increase. With surface deformation the model goes through the origin, i.e. at zero load cycles there is zero deformation. By taking logarithms and using least squares regression, a best fit Kinder–Lay model can be developed for each pavement segment. The best-fit parameters are listed in Table 10.9. As shown above, a in the Kinder–Lay model corresponds to the exponent in the power law and the values of a in Table 10.9 are similar to the best-fit power law exponents given in Figure 9.6.

The reason they are not identical is that the Kinder–Lay model also fits a power relationship to the VSD against load cycles curve which is the same for both the 40 kN axle load and the 60 kN axle load.

**Table 10.9	Coefficients of best fit Kinder–Lay models with Stage 3 dataset.**
(C only is common)

Segment	*K*	*C*	*m*	*a*	Mean error (mm)
A	1.0	0.124	1.30	2.28	0.36
B	2.2	0.124	1.69	3.83	0.28
C	1.8	0.124	1.43	2.94	0.27
D	3.3	0.124	1.59	4.25	0.33

Figure 10.5 shows a comparison of the VSD versus load cycle curves predicted by these Kinder–Lay type models with the measured data. As can be seen the fit is quite good. However, these models suffer from exactly the same problem as the equations shown previously, namely that, although the four pavement segments are quite similar, the best-fit coefficients are very different from each other. Thus it is difficult to use the model as a predictive tool because the coefficients cannot be determined in advance. Ideally *m* and *a* should be the same for all similar pavements, and *K* should be pavement-specific and relate to its underlying wear resistance or strength.

By using Segment A as the reference level and dividing the VSD values for each of the other three segments by the Segment A value at each measurement point, a best estimate of *K* for each pavement segment relative to the *K* (= 1.00) for Segment A can be determined. Adjusting the data for these *K* values, we can then find least squares estimates of the *m* and *a* for the whole dataset and *K* for Segment A (Table 10.10).

Table 10.10 Coefficients of a single best fit Kinder–Lay model with the Stage 3 dataset.
(Coefficients *C, m, a* are common)

Segment	*K*	*C*	*m*	*a*	Mean error (mm)
A	1.00	0.207	1.47	3.07	0.46
B	1.14	0.207	1.47	3.07	0.38
C	1.09	0.207	1.47	3.07	0.28
D	1.07	0.207	1.47	3.07	0.33

Stage 3, Segments A to D
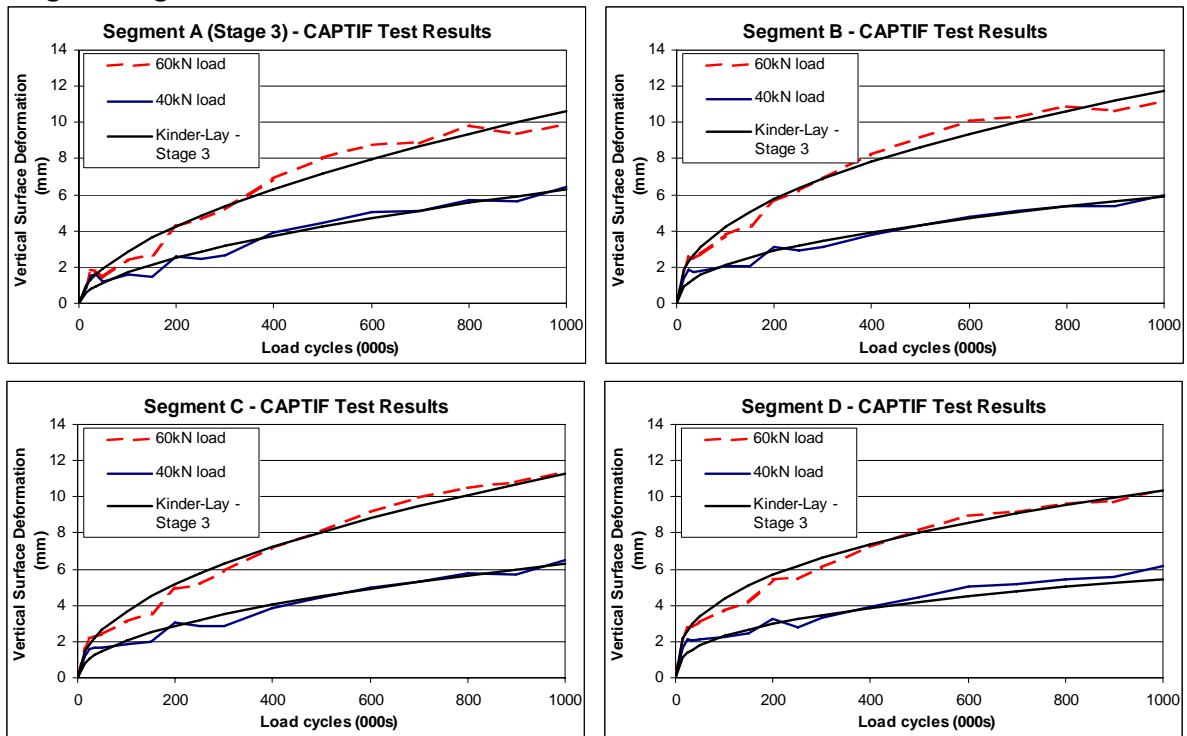
Figure 10.5 Comparison of Kinder-Lay type models using best fit coefficients with Stage 3 measured data. *(C is common)*

Stage 3, Segments A to D
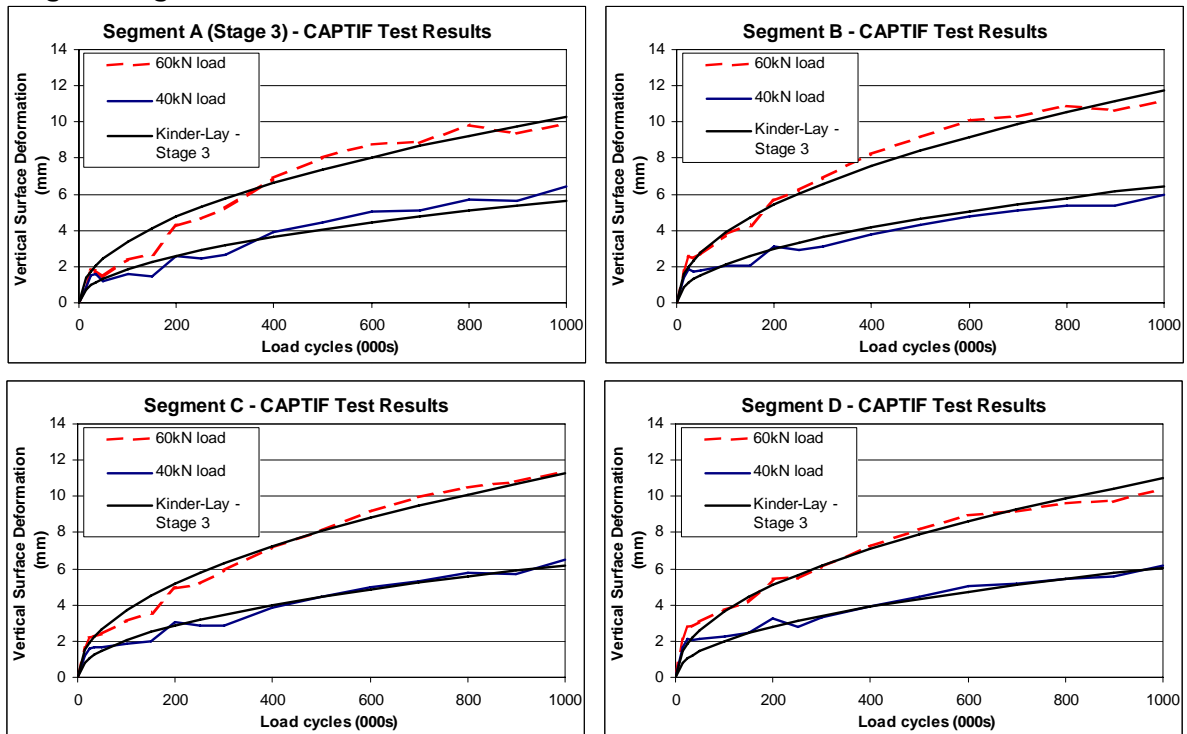
Figure 10.6 Comparison of Kinder–Lay type models using common coefficients (*C, m, a*) with Stage 3 measured data.

Stage 3 data
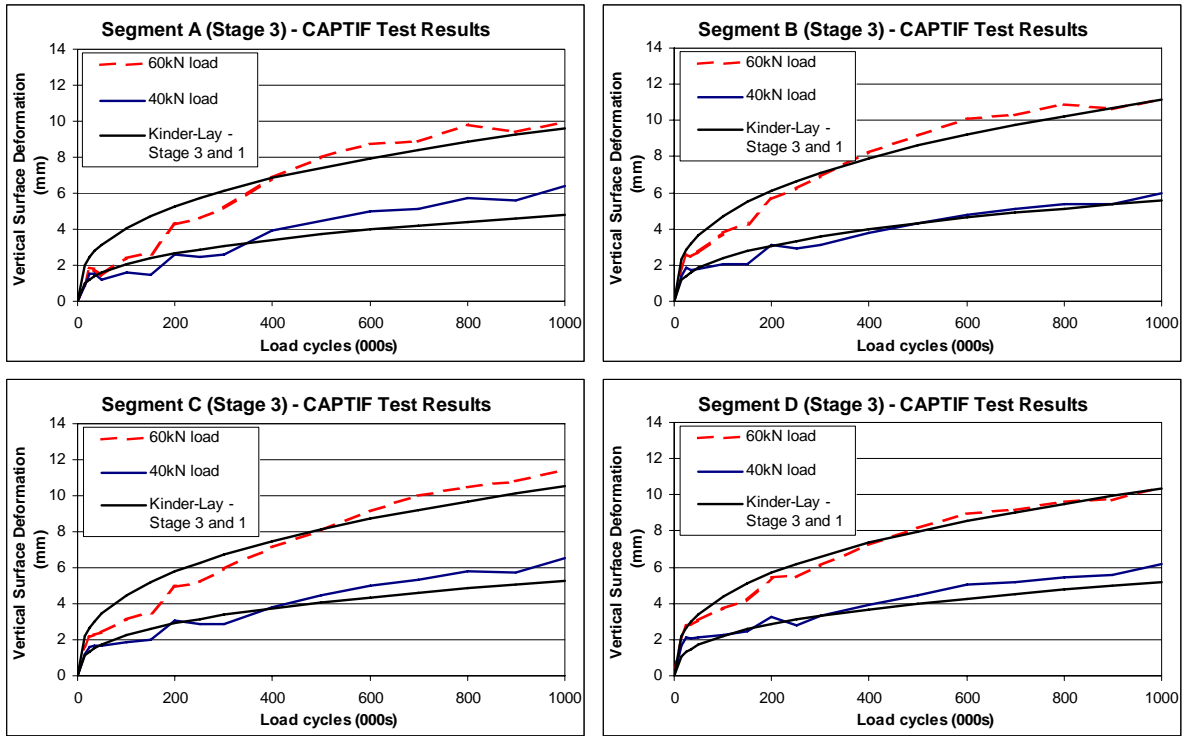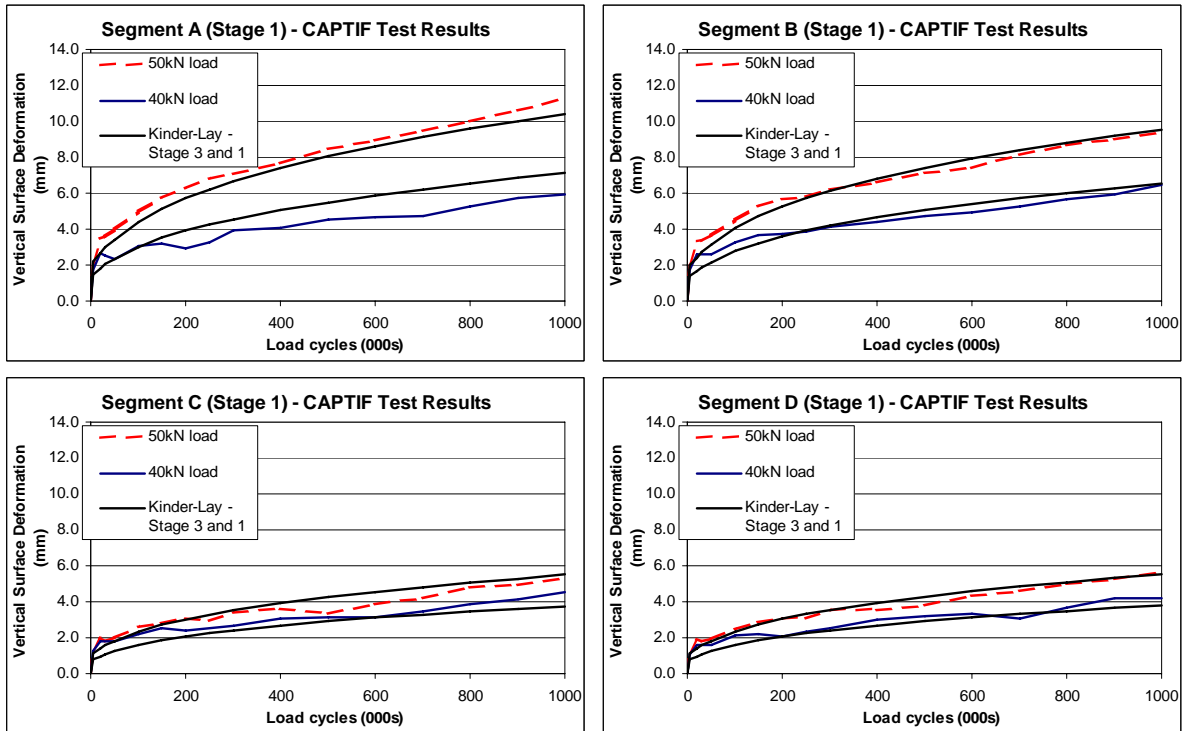
Stage 1 data

Figure 10.7 Comparison of Kinder–Lay type models using common coefficients found for best fit to Stage 3 and Stage 1 data with measured data.

This model is suitable for predictive purposes with a single *m* and *a* (the exponent for the mass effect is 3.07, i.e. approximately 3). The *K* values represent the propensity of the pavement to VSD, with a higher value indicating greater VSD for the same load. Thus all segments are similar to each other. Figure 10.6 shows a comparison of the predictions of this single Kinder–Lay model with the measured data for each of the four pavement segments. This model produces a good match for all segments.

Common coefficients for the Kinder-Lay model were determined when the Stage 1 dataset was included with the Stage 3 results. Best-fit coefficients for the Stage 1 segments varied significantly, and adding this dataset reduces the goodness of fit to the measured data. Table 10.11 and Figure 10.7 show the results of coefficients determined using the least squares method to find the best fit across all the datasets.

Table 10.11 Coefficients of a single best fit Kinder–Lay model to the Stages 3 and 1 datasets. (Coefficients *C, m, a* in common)

Segment	*K*	*C*	*m*	*a*	Mean error (mm)
Stage 3					
A	1	0.370	1.70	4.59	0.73
B	1.16	0.370	1.70	4.59	0.37
C	1.10	0.370	1.70	4.59	0.58
D	1.08	0.370	1.70	4.59	0.37
Stage 1					
A	1.48	0.370	1.70	4.59	0.54
B	1.36	0.370	1.70	4.59	0.33
C	0.78	0.370	1.70	4.59	0.30
D	0.79	0.370	1.70	4.59	0.29

Apart from the 40 kN load case for Segment A in both Stages 1 and 3, using common coefficients in the Kinder–Lay model fits the data fairly well. An exponent value *a* of 4.6 was found to give the best fit to both the Stage 3 and Stage 1 data.

10.3   Wolff and Visser model

Pidwerbesky (1996) reported that the Wolf & Visser (1994) model provided a better estimate of the permanent surface deformation in thin-surfaced unbound granular pavements than other models. The model proposed by Wolff & Visser (1994) is as follows:

$$y = (a + mx)(1 - e^{-bx})$$ Equation 10.6

where:
   a, *m* and *b* are constants
   x   is the number of wheel passes
   e   is the exponential

This model has been modified similar to the compaction–wear and Kinder–Lay models to account for the pavement type and the load, and takes the form of Equation 10.7.

$$VSD = k\left(\frac{P}{40kN}\right)^c (a + mN)\left(1 - e^{-bN}\right)$$ Equation 10.7

where:

VSD   is vertical surface deformation (mm)
P   is the load in kN
k   is a constant particular to the pavement
c, a, m and b are constants

A first look at Equation 10.7 indicates it is similar to the compaction–wear model with a blending function. The *(1 − e^{-bN})* is the blending part to the linear function *a+mN*. As *N* increases the blending part nearly equals 1 and therefore has little influence on the linear function. Best-fit constants for the Stage 3 data where the 60 kN load was compared with the 40 kN load are given in Table 10.12. Figure 10.8 shows the resulting functions for each pavement segment plotted against the measured data. As can be seen, the fit is fairly good.

Table 10.12 Pidwerbesky/Wolff & Visser model coefficients that are the best fit to the measured Stage 3 dataset for each pavement segment. (*k* is common)

Segment	*k*	*a*	*m*	*b*	*c*	Mean error (mm)
Stage 3						
A	1.0	6.072	0.00039	0.0025	1.31	0.37
B	1.0	2.212	0.00387	0.0219	1.70	0.42
C	1.0	1.592	0.00515	0.0443	1.46	0.32
D	1.0	2.091	0.00427	0.0501	1.37	0.32

Single coefficients for the model that provided the best fit to only the Stage 3 data and to the Stages 3 and 1 data combined were also determined. Tables 10.13 and 10.14 report the coefficients and Figures 10.9 and 10.10 compare the single coefficient model with the measured data for Stage 3 dataset and Stages 3 and 1 datasets combined.

Table 10.13 Pidwerbesky/Wolff & Visser model using common coefficients (*a, m, b, c*) to the measured Stage 3 dataset.

Segment	*k*	*a*	*m*	*b*	*c*	Mean error (mm)
Stage 3						
A	1.000	1.70	0.00427	0.0352	1.47	0.54
B	1.141	1.70	0.00427	0.0352	1.47	0.48
C	1.096	1.70	0.00427	0.0352	1.47	0.34
D	1.070	1.70	0.00427	0.0352	1.47	0.40

Stage 3 data, Segments A to D
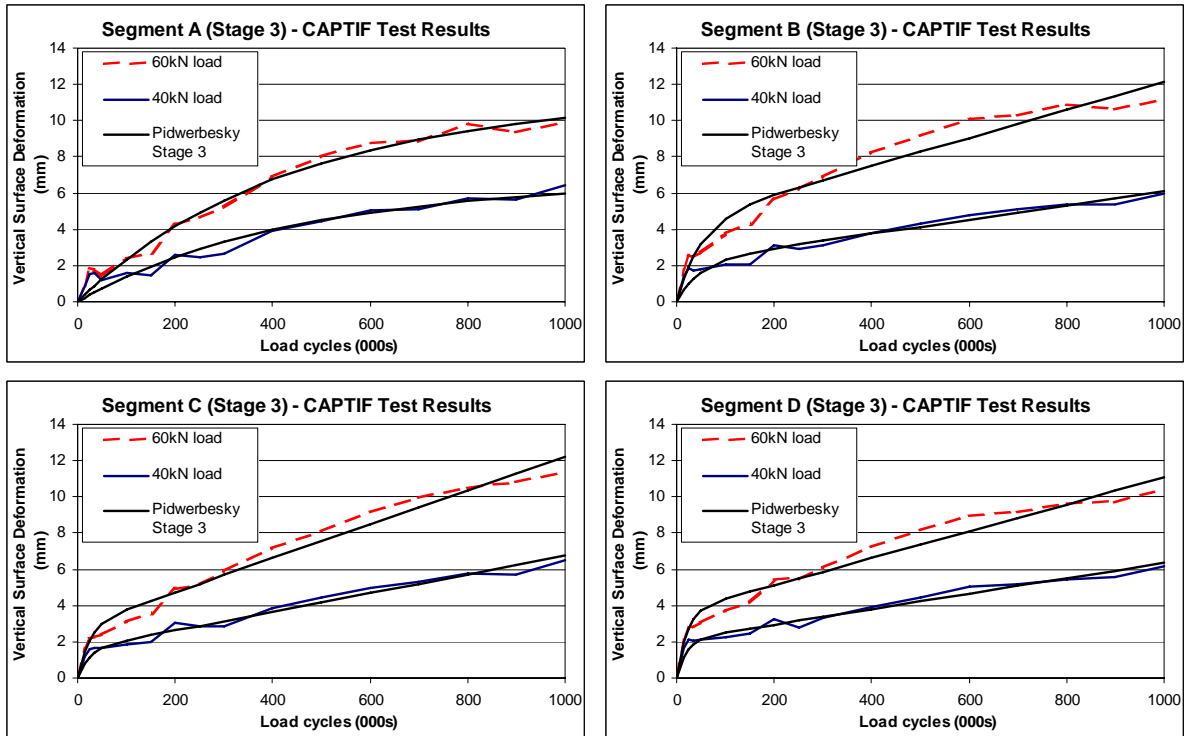
Figure 10.8 Pidwerbesky/Wolff & Visser model with coefficients that are the best fit to the Stage 3 data for each pavement segment, compared to measured data.

Stage 3 data, Segments A to D
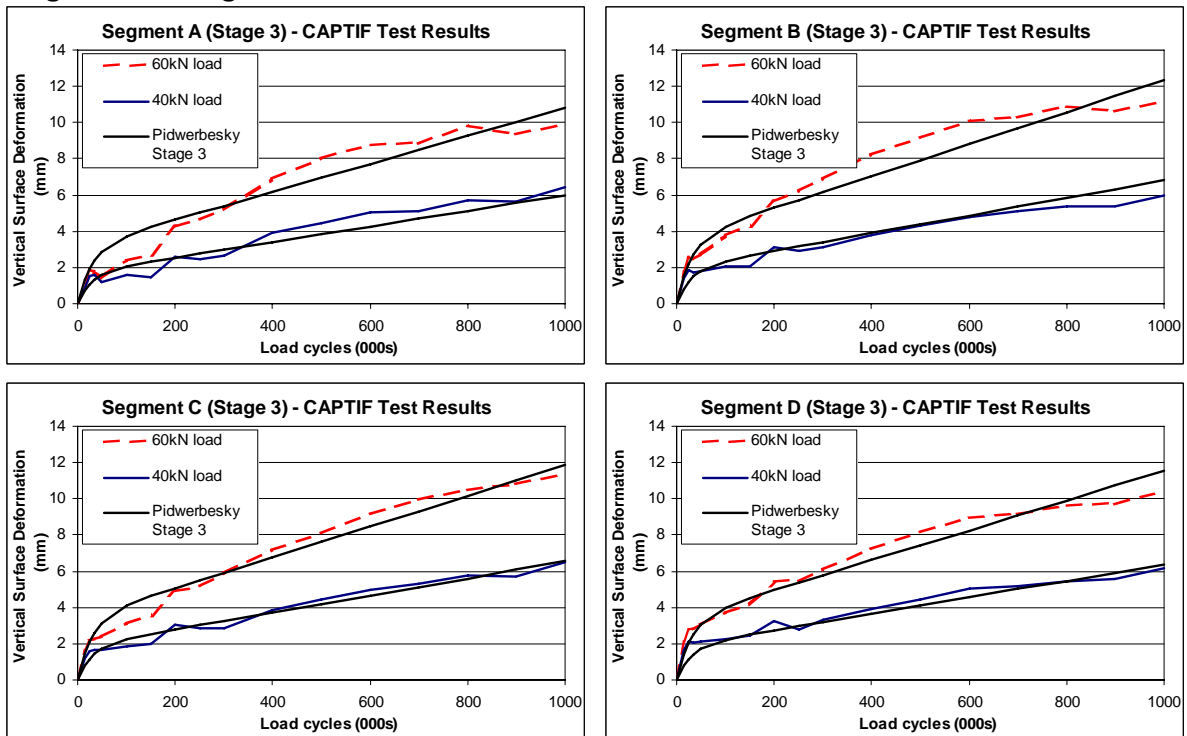
Figure 10.9 Pidwerbesky/Wolff & Visser model with common coefficients (*a, m, b, c*) compared to measured Stage 3 data.

Stage 3 data
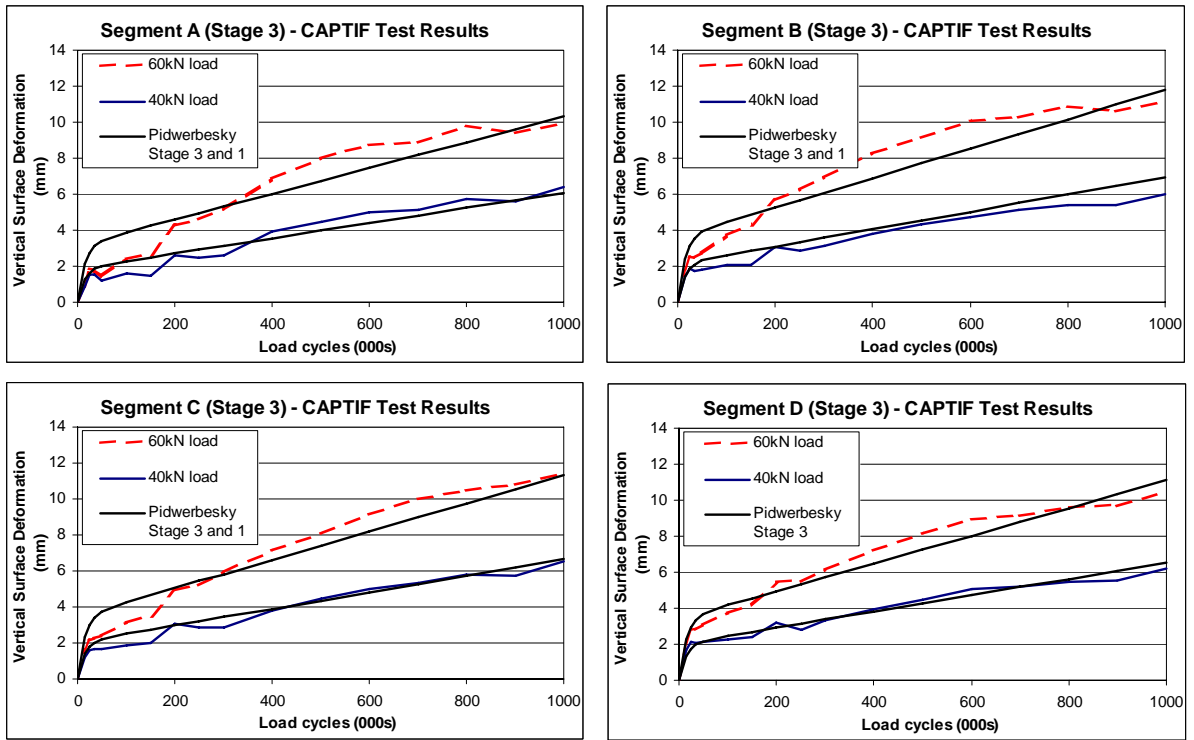
Stage 1 data
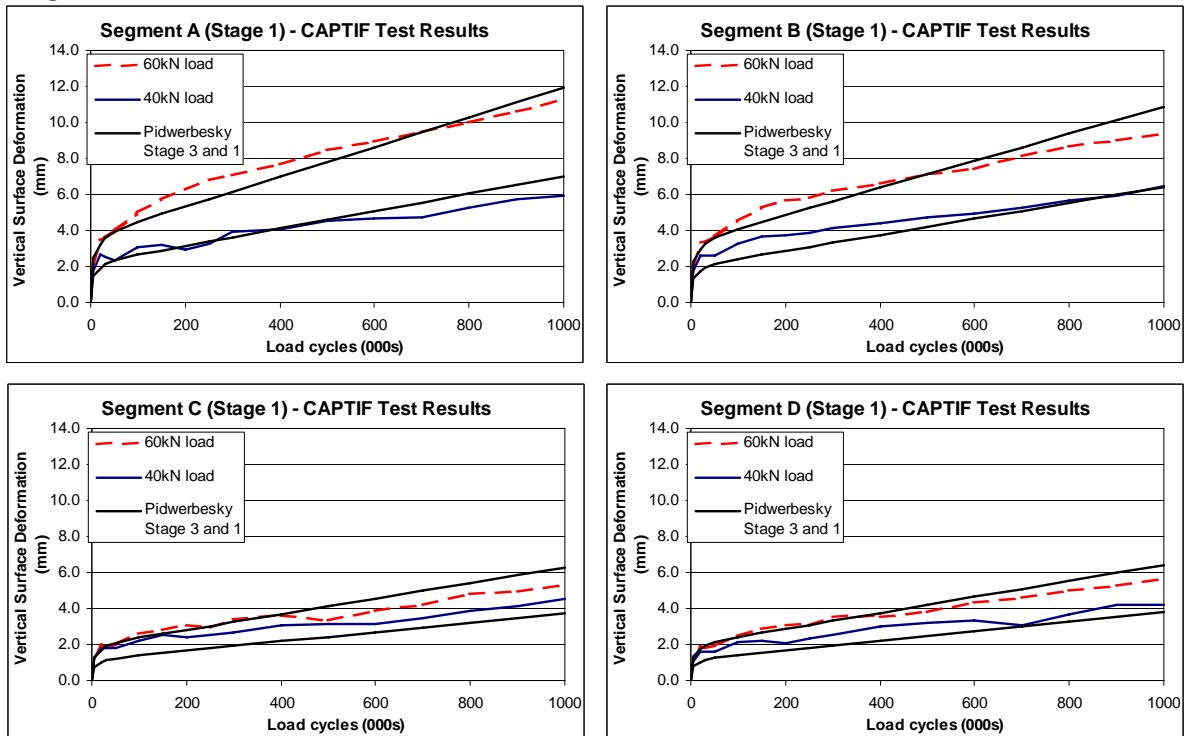
Figure 10.10   Pidwerbesky/Wolff & Visser model with common coefficients (*a, m, b, c*) from Stages 3 and 1 data, compared to measured values.

Table 10.14   Pidwerbesky/Wolff & Visser model using common coefficients (*a, m, b, c*) from Stages 3 and 1 datasets, compared with Stage 3 Segment A (=1.00).

Segment	*k*	*a*	*m*	*b*	*c*	Mean error (mm)
Stage 3						
A	1.000	1.87	0.00421	0.0691	1.31	0.64
B	1.143	1.87	0.00421	0.0691	1.31	0.60
C	1.097	1.87	0.00421	0.0691	1.31	0.46
D	1.076	1.87	0.00421	0.0691	1.31	0.34
Stage 1						
A	1.156	1.87	0.00421	0.0691	1.31	0.45
B	1.056	1.87	0.00421	0.0691	1.31	0.51
C	0.610	1.87	0.00421	0.0691	1.31	0.52
D	0.622	1.87	0.00421	0.0691	1.31	0.38

10.4   Summary

The models that gave the best fit to the measured data are those with the lowest average mean error in Table 10.15. Mean error is the average difference between calculated and measured values. As can be seen, all models report a mean error less than 0.6 mm which would be considered sufficient accuracy when predicting rut depth in a pavement. Kinder–Lay, best fit blended compaction wear, and best fit Wolff & Visser models showed the best fits to the measured data.

Table 10.15 Summary of mean errors for the deformation models tested.

Table	Deformation Model	Average Mean Error (mm)
10.9	Coefficients of best-fit Kinder–Lay models with Stage 3 dataset	0.31
10.7	Best fit coefficients of single blended compaction–wear model with Stage 3 dataset	0.33
10.10	Coefficients of single best fit Kinder–Lay model to Stage 3 dataset	0.36
10.12	Pidwerbesky/Wolff & Visser model coefficients that are the best fit to the measured Stage 3 dataset	0.36
10.11	Coefficients of a single best-fit Kinder–Lay model to the Stages 3 and 1 datasets	0.44
10.13	Pidwerbesky/Wolff & Visser model using common coefficients to the measured Stage 3 dataset	0.44
10.14	Pidwerbesky/Wolff & Visser model using common coefficients from Stages 3 and 1 datasets	0.49
10.5	Compaction–wear best fit with common coefficients for Stage 3 results	0.49
10.1 & 10.2	Linear best fit to VSD results for Stage 3 dataset	0.50
10.6	Compaction–wear best fit with common coefficients for Stages 1 and 3 results combined	0.51
10.8	Common coefficients of single blended compaction–wear model with Stage 3 dataset	0.57

11. Implications

11.1 Network deterioration

Two distinct methods are used in assessing the effect on pavement life for a change in mass limits: a general power law relationship, and deterioration modelling.

The first, a general power law relationship (Equation 9.1), in theory, can be directly applied in pavement design for calculating Equivalent Standard Axles (ESAs) and appropriate Road User Charges (RUC). Further, a general power law relationship can easily be used to estimate the reduction in pavement life if, for example, the 40 kN axles were replaced by 60 kN axles. However, a range of exponents were used for the power law calculated from the results. This makes computing the correct ESAs or RUC difficult because of the sensitivity of the result to the exponent value.

The second method for assessing the effect on pavement life is essentially deterioration modelling. Various forms of equations are proposed that predict the value of VSD with the number of load cycles. The constants for these equations are determined by minimising the differences between the measured and predicted values of VSD. This approach does result in much less variation in predicting the relative damaging effect of axle loads compared with the standard reference axle load of 40 kN. However, as these equations predict VSD, it is difficult to relate them to predictions made with a general power law relationship.

An imaginary road network was therefore formulated to test and understand how the various methods are used in predicting the damaging effect caused by an increase from 40 kN to 60 kN axle loads. Various simplifying assumptions are used for this road network as detailed in Table C1 in Appendix C. A key but simplistic question that has been answered, is how the existing programme of annual pavement rehabilitation will be affected if the 40 kN axles were suddenly all replaced by 60 kN axles.

On reviewing the results from the deterioration modelling on the network in Appendix C, it is interesting to note the initial increase in rehabilitation required in the first year after the change in axle loads. This initial increase is predictable and has been discussed in this Stage 3 report as the compaction component of VSD increase. Table 11.1 summarises the predicted average rehabilitation requirements both including and excluding the first year determined for each model using the 60 kN axle loads. In addition, the exponent values are calculated that relate rehabilitation requirements to axle load with a power law relationship (Equation 11.1).

$$\frac{Numb.\,Re\,habs_{60kN}}{Numb.\,Re\,habs_{40kN}} = \left[\frac{60kN}{40kN}\right]^n \qquad\qquad \text{Equation 11.1}$$

Table 11.1   Average rehabilitation requirements and appropriate power law exponents predicted for an increase from 40 kN to 60 kN axle loads.

Rehab requirements	Base Power Model	Best fit C-W	Common coeff. C-W	Best fit Wolff & Visser	Common coeff. Wolff & Visser
For 40 kN:					
avg no./year	1	1	1	1	1
For increase to 60 kN:					
actual no. in year 1	8	5	7	6	10
avg/year excl year 1	3.5	1.9	2.0	2.0	2.0
avg/year incl year 1	3.6	2.0	2.1	2.1	2.0
Rehab power law exponent:					
for Year 1	5.1	4.0	4.8	4.4	5.7
avg (excl year 1)	3.1	1.6	1.7	1.7	1.7
avg (incl year 1)	3.2	1.7	1.8	1.9	1.7

C–W   compaction–wear model

Reviewing results in Table 11.1 shows little difference is made to the Rehabilitation power law exponent by separating the additional rehabilitation requirements in year 1. Also the Rehabilitation power law exponent of 3.2 predicted using the base power model is the same as that determined for a traditional power law for a known VSD at end-of-life (Table C2). As the base power model matches the measured data for Segment C (Stage 3) better than all the other relationships, it can be argued that results using this relationship are best.

However, the base power model may not be appropriate for extrapolation beyond the measured data as this assumes the rate of increase in VSD decreases with increasing load cycles. This has the effect of putting a greater separation between the VSD curves for the 60 kN and 40 kN axle loads (i.e. increase the power law exponent for relative damage). Therefore, the linear relationships such as the compaction–wear and Wolff & Visser models may be more appropriate.

11.2   Low strength pavements

Segment E that used rounded aggregate failed quickly and power exponents as high as 6 were calculated from the general power relationship (Equation 9.1). Due to the rapid nature of the failure, the final exponent was calculated as 2.6. This is an important result and has implications in predicting the damage that may be caused to the New Zealand road network should an increase in mass limits occur. There are roads in New Zealand constructed using marginal quality aggregates that, if trafficked by higher loads, will fail very quickly. This will result in more rehabilitations required in the first year than that predicted with the network deterioration modelling. The amount will depend on the length of low strength pavements that are either thin or constructed with marginal aggregates.

Research at the University of Nottingham (Arnold et al. 2002) showed three possible permanent strain responses to repeated load (Ranges A, B or C). Figure 11.1 illustrates these different behaviour ranges.

- Range A response is a stable response where the permanent strain rate (i.e. VSD increase per load cycle) appears to be decreasing with increasing load cycles.

- Range B response is where the permanent strain rate, after an initial compaction period, appears to remain constant with increasing load cycles.

- Premature failure is categorised as a Range C response.

The research also showed that there is a clear stress boundary between the responses and only a small change in load can result in a different Range response. Therefore it is possible that a change from 60 kN load from 40 kN could result in a change from a Range B response to a Range C response and thus to early failure.
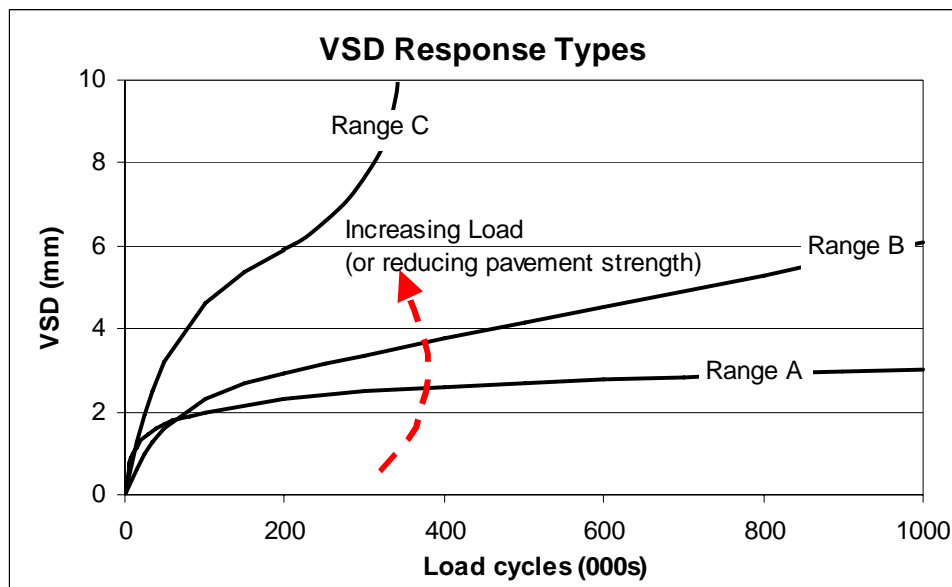
Figure 11.1 Illustration of the range of VSD responses with load cycles.

Perhaps one of the reasons why Segment E performed poorly was the apparently low level of compaction. As this material has been used extensively in some areas but not recently, it is difficult to determine if the density is typical of that observed in the field. This material in the field would have been compacted to a plateau density, rather than to a percentage of maximum dry density. Although the material did not meet current Transit standards, it did meet the requirements of the Christchurch City Council who use a fixed density as a target. Therefore, it is difficult to tell if the early failure of this section is or is not significant.

12. Predicting pavement damage for other loads, tyre types and contact stress

Analysis of Stage 3 and Stage 1 data have produced some useful equations for predicting VSD progression in a pavement. Some of these equations require the axle load as one of the inputs, which enables VSD predictions for loads other than those tested. Therefore, a series of plots of VSD versus axle passes for different axle loads can be produced. The relative damage caused by these different axle loads can be determined by comparing the results to the standard 40 kN load case from the Stage 1 research. However, the VSD equations derived from Stages 3 and 1 data are from a particular tyre type and tyre contact stress. Therefore, axle load alone may not be appropriate to predict the damage caused by different tyre types and tyre pressures to those used to obtain the original VSD equations.

Another approach is to use pavement response data for predicting the damage for other loads, tyre types and contact stress. However, this approach has not been validated but is included as a possible way forward to predict the damage caused by tyre types and loads other than those tested.

At CAPTIF, resilient strains are measured within the pavement at various depths. It is reasonable to assume that permanent strain in terms of VSD is directly proportional to the resilient strain measured. For the CAPTIF tests (Stages 3 and 1) it is possible at each strain-measuring coil pair to find a linear relationship between axle load (P) and measured resilient strain. From these relationships an equivalent axle load (P') can be obtained from measured strains for other tyre types, loads and contact stresses. This equivalent axle load can then be used directly in the equations that predict VSD. It is likely that for single wide tyres the equivalent axle load calculated would be markedly different from the actual axle load.

Strains and stresses within the pavement have been measured at CAPTIF as part of an Austroads research project (Vuong & Sharp 2001), for a range of different tyre types, loads and contact stress (Table 12.1). A linear equation relating axle load to measured strain was derived for each coil pair from measurements obtained from the standard tyre type (11R22.5) and tyre contact stress of 750 kPa. This tyre type and pressure is the closest match to the tyre types and pressures used in determining the VSD relationships in the Stages 3 and 1 research projects. The relationship between axle load and strain was then applied to the measured strains for the other tyre types, loads and pressures (Table 12.1). Results of this analysis are shown in Appendix D and, as can be seen, the equivalent axle load for single wide tyres is up to 3 times higher than the actual load at individual gauge points.

Table 12.1   Range of tyre types, pressure and loads for which strain measurements were obtained.

No.	Tyre Type	Load (kN)	Pressure (kPa)
1	11 R 22.5	40	650
*2	11 R 22.5	40	750
3	11 R 22.5	40	850
*4	11 R 22.5	50	750
5	11 R 22.5	50	850
*6	11 R 22.5	60	750
7	11 R 22.5	60	850
8	385/65* (Super Single)	40	750
9	385/65 (Super Single)	40	850
10	385/65 (Super Single)	50	750
11	385/65 (Super Single)	50	850
12	385/65 (Super Single)	60	850
13	11 R 22.5	40	650

* These tyre types, pressures and loads were used as the standard reference loads where a linear relationship between load and measured strain was obtained for each coil pair.

Results in Appendix D show that the equivalent load value calculated is very dependent on pavement depth where the strain was measured. This is not surprising as tyre pressure has a greater influence in the upper layers of the pavement. An average equivalent axle load was calculated over all depths as it is assumed that permanent deformation occurs equally in all the layers. If this is not the case, then a weighted average could be used with a likely bias towards the upper layers in the pavement. Average equivalent loads are compared with the actual loads for each tyre type by determining the effect on the exponent for a general power law (Equation 12.1) reported in Table 12.2. The average equivalent loads exclude the values calculated from strains measured in the top pavement layers. Strains measured between the dual tyres are significantly less than those measured directly under the super single tyres at the top of the pavement.

$$\left[\frac{P}{40} \right]^{n'} = \left[\frac{P'}{40} \right]^{n}$$

Equation 12.1

where:

n is the original exponent value

P is the actual axle load in kN

P' is the equivalent axle load as calculated from measured strains

n' is the new adjusted exponent that is calculated from this equation

Table 12.2   Average equivalent load determined from strain measurement and its effect on the power law exponent for damage.

*No.	Tyre Type	Load (kN)	Average Equivalent Load (kN)	Existing power exponent		
				2	3	4
				Adjusted power exponent		
1	Dual	40	41	–	–	–
2	Dual	40	42	–	–	–
3	Dual	40	43	–	–	–
4	Dual	50	48	1.6	2.3	3.1
5	Dual	50	53	2.5	3.7	5.0
6	Dual	60	60	2.0	3.0	4.0
7	Dual	60	64	2.3	3.5	4.6
8	Single	40	62	–	–	–
9	Single	40	64	–	–	–
10	Single	50	62	3.9	5.9	7.9
11	Single	50	74	5.5	8.2	10.9
12	Single	60	70	2.8	4.1	5.5
13	Dual	40	37	–	–	–

*   See Table 12.1 for full description.

– As the reference load in Equation 12.1 is 40 a new exponent value cannot be calculated.

Results show that, when predicting VSD for the Super Single tyres, the value of axle load needs to be factored up, in some cases as much as 60%. For the dual-tyred case the differences are less than 10%. The new exponent values shown in Table 12.2 are to illustrate the additional damaging effect caused by different tyre types. An adjusted exponent value does not need to be used except in equations that predict damage (i.e. VSD and general power law relationships) as defined in this report. The equivalent axle load determined from strain measurements should be used in place of the actual axle load in the determination of ESAs.

13.   Discussion

13.1   Effect of increasing axle load

This research project has clearly shown that an increase in axle load will result in an increase in VSD (Vertical Surface Deformation). VSD is related to rutting and roughness and therefore this result can be translated into what may occur on the New Zealand road network should mass limits increase. In pavement design, different axle loads are converted into a number of Equivalent Standard Axles (ESAs). The idea behind this approach is to determine **the number of passes of an ESA** (e.g. 40 kN axle) **that will cause the same damage as passes of the axle load in question** (e.g. 60 kN). To calculate the number of ESAs a general power law relationship is used where the ratio of the two axle loads is raised to a power, usually 4. This is commonly known as the fourth power law which is also used in the wear component of the Road User Charges (RUCs).

The philosophy behind the ESA approach was applied to the VSD versus load cycle results obtained at CAPTIF for the reference load of 40 kN, and for an alternate load of either 60 kN (Stage 3 tests) or 50 kN (Stage 1 tests). The exponent for the general power law was found to change depending on the value of damage chosen (i.e. VSD), and pavement type. Exponents for Stage 1 results ranged from 2 to 9 while a range of 2 to 4 was found in Stage 3 research if Segment E is excluded. Segment E failed within 250,000 load cycles and exponent values for this section were as high as 6. The influence of initial density needs to be considered as it has a great influence on the initial results during the first 100,000 load cycles.

This scatter in calculated power law exponent values makes it difficult to decide on a new exponent to use for the calculation of ESAs and RUCs. However, this result should not be discounted as other researchers have also found similar scatter in their results. Roads in New Zealand vary in strength and RCAs need to be aware that changes in mass limits will have a mixed effect on their network. It is likely that the stronger sections in the road network will feel little impact caused by an increase in mass limits, perhaps requiring a power law of around 2. For weaker sections in the pavement, increases in mass limits could have a dramatic effect in increasing roughness or damage. For these weak pavements the power exponent could be around 4 to 9.

13.2   Components of VSD

All the VSD results appeared to consist of two components:

1. An initial compaction component, where in the first 100,000 load cycles a disproportionate amount of deformation occurs, with as much as half the total deformation in 1,000,000 load cycles occurring in this period;

2. A wear-related component, which is related to the linear part of the VSD curve after 100,000 load cycles.

Equations that were basically linear, power, or linear plus blending were fitted to the VSD data. If the equation was multiplied by a constant relating to the pavement type (i.e. Segment) and by the ratio of axle load to the reference axle load raised to the power of an exponent, then the coefficients showed a fairly good match to all the VSD results in both the Stage 3 and Stage 1 tests. This is promising because if an appropriate constant for the pavement type is known, then VSD can be predicted and this is similar to the HDM modelling approach.

All the equations for VSD predicted a significant amount of deformation to occur, either immediately as with the linear case or in the first 100,000 load cycles. To understand the implications of this, a few equations for predicting VSD were applied to an imaginary network. The imaginary network consisted of 40 sections aged 1 to 40 years, where one section is rehabilitated per year when the amount of traffic consists of 100,000 40 kN axles. VSD equations were then used to predict the rehabilitation requirements should all the traffic change to 100,000 passes of a 60 kN axle. The results were quite dramatic as in the first year 5 to 8 sections required rehabilitation and after this at least 2 sections per year required rehabilitation. In addition, the 5 to 8 sections rehabilitated in the first year all require rehabilitation again at the same time (i.e. in 13 to 22 years time).

The equation that used the base power model most closely matched the measured data. This model predicted over twice the rehabilitation requirements than the number predicted by the other models used. The other models were essentially linear in the way VSD was predicted beyond the measured data, and this could be the reason for the difference. It is possible that, if the CAPTIF tests had been continued, the VSD relationship would be linear in which case the base power model shows the extreme case.

13.3   Prediction of rehabilitation requirements

Rehabilitation requirements predicted by the models were used to determine an exponent to predict relative damage. Removing the first year rehabilitation requirements was found to make little difference to the exponent value. This negates the need to have a one-off RUC for vehicles with increased mass limits. The exponent value was around 2 except for the base power model where a value of 3.2 was recorded. As expected the value of 3.2 matched the exponent obtained for a traditional power law from a known VSD at the pavement end-of-life. The other rehabilitation exponent values were not the same as the traditional power law exponent values as the equations used to predict wear were linear.

This analysis for predicting rehabilitation requirements was based on the equations for Segment C only. Therefore, different results will be obtained depending on the pavement type chosen. Further, the example is hypothetical and a simulation is required over a real network with the correct traffic spectrum both before and after a change in mass limits, to gauge the real impact. This real impact will be much less than predicted in the hypothetical case as not all heavy vehicles will need to change to the new mass limits, and also more freight may be carried per trip. However demand would theoretically increase as prices for moving freight decreased.

13.4   Predicting damage from increased axle loads

The equations developed to predict the damage caused by axle loads greater than the standard reference load (of 40 kN) were from tests conducted with a certain type of dual tyres with a set tyre pressure. With previous tests at CAPTIF for the same axle load, changes in tyre pressure were found to have had small effect on measured strains within the pavement. However, the change to Super Single tyres significantly increased the measured strains.

Therefore, when predicting damage caused by tyre types and pressures that were not tested at CAPTIF, it was thought prudent to adjust the value of axle load. We have proposed that this adjustment is calculated from the measured strain value, where the adjusted axle load is the axle load with the standard tyres and pressures used at CAPTIF that causes the same strain. The result is an increase in axle load for Super Single tyres with a slight increase or decrease in axle load, depending on the tyre pressure. Ideally, when predicting damage for other tyre types and pressures, the strains should be measured and the axle load adjusted accordingly.

14.   Conclusions

The aim of this study was to compare the pavement wear generated by a 60 kN axle load with that of a standard 40 kN axle, with a view to predicting the implications in terms of pavement damage of a change in the legal axle load limit allowed on New Zealand highways. A pavement was tested at CAPTIF which comprised five distinct segments consisting of a combination of basecourse aggregates and pavement depths. One of the SLAVE units at CAPTIF was configured to generate a 40 kN wheel load (equivalent to an 8.2 tonne axle) and the other was configured for a 60 kN wheel load (equivalent to just over a 12 tonne axle load). The two SLAVEs were then used to apply 1,000,000 load cycles to parallel wheelpaths on the pavement. During the testing, measurements were taken to record the pavement wear, the pavement condition, the pavement response to the vehicle loading, and the vehicle response to the pavement.

From these measurements a number of important findings were deduced:

- VSD (vertical surface deformation), which is a fundamental form of pavement wear that results in both rutting and increased surface roughness, again proved to be the most useful measure for monitoring pavement wear at CAPTIF.

- The 60 kN axle load resulted in VSD values nearly twice those obtained with the 40 kN axle load in all the pavement segments.

- Segment E, in which a lower quality aggregate (complying with the former TNZ M/5 specification) was used, failed at 87,000 load cycles under the 60 kN load and at 250,000 load cycles under the 40 kN load.

- A conventional power law relationship was fitted to describe the differences in VSD between the two levels of loading for each of the five pavement segments. The exponent for the power law ranged from 2 to 4 for Segments A, B, C and D.

- The value of the exponent depended on the pavement type and the value of VSD taken to be the end-of-pavement life.

- Reviewing the progression of VSD with load cycles shows that the pavement underwent two distinct phases of VSD. An initial period of rapid change was observed, here called compaction, followed by a period with a constant (linear) rate of change called wear. Least squares regression can be used to fit a straight line to the linear part of the VSD versus load cycles curve. The intercept of this line with the y-axis then gives the compaction component, and the slope gives the wear component.

- The compaction–wear linear relationship was modified to include a multiplier for the pavement type and the ratio of axle load to the reference load of 40 kN. This relationship with common coefficients could be fitted to all the VSD data from this research. In Stage 1 where a 50 kN axle load was compared to the 40 kN load, this relationship has the advantage of being able to predict VSD for other pavement types and axle loads.

14.   Conclusions

- A power law model (Kinder–Lay model, 1988) and a linear model with a blending function that models the initial progression of VSD in the compaction stage (Wolff & Visser model, 1994) were also fitted to the VSD data, using both best-fit coefficients (where the coefficients were changed for each pavement segment) and common coefficients across the whole dataset.

- All equations used to predict VSD fitted the data fairly well. Probably the power law model (Kinder–Lay) gave the best fit but its use in extrapolating the results may not be appropriate as it predicts an ever-decreasing rate of change in VSD with increasing load cycles.

Many different equations were determined that predicted VSD for a known pavement type and axle load. A selection of the above equations were applied to an imaginary network to predict deterioration in terms of VSD, and thus the rehabilitation requirements each year should the traffic change from 100,000 passes per year for a 40 kN axle to 100,000 passes per year of a 60 kN axle. It was assumed that the imaginary network consisted of 40 road sections and that, with the 40 kN axles, only one section would require rehabilitation per year. A summary of the analysis follows.

- All equations predicted that 5 to 10 sections would need rehabilitation in the first year. After this, the linear-type equations (compaction–wear and Wolff & Visser) predicted, on average, around 2 sections per year would need rehabilitation. The base power model, which was a power model fitted to each load, predicted on average 3.6 sections per year would require rehabilitation. Note that this must be tempered with the fact that the 60 kN axle would carry considerably more freight per axle pass.

- The power exponent that relates damage (number of rehabilitations per year) to the ratio of axle load to reference load of 40 kN raised to this power exponent, ranged from 1.7 to 1.9 for the linear model, and was 3.2 for the base power model.

- The large number of pavement sections requiring rehabilitation in the first year after the new 60 kN axle loads were introduced, all required rehabilitation again at the same time (from 8 years to 22 years depending on the model used).

- Removing the first year rehabilitation requirements made very little difference to the power law exponent and thus this negates the need for a one-off payment to be included in the RUC for new vehicles operating at the higher mass limits.

- The average number of rehabilitations required each year predicted by the base power model (3.6 per year) was significantly higher than the other models (2.0 per year). The base power model was the best match to the measured data. However, this large difference in results is partly related to the way the VSD results are extrapolated beyond the measured data. The base power model predicts an ever-decreasing rate of change in VSD while the linear type models predicts a constant increase.

- The results of network deterioration highlighted that caution should be taken when applying the more simple linear models to VSD, as the prediction of pavement wear is likely to be much less than what will occur with an increase in mass limits.

- For Segment E constructed with low strength rounded aggregates that failed within 250,000 load cycles, exponent values as high as 6 were calculated as the test progressed. However, the rapid nature of the final failure reduced the exponent to 2.6 at the end of testing. This result illustrates that weaker sections in the road network which are adequate at present could fail quickly with the introduction of higher mass limits.

- When applying the equations used in this study to predict the damage caused by other tyre types and pressures not used here, then an adjustment is required to the axle load. This adjustment can be calculated from the measured strain value where the adjusted axle load is the axle load with the standard tyres and pressure used at CAPTIF that causes the same strain. The result is an increase in axle load for Super Single tyres with a slight increase or decrease in axle load, depending on the tyre pressure.

- The result of this accelerated pavement test principally provides an indication of the performance of a relatively strong pavement, on a strong dry subgrade, in ideal dry environmental conditions. The behaviour of weaker or saturated subgrades has not been investigated, nor have the effects on older and/or poorly maintained surfaces where moisture may be entering the base.

15. Recommendations

- Further validation is required of the models proposed to predict VSD with load cycles based on pavement type and axle load.

- Equations that predict VSD with load cycles are based on measured data up to 1,000,000 load cycles. The pavement had not reached the terminal functional condition and, to be sure of the correct equation form (either a power law or linear function), a test that reaches terminal condition is required for both the reference axle load of 40 kN and that of 60 kN.

- Analysis of the pavement types tested in this Stage 3 to determine how the results affect current pavement design practices is required. For example, in the tests reported here, some of the thinner pavement segments had a similar life to the thicker pavement segments.

- On the existing pavement, strain measurements should be undertaken for a range of tyre pressures and loads other than those tested. These data will help decide how to interpolate the results for other tyre types, pressures and loads.

- From these results of a rather simple deterioration study, the compaction–wear model and other linear type models should be used cautiously, particularly when predicting the relative damage to the pavement caused by an increase in axle loads.

- Some of the models developed that predict VSD have a multiplier depending on the pavement type. So that these models can be applied to other pavement types, a relationship needs to be developed with a common pavement parameter like the structural number and/or FWD measurements.

16.   References

Arnold, G., Alabaster, D.A., Steven, B.D. 2001. Prediction of pavement performance from repeat load tri-axial tests on granular materials. *Transfund New Zealand Research Report No. 214.* 120pp.

Arnold, G., Dawson, A., Hughes, D., Robinson, D. 2002. The application of shakedown approach to granular pavement layers*. Ninth International Conference on Asphalt Pavements.* Copenhagen, Denmark: International Society for Asphalt Pavements.

Austroads. 1992. *Pavement design: A guide to the structural design of road pavements*. Austroads, Sydney, Australia.

Cebon, D. 1999. *Handbook of vehicle-road interaction.* Swets & Zeitlinger, Lisse, Netherlands.

Council of the European Communities. 1992. *Annex III of the Council Directive 92/7/EEC amending Directive 85/3/EEC on the weights, dimensions and certain technical characteristics of certain road vehicles.* Council of European Communities, Brussels.

de Pont, J. 1997. OECD DIVINE project - Element 1. Longitudinal pavement profiles. *Industrial Research Limited IRL Report No.708.*

de Pont, J., Steven, B., Pidwerbesky, B. 1999. The relationship between dynamic wheel loads and road wear. *Transfund New Zealand Research Report No. 144.* 88pp.

de Pont, J., Steven, B., Alabaster, D., Fussell, A. 2001. Effect on pavement wear of an increase in mass limits for heavy vehicles [Stage 1]. *Transfund New Zealand Research Report No. 207.* 55pp.

de Pont, J., Steven, B., Alabaster, D., Fussell, A. 2002. Effect on pavement wear of an increase in mass limits for heavy vehicles – Stage 2. *Transfund New Zealand Research Report No. 231.* 50pp.

Kinder, D.F., Lay, M.G. 1988. Review of the fourth power law. *Australian Road Research Board ARRB Internal Report MR 000-248.*

OECD. 1998. Dynamic interaction between vehicles and infrastructure experiment (DIVINE). *OECD Technical Report IRKD 899920.*

Patrick, J.P., Alabaster, D.J., Dongol, D.M.S. 1998. Pavement density. *Transfund New Zealand Research Report 100.*

Pidwerbesky, B.D. 1995. Accelerated dynamic loading of flexible pavements at the Canterbury accelerated pavement testing indoor facility. *Transportation Research Record 1482:* 79-86.

Pidwerbesky, B.D. 1996. Fundamental behaviour of unbound granular pavements subjected to various loading conditions and accelerated trafficking. *University of Canterbury Research Report 96-13.*

16. References

Sayers, M.W., Gillespie, T.D., Paterson, W.D.O. 1986. Guidelines for conducting and calibrating road roughness measurements. *World Bank Technical Paper 46.*

SA (Standards Australia). 1995. Soil strength and consolidation tests – Determination of the resilient modulus and permanent deformation of granular unbound pavements. *AS1289.6.8.1:1995.*

SANZ (Standards Association of New Zealand). 1986. Methods of testing soils for civil engineering purposes. Soil compaction tests. *NZ4402:1986 Test 4.1.3.*

SANZ. 1991. Methods of sampling and testing road aggregates. Laboratory tests. *NZ4407:1991 Tests 3.1, 3.8.1, 3.14.*

Vuong, B., Sharp, K. 2001. Impact of new heavy vehicles on pavement wear and surfacings: Responses-to-load testing using CAPTIF. *Austroads Project T&E.P.N.004. APRG Report 01/08 (LO).* 76pp. ARRB Transport Research Ltd, Vermont South, Victoria, Australia.

Wolff, H., Visser, A.T. 1994. Incorporating elasto-plasticity in granular layer pavement design. *Proceedings of Institution of Civil Engineers Transportation 105:* 259-272.

APPENDICES

Appendix A: Laboratory Characterisation of Aggregates

Fulton Hogan Canterbury Laboratory
PO Box 16-064, Hornby, Christchurch. 325 Pound Rd, Yaldhurst, Christchurch.
Telephone: 03 349 9142 - Fax: 03 349 9143 - Manager's Mobile: 025 377 318

Laboratory Reference: 2002/0323/2

Page 1 of 1

BASECOURSE AGGREGATE TEST REPORT

ATTENTION: **Allan Fussell**

CLIENT:	TRANSIT New Zealand
PRODUCT:	Montrose Rock (AP20)
CONDITION AS RECEIVED:	Natural, sealed plastic bag
SAMPLED FROM:	Ex Australia (Montrose Rock), Stockpile @ Captif
SAMPLING METHOD USED:	NZS 4407:1991 Part 2.4.6.2.1
TEST METHODS USED:	NZS 4407:1991 Tests 3.8.1 & 3.14
SAMPLED BY:	J Hansby on 19/2/2002
TESTED BY:	Max Burford on 26/2/2002

Sieve Size (mm)	% Passing Sieve
37.5	100
19	99
9.5	78
4.75	61
2.36	45
1.18	31
0.6	22
0.3	16
0.15	12
0.075	9

% passing finest sieve obtained by difference

Size Range	% Crushed
19-37.5	100
9.5-19	100
4.75-9.5	100

Montrose Rock - Particle Size Distribution

— Sample Grading

(graph: % Passing Sieve vs Sieve Size (mm), showing sample grading curve)

Report Issued By: Max Burford on 26/2/2002

Report Checked By: _[signature]_   Approved Signatory: _[signature]_

A member of the Fulton Hogan Ltd. Group   Report Template: Basecourse(Wet).doc Template Issued: 2nd August 2001

Fulton Hogan Canterbury Laboratory
PO Box 16-064, Hornby, Christchurch. 325 Pound Rd, Yaldhurst, Christchurch.
Telephone: 03 349 9142 - Fax: 03 349 9143 - Manager's Mobile: 025 377 318

Page 1 of 1

Laboratory Reference: 2002/0323/1

NZ VIBRATING HAMMER COMPACTION TEST

ATTENTION: **Allan Fussell**

CLIENT:	TRANSIT New Zealand
MATERIAL:	Montrose Rock (AP20)
CONDITION AS RECEIVED:	Natural, sealed plastic bag
SAMPLE SOURCE:	Ex Australia (Montrose Rock), Stockpile @ Captif
SAMPLED BY:	J Hansby on 19/2/2002
SAMPLING METHOD USED:	NZS 4407:1991 Part 2.4.6.2.1
TEST METHOD USED:	NZS 4402:1986 Test 4.1.3 – performed on whole material in natural state
TESTED BY:	Max Burford on 26/2/2002

Moisture Content (%)	Dry Density (t/m³)
4.1	2.15
5.2	2.24
6.2	2.26
7.2	2.22
8.5	2.20

Optimum Water Content   = 6.0 %
Maximum Dry Density   = 2.26 t/m³
Solid Density of Coarse Particles   = 2.72 t/m³ (Assumed)

NZ Vibrating Compaction Curve

Report Issued By: Max Burford on 26/2/2002

Report Checked By: _____   Approved Signatory: _____

A member of the Fulton Hogan Ltd. Group   Report Template: Vibrating Compaction.doc Template Issued: 27th May 1999

Fulton Hogan Canterbury Laboratory
PO Box 16-064, Hornby, Christchurch. 325 Pound Rd, Yaldhurst, Christchurch.
Telephone: 03 349 9142 - Fax: 03 349 9143 - Manager's Mobile: 025 377 318

Laboratory Reference: 2002/0324/2A Page 1 of 2
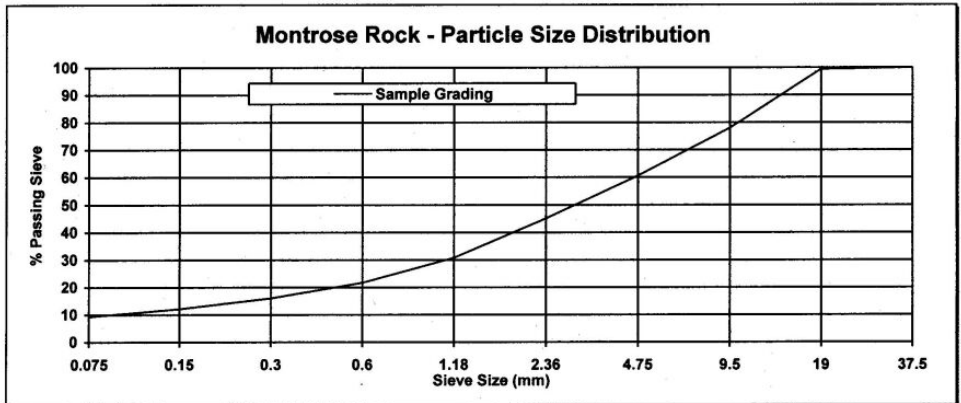
BASECOURSE AGGREGATE TEST REPORT

ATTENTION: Alan Fussell

CLIENT:	TRANSIT New Zealand
PRODUCT:	TNZ M/4 AP40 Basecourse
CONDITION AS RECEIVED:	Natural, sealed plastic bag
SAMPLED FROM:	Ex Pound Road, Stockpile @ Captif
SAMPLING METHOD USED:	NZS 4407:1991 Part 2.4.6.2.1
TEST METHODS USED:	NZS 4407:1991 Tests 3.8.1 & 3.14
SAMPLED BY:	J Hansby on 19/2/2002
TESTED BY:	Max Burford on 26/2/2002

Sieve Size (mm)	% Passing Sieve	TNZ M/4: 1995
37.5	100	100
19	77	66 - 81
9.5	56	43 – 57
4.75	43	28 – 43
2.36	30	19 – 33
1.18	21	12 – 25
0.6	16	7 – 19
0.3	12	3 – 12
0.15	8	0 – 10
0.075	5	0 - 7

% passing finest sieve obtained by difference

Size Range	% Crushed
19-37.5	100
9.5-19	100
4.75-9.5	100

TNZ M/4 AP40 - Particle Size Distribution

Report Reissued By: Max Burford on 24/4/2002

Report Checked By: _____   Approved Signatory: _____
Laboratory Manager

This Laboratory is accredited by International Accreditation New Zealand. The tests reported herein (unless otherwise indicated by an *) have been performed in accordance with the laboratory's certificate to the schedule of accreditation. This report may not be reproduced except in full. The results given in this report apply only to the sample as received by the laboratory.
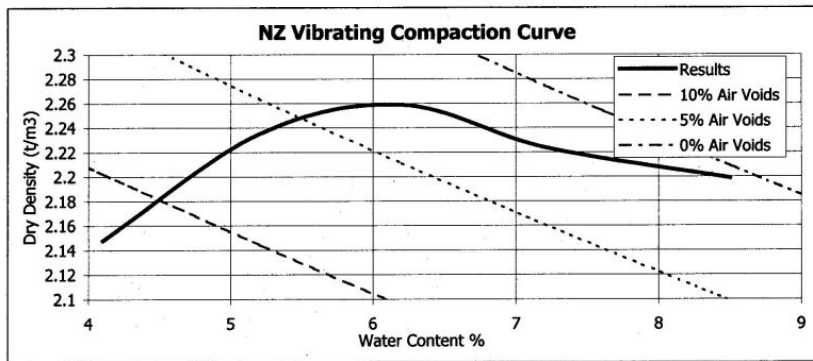
A member of the Fulton Hogan Ltd. Group Report Template: Basecourse(Wet).doc Template Issued: 2nd August 2001

Fulton Hogan Canterbury Laboratory

PO Box 16-064, Hornby, Christchurch. 325 Pound Rd, Yaldhurst, Christchurch.
Telephone: 03 349 9142 - Fax: 03 349 9143 - Manager's Mobile: 025 377 318

Laboratory Reference: 2002/0324/1 Page 1 of 1
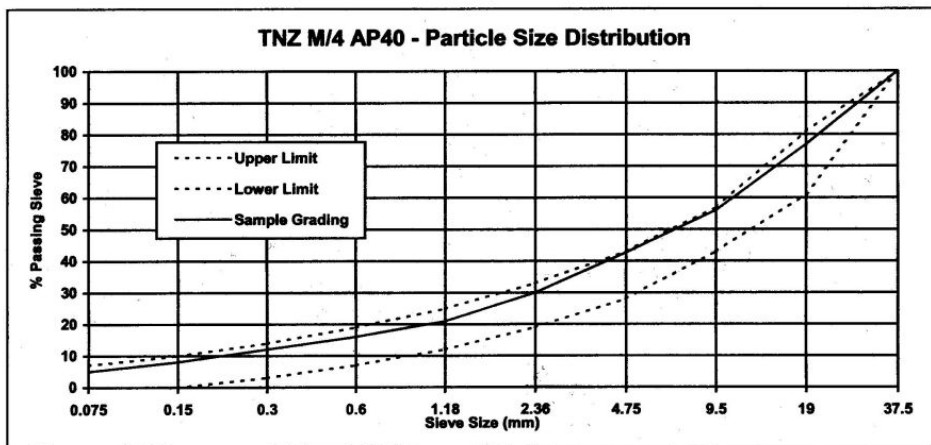
NZ VIBRATING HAMMER COMPACTION TEST

ATTENTION: **Allan Fussell**

CLIENT: TRANSIT New Zealand
MATERIAL: TNZ M/4 AP40 Basecourse
CONDITION AS RECEIVED: Natural, sealed plastic bag
SAMPLE SOURCE; Ex Pound Road, Stockpile @ Captif
SAMPLED BY: J Hansby on 19/2/2002
SAMPLING METHOD USED: NZS 4407:1991 Part 2.4.6.2.1
TEST METHOD USED: NZS 4402:1986 Test 4.1.3 – performed on whole material in natural state
TESTED BY: Max Burford on 26/2/2002

Moisture Content (%)	Dry Density (t/m³)
4.6	2.23
5.1	2.19
5.9	2.25
6.2	2.24
7.8	2.18

Optimum Water Content = 6.0 %
Maximum Dry Density = 2.25 t/m³
Solid Density of Coarse Particles = 2.65 t/m³ (Assumed)

NZ Vibrating Compaction Curve

Report Issued By: Max Burford on 26/2/2002

Report Checked By: _____ Approved Signatory: _____

Fulton Hogan Canterbury Laboratory

PO Box 16-064, Hornby, Christchurch. 325 Pound Rd, Yaldhurst, Christchurch.
Telephone: 03 349 9142 - Fax: 03 349 9143 - Manager's Mobile: 025 377 318

Page 1 of 1

Laboratory Reference: 2002/0322/2

ROADING AGGREGATE SIEVE ANALYSIS TEST REPORT

ATTENTION: **Allan Fussell**

CLIENT:	TRANSIT New Zealand
PRODUCT:	TNZ M/4 Table 5 Christchurch Uncrushed River Gravel
CONDITION AS RECEIVED:	Natural, sealed plastic bag
SAMPLED FROM:	Ex Coutts Island, Stockpile @ Captif
SAMPLING METHOD USED:	NZS 4407:1991 Part 2.4.6.2.1
TEST METHODS USED:	NZS 4407:1991 Test 3.1 & 3.8.1
SAMPLED BY:	J Hansby on 19/2/2002
TESTED BY:	Max Burford on 26/2/2002

Sieve Size (mm)	Passing Sieve (%)	TNZ M/4 Table 5 Christchurch Uncrushed River Gravel
37.5	100	-
19.0	80	60 – 80
9.5	48	40 - 60
4.75	31	25 – 45
2.36	23	18 – 36
1.18	20	11 – 28
0.60	18	6 – 22
0.30	13	2 – 17
0.15	6	0 – 12
0.075	4	0 - 7

% passing finest sieve obtained by difference

Report Issued By: Max Burford on 26/02/2002

Report Checked By: _____   Approved Signatory: _____

Christchurch Uncrushed River Gravel - Particle Size Distribution

- - - - - Upper Limit   - - - - - Lower Limit   ——— Sample Grading

Report Template: Grading 381.doc Template Issued: 27/10/1999

A member of the Fulton Hogan Ltd. Group

Fulton Hogan Canterbury Laboratory

PO Box 16-064, Hornby, Christchurch. 325 Pound Rd, Yaldhurst, Christchurch.
Telephone: 03 349 9142 - Fax: 03 349 9143 - Manager's Mobile: 025 377 318

Page 1 of 1

Laboratory Reference: 2002/0322/1

NZ VIBRATING HAMMER COMPACTION TEST

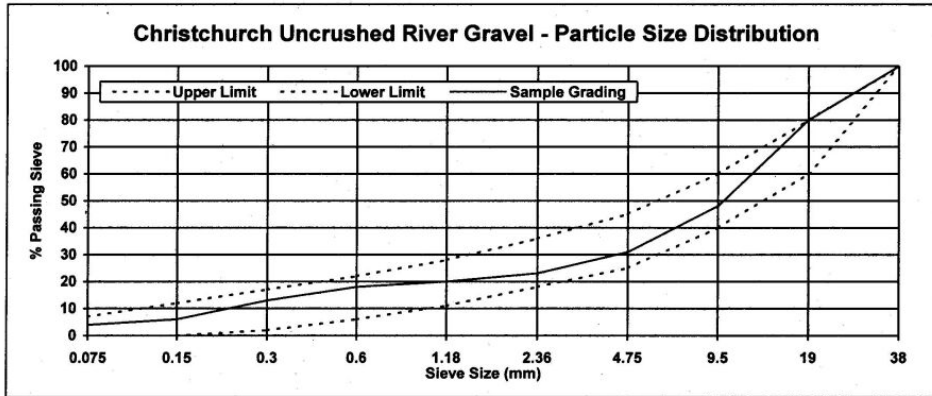**ATTENTION:**   **Allan Fussell**

CLIENT:	TRANSIT New Zealand
MATERIAL:	TNZ M/4 Table 5 Christchurch Uncrushed River Gravel
CONDITION AS RECEIVED:	Natural, sealed plastic bag
SAMPLE SOURCE:	Ex Coutts Island, Stockpile @ Captif
SAMPLED BY:	J Hansby on 19/2/2002
SAMPLING METHOD USED:	NZS 4407:1991 Part 2.4.6.2.1
TEST METHOD USED:	NZS 4402:1986 Test 4.1.3 – performed on whole material in natural state
TESTED BY:	Erin McDonald on 26/2/2002

Moisture Content (%)	Dry Density (t/m³)
2.6	2.30
3.4	2.31
4.0	2.38
4.5	2.38
5.6	2.23

Optimum Water Content   = 4.2 %
Maximum Dry Density   = 2.38 t/m³
Solid Density of Coarse Particles   = 2.67 t/m³ (Assumed)

NZ Vibrating Compaction Curve

Report Issued By: Max Burford on 26/2/2002

Report Checked By: _[signature]_   Approved Signatory: _[signature]_

A member of the Fulton Hogan Ltd. Group   Report Template: Vibrating Compaction.doc Template Issued: 27th May 1999

Fulton Hogan Canterbury Laboratory

PO Box 16-064, Hornby, Christchurch. 325 Pound Rd, Yaldhurst, Christchurch.
Telephone: 03 349 9142 - Fax: 03 349 9143 - Manager's Mobile: 025 377 318

Laboratory Reference: 2002/1043/1   Page 1 of 1

DETERMINATION OF THE CONE PENETRATION LIMIT, PLASTIC LIMIT, PLASTICITY INDEX OF A SOIL & THE SAND EQUIVALENT

ATTENTION: **Alan Fussell**

CLIENT:	TRANSIT New Zealand
CLIENT REFERENCE:	Transfund Project PR3-0604
MATERIAL:	TNZ AP40 M/5, TNZ AP40 M/4 & Australian AP20 (Montrose Rock)
CONDITION AS RECEIVED:	Natural in 3 sealed plastic bags
SAMPLED FROM:	Captif Test Track Stockpiles, Harewood
SAMPLING METHOD USED:	NZS 4407:1991 Part 2.4.6.2.1
TEST METHODS USED:	NZS 4407:1991 Test 3.1, 3.2, 3.3 & 3.4
	NZS 4407:1991 Test 3.6 (Mechanical shaking used)
SAMPLED BY:	Martin Clay on 6/05/2002
RECEIVED ON:	6/05/2002
TESTED BY:	Max Burford on 13/05/2002

RESULTS:

Material:		TNZ AP40 M/5	TNZ AP40 M/4	Australian AP20
Cone Penetration Limit:	CPL	19	20	22
Plastic Limit:	PL	NP	NP	18
Plasticity Index:	PI	NP	NP	4
Sand Equivalent:	SE	53	31	31

Report Issued By: Max Burford on 14/05/2002

Report Checked By: _____

Approved Signatory: _____
           Laboratory Manager

Report Template: PI & Shrinkage.doc Template Issued: 27/10/1999

A member of the Fulton Hogan Ltd. Group

Fulton Hogan Canterbury Laboratory

PO Box 16-064, Hornby, Christchurch. 325 Pound Rd, Yaldhurst, Christchurch.
Telephone: 03 349 9142 - Fax: 03 349 9143 - Manager's Mobile: 025 377 318

Laboratory Reference: 2002/0545/1

Page 1 of 1

ASPHALTIC CONCRETE TEST REPORT

ATTENTION: **Allan Fussell**

CLIENT:	TRANSIT New Zealand
CLIENT REFERENCE:	11/03/02
PRODUCT:	AC 10 - TNZ
CONDITION AS RECEIVED:	As Manufactured, in a brown paper bag. Temperature not recorded
SAMPLED FROM:	Transit CAPTIF faciility, McLeans Island Rd
SAMPLING METHOD USED:	ASTM D 979 - 96 Section 5.2.2
TEST METHODS USED:	NSZ 4407: 1991 Test 3.8.1, ADL 4.02/15a-90, ASTM D 2041 – 00, ASTM D3203-94, ASTM D2726-00, ASTM D1559-89, Igniter FHCL T4 1999 (Not IANZ Accredited)
COMPACTION TEMP:	138 - 145°C @ 75 blows
SAMPLED BY:	Martin Clay on 14/3/02
RECEIVED ON:	14/3/02
TESTED BY:	Martin Clay on 15/3/02

Sieve Size (mm)	% Passing Sieve	TNZ M/10 Mix 10, Jun 1975
9.5	100	100
6.7	92	-
4.75	86	70-85
2.36	60	55-75
1.18	43	40-60
0.6	33	27-47
0.3	24	18-33
0.15	14	12-22
0.075	8	6-12

% passing finest sieve obtained by difference
sample extracted via igniter

Asphalt Properties		Results	TNZ M/10 Mix 10, Jun 1975	Reporting Information
Binder Content	(%)	6.2	6.5-8	1.4 kg used
Bulk SG		2.334		Tested at 25°C, 3 blocks used @ 1.2 kg
Bulk Density	(kg/m³)	2327		
Air Voids	(%)	3.5	-	
Max Theoretical SG		2.420		Flask Type C, weighed in air / Tested at 25°C, 1 samples tested @ 2.4 kg
Stability	(kN)	17.2	>= 7	Tested at 60°C
Flow	(mm)	3.4		
Water Absorption	(%)	0.2		3 blocks tested at 25°C

Particle Size Distribution

Report Issued By: Martin Clay on 15/3/02

Report Checked By: _____   Approved Signatory: _____
Laboratory Manager

Report Template: AC-All381.doc Template Issued: 2nd August 2001

REPEATED LOAD TRIAXIAL
Resilient Modulus Test

OPUS
INTERNATIONAL
CONSULTANTS

Project:	PR3-0610 Basecourse Materials	Report No.	522900/640
Client:	Transit NZ, CAPTIF	Sample No.	2-02/198
Client ref:	O/n 1241	Project No:	522900.95

Sampled by:	Fulton Hogan Canterbury Laboratory	Date sampled:	19.2.02
Source:	CAPTIF stockpile, ex. Australia	Sampling method:	
Description:	Montrose AP20	NZS 4407: 1991 Part 2.4.6.2.1	

Sample prep:	w/c=3.9%	Sample diameter:	150mm
Compaction:	Vibrating hammer, 6 layers	Sample height:	295mm
Comp. w/c:	3.9%	Date tested:	4-5.11.02
Comp. ρd:	2.17 t/m^3	Curing time:	n/a
Test cond:	w/c=3.9%, unconsolidated, undrained	Confining pressure:	various
Notes:		Deviator stress:	various

Resilient Modulus v Mean Principal Stress

Test method: Load pulse to AS1289.6.8.1: 1995, test stress sequence to client specifications

Page 1 of 2

REPEATED LOAD TRIAXIAL
Resilient Modulus Test

OPUS
INTERNATIONAL CONSULTANTS

Project:	PR3-0610 Basecourse Materials	**Report No.**	522900/640
Client:	**Transit NZ, CAPTIF**	**Sample No.**	2-02/198
Client ref:	O/n 1241	**Project No:**	522900.95

Sampled by:	Fulton Hogan Canterbury Laboratory	Date sampled:	19.2.02
Source:	CAPTIF stockpile, ex. Australia	Sampling method:	
Description:	**Montrose AP20**	NZS 4407: 1991 Part 2.4.6.2.1	

Sample prep:	w/c=3.9%	Sample diameter:	150mm
Compaction:	Vibrating hammer, 6 layers	Sample height:	295mm
Comp. w/c:	3.9%	Date tested:	4-5.11.02
Comp. ρd:	2.17 t/m^3	Curing time:	n/a
Test cond:	w/c=3.9%, unconsolidated, undrained	Confining pressure:	various
Notes:		Deviator stress:	various

stage #	σ_1 (kPa)	σ_3 (kPa)	$(\sigma_1-\sigma_3)$ (kPa)	$(\sigma_1+\sigma_3)/2$ (kPa)	Resilient Modulus (MPa)
1	84	14	70	49	107
2	168	28	140	98	148
3	252	42	210	147	199
4	323	54	269	189	257
5	480	80	400	280	380
6	638	106	531	372	486
7	503	151	352	327	522
8	705	212	494	459	711
9	578	231	347	405	655
10	750	300	450	525	858
11	750	503	248	627	990
12	338	34	304	186	227
13	525	53	473	289	315
14	208	21	187	115	177
15	138	14	124	76	138
16	70	7	63	39	98
17	138	14	124	76	-
18	206	21	186	114	179
19	338	34	304	186	237

Test method: Load pulse to AS1289.6.8.1: 1995, test stress sequence to client specifications

Page 2 of 2

REPEATED LOAD TRIAXIAL
Resilient Modulus Test

OPUS
INTERNATIONAL CONSULTANTS

Project:	PR3-0610 Basecourse Materials	Report No.	522900/640
Client:	Transit NZ, CAPTIF	Sample No.	2-02/199
Client ref:	O/n 1241	Project No:	522900.95

Sampled by:	Fulton Hogan Canterbury Laboratory	Date sampled:	19.2.02
Source:	EX. Pound Road, CAPTIF Stockpile	Sampling method:	
Description:	**TNZ M/4 AP40 Basecourse**	NZS 4407: 1991 Part 2.4.6.2.1	

Sample prep:	w/c=2.7%	Sample diameter:	150mm
Compaction:	Vibrating hammer, 6 layers	Sample height:	295mm
Comp. w/c:	2.7%	Date tested:	13-14.11.02
Comp. ρd:	2.16t/m^3	Curing time:	n/a
Test cond:	w/c=2.7%, unconsolidated, undrained	Confining pressure:	various
Notes:		Deviator stress:	various

Resilient Modulus v Mean Principal Stress

Resilient Modulus (MPa) vs Mean Principal Stress P ($\sigma_1 + \sigma_3$)/2 (kPa)

▲ 2-02/199 TNZ M/4 AP40

Test method: Load pulse to AS1289.6.8.1: 1995, test stress sequence to client specifications

Page 1 of 2

Opus International Consultants Limited
Central Laboratories
Quality Management Systems Certified to ISO 9001

138 Hutt Park Road
PO Box 30 845, Lower Hutt
New Zealand

Telephone +64 4 587 0600
Facsimile +64 4 587 0604
Website www.opus.co.nz
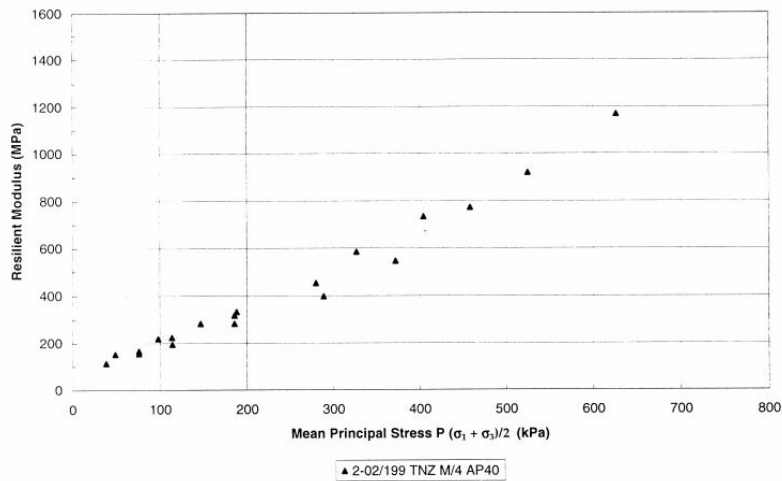
REPEATED LOAD TRIAXIAL
Resilient Modulus Test

OPUS
INTERNATIONAL
CONSULTANTS

Project:	PR3-0610 Basecourse Materials	Report No.	522900/640
Client:	Transit NZ, CAPTIF	Sample No.	2-02/199
Client ref:	O/n 1241	Project No:	522900.95

Sampled by:	Fulton Hogan Canterbury Laboratory	Date sampled:	19.2.02
Source:	EX. Pound Road, CAPTIF Stockpile	Sampling method:	
Description:	**TNZ M/4 AP40 Basecourse**	NZS 4407: 1991 Part 2.4.6.2.1	

Sample prep:	w/c=2.7%	Sample diameter:	150mm
Compaction:	Vibrating hammer, 6 layers	Sample height:	295mm
Comp. w/c:	2.7%	Date tested:	13-14.11.02
Comp. ρd:	2.16t/m^3	Curing time:	n/a
Test cond:	w/c=2.7%, unconsolidated, undrained	Confining pressure:	various
Notes:		Deviator stress:	various

stage #	σ_1 (kPa)	σ_3 (kPa)	$(\sigma_1-\sigma_3)$ (kPa)	$(\sigma_1+\sigma_3)/2$ (kPa)	Resilient Modulus (MPa)
1	84	14	70	49	152
2	168	28	140	98	218
3	252	42	210	147	282
4	323	54	269	189	332
5	480	80	400	280	452
6	638	106	531	372	545
7	503	151	352	327	583
8	705	212	494	459	772
9	578	231	347	405	734
10	750	300	450	525	919
11	750	503	248	627	1168
12	338	34	304	186	282
13	525	53	473	289	397
14	208	21	187	115	194
15	138	14	124	76	155
16	70	7	63	39	113
17	138	14	124	76	166
18	206	21	186	114	224
19	338	34	304	186	317

Test method: Load pulse to AS1289.6.8.1: 1995, test stress sequence to client specifications

Page 2 of 2

REPEATED LOAD TRIAXIAL
Resilient Modulus Test

OPUS
INTERNATIONAL CONSULTANTS

Project:	PR3-0610 Basecourse Materials	Report No.	522900/640
Client:	Transit NZ, CAPTIF	Sample No.	2-02/200
Client ref:	O/n 1241	Project No:	522900.95

Sampled by:	Fulton Hogan Canterbury Laboratory	Date sampled:	19.2.02
Source:	Ex. Coutts Island, stockpile @ CAPTIF	Sampling method:	
Description:	**TNZ M/4 Table 5 CHCH Uncrushed River Gravel**	NZS 4407: 1991 Part 2.4.6.2.1	

Sample prep:	w/c=2.6%	Sample diameter:	150mm
Compaction:	Vibrating hammer, 6 layers	Sample height:	295mm
Comp. w/c:	2.6%	Date tested:	19-20.11.02
Comp. ρd:	2.22 t/m³	Curing time:	n/a
Test cond:	w/c=2.6%, unconsolidated, undrained	Confining pressure:	various
Notes:		Deviator stress:	various

Resilient Modulus v Mean Principal Stress

Test method: Load pulse to AS1289.6.8.1: 1995, test stress sequence to client specifications

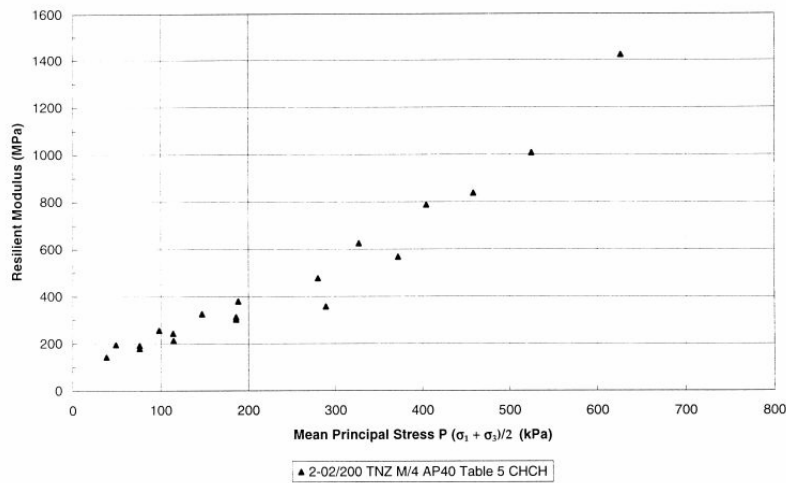Page 1 of 2

REPEATED LOAD TRIAXIAL
Resilient Modulus Test

OPUS
INTERNATIONAL
CONSULTANTS

Project:	PR3-0610 Basecourse Materials	Report No.	522900/640
Client:	Transit NZ, CAPTIF	Sample No.	2-02/200
Client ref:	O/n 1241	Project No:	522900.95

Sampled by:	Fulton Hogan Canterbury Laboratory	Date sampled:	19.2.02
Source:	Ex. Coutts Island, stockpile @ CAPTIF	Sampling method:	
Description:	**TNZ M/4 Table 5 CHCH Uncrushed River Gravel**	NZS 4407: 1991 Part 2.4.6.2.1	

Sample prep:	w/c=2.6%	Sample diameter:	150mm
Compaction:	Vibrating hammer, 6 layers	Sample height:	295mm
Comp. w/c:	2.6%	Date tested:	19-20.11.02
Comp. ρd:	2.22 t/m^3	Curing time:	n/a
Test cond:	w/c=2.6%, unconsolidated, undrained	Confining pressure:	various
Notes:		Deviator stress:	various

stage #	σ_1 (kPa)	σ_3 (kPa)	$(\sigma_1-\sigma_3)$ (kPa)	$(\sigma_1+\sigma_3)/2$ (kPa)	Resilient Modulus (MPa)
1	84	14	70	49	195
2	168	28	140	98	256
3	252	42	210	147	325
4	323	54	269	189	379
5	480	80	400	280	476
6	638	106	531	372	567
7	503	151	352	327	624
8	705	212	494	459	836
9	578	231	347	405	787
10	750	300	450	525	1008
11	750	503	248	627	1422
12	338	34	304	186	302
13	525	53	473	289	357
14	208	21	187	115	213
15	138	14	124	76	179
16	70	7	63	39	142
17	138	14	124	76	192
18	206	21	186	114	243
19	338	34	304	186	312

Test method: Load pulse to AS1289.6.8.1: 1995, test stress sequence to client specifications

Page 2 of 2

Appendix B: Photos of the construction

Sorry photos 1 – 11 (pp. 101 – 106 of report) unavailable in electronic copy

Appendix C: Example of Network Deterioration Modelling

Appendix C: Example of Network Deterioration Modelling

Two approaches to modelling deterioration on a simple network have been investigated. The first is the traditional power law relationships developed in Chapter 9 of the report and the second is using the VSD relationships developed in Chapter 10 of the report. The network is based on Section C data and the assumptions made for the network are given in Table C1.

Table C1   Assumptions used in imaginary road network for existing condition.

Item	Assumptions
No. of road sections	40
Pavement types	All 40 pavement sections are the same type as Segment C tested in this Stage 3 research.
Age	Each section with a different age ranging from 1 to 40 years.
Existing Traffic	100,000 passes of a 40 kN axle per year (*i.e. no 60 kN axles*).
Rehabilitation	1 section per year or pavement life = 40 years.
VSD when rehabilitation required	VSD value when rehabilitation required is the value determined for 4,000,000 passes of a 40 kN axle from either the best fit function to measured date or the VSD function being tested for Segment C.
Existing VSD	As predicted for each road section of ages 0 to 40 years with the VSD equation for 40 kN that is being tested.
New Traffic	*100,000 passes of a 60 kN axle per year (i.e. no 40 kN axles).*

Traditional power law relationships

Using a traditional power law relationship (Equation 9.1, Chapter 9 of report) simplifies the analysis as the calculation involves determining the number of Equivalent Standard Axles (ESAs, i.e. no. of 40 kN axles). The existing life of the pavement in the imaginary network (Table C1) is 40 years. This equates to 100,000 x 40 passes of a 40 kN axle to consume the life of the pavement. In other words 4,000,000 ESAs are required before pavement rehabilitation is required.

For Segment C (Stage 3) a best-fit exponent of 2.5 (Figure 9.6) was determined for a traditional power law. For a compaction–wear type model the exponents calculated were 1.41 for the compaction/intercept component and 1.52 for the slope component (Table 10.3). The average exponent value for the compaction–wear model is 1.47. A traditional exponent value for Segment C (Stage 3) can also be determined from Figure 9.2 for a known VSD at the pavement's end-of-life. The VSD at end-of-life needs to be determined by extrapolating the measured VSD data for the 40 kN axle load on Segment C (Stage 3) to 4,000,000 passes. A power equation used to smooth the results for Segment C (Stage 3, Figure 9.1) was used for this extrapolation. This resulted in a VSD of 12.1 mm at end of the pavement life (i.e. after 4,000,000 ESAs). Therefore, from Figure 9.2 the exponent value for Segment C (Stage 3) at a VSD of 12.1 mm is 3.2. In summary, the exponent values to investigate for use in the general power law relationship are: 2.5 (best fit), 1.47 (compaction-wear), and 3.2 (for a known VSD).

A form of the general power law relationship (Equation 9.1) is used to determine the number of ESAs (Equation C1) and this value is then used to determine the affect of 60 kN axle loads replacing the 40 kN axle loads on the imaginary network (Table C1).

$$ESA = N_{60kN} \left[\frac{60kN}{40kN} \right]^n$$

Equation C1

where:

ESA is the number of Equivalent Standard Axles (i.e. 40 kN axles)

n is the exponent for the power law

N_{60kN} is the number of passes of the 60 kN axle

Currently in the imaginary network of 40 sections with 100,000 40 kN axle passes (or ESAs) per year, 1 section out of 40 is rehabilitated per year. Based on the new value of ESAs determined from Equation C1, an estimate on the average number of rehabilitations per year can be determined for the new 60 kN axle loads. Table C2 shows the results for the 3 different exponent values determined.

Table C2   Effect on imaginary network (Table C1) when traffic changes from 40 kN axles to 100,000 passes per year of 60 kN axles.

Method	Exponent, *n*	ESAs per year (Equation C1)	*Average number sections out of 40 rehabilitated per year
Best fit	2.5	276	2.76
Compaction-wear	1.47	181	1.81
From VSD at end of life	3.2	366	3.66

* for the 100,000 passes of the 40 kN axles, only 1 out 40 sections was rehabilitated per year.

Based on the above analysis (Table C1) an RCA's budget will need to increase from 1.8 to 3.7 times to ensure the road network is maintained at the same level for the 60 kN axles. However, this is an extreme case as not all vehicles will change to the new loads of 60 kN should a change in the law occur.

VSD relationships

To estimate the effect on the imaginary road network (Table C1) should the axle loads increase to 60 kN, a VSD relationship can be used. In Chapter 10 of this report many different relationships for VSD were determined. A few have been selected to simulate the effect on VSD for each pavement section in the network caused by an increase in axle loads to 60 kN over the next 40 years. This information is then in turn used to estimate the new average number of sections rehabilitated per year and thus the number of ESAs and exponent value, *n*. The range of relationships for VSD selected are summarised in Table C3.

Table C3   Relationships used to predict VSD on imaginary network for a Segment C (Stage 3) type pavement.

VSD Model	Description
Base power model: $$VSD_{40kN} = 0.2235N_{40kN}^{0.4814}$$ $$VSD_{60kN} = 0.2893N_{60kN}^{0.5345}$$	This is in effect the best fit smoothing curve applied to the real measured data for Segment C (Stage 3) (see Figure 9.1).
Best fit compaction–wear model: $$VSD_{40kN} = 1.63 + 0.00504N_{40kN}$$ $$VSD_{60kN} = 2.89 + 0.00933N_{60kN}$$	This is the best fit linear equation to the measured data for Segment C (Stage 3) after the initial compaction period (i.e. after 100,000 load passes).
Common coefficients compaction–wear model: $$VSD = 1.09\left[\frac{P}{40}\right]^{1.59}(1.8 + 0.00384N)$$	This is the compaction–wear model using common coefficients for best fit to both Stages 3 and 1 data. The 1.09 multiplier is unique for Segment C (Stage 3) pavement.
Best fit Wolff and Visser: $$VSD = \left(\frac{P}{40}\right)^{1.46}(1.59 + 0.00515N)(1 - e^{-0.0443N})$$	The coefficients calculated for this model are those that provide the best fit to the Segment C (Stage 3) measured data.
Common coefficients Wolff and Visser: $$VSD = 1.097\left(\frac{P}{40}\right)^{1.31}(1.87 + 0.00421N)(1 - e^{-0.0691N})$$	The coefficients calculated for this model are those that provide the best fit to all the data from Stages 3 and 1. The 1.097 multiplier is unique for Segment C (Stage 3) pavement.

N_{60kN} and N_{40kN} are the number of 1/1000th axle passes with the 60 kN and 40 kN axle load respectively.

N is the number of 1/1000th axle passes for a given load P in kN.

The units of N are in per 1000 axle passes (i.e. a N value of 100 is 100,000 passes).

Method of applying VSD models

The first step in applying these models to the imaginary network is to determine the existing VSD for each of the 40 pavement sections aged from 0 to 40 years. For the relationship in question, the VSD for the pavement section is determined by the relationship for the 40 kN axle and number of passes is the pavement age multiplied by 100,000 (i.e. 100,000 40 kN axle passes per year). The current life of the pavement is 40 years or 4,000,000 passes of the 40 kN axle (i.e. 4,000,000 ESA). Therefore, the VSD at the terminal condition when rehabilitation is required is the VSD calculated for 4,000,000 passes of a 40 kN axle.

After the existing condition in terms of VSD and the VSD at the end-of-life are determined, the next step is to predict the VSD progression in subsequent years using the appropriate model for the 60 kN axle load. It is assumed in these subsequent years that the pavement section is rehabilitated as soon as the VSD at the end-of-life is exceeded. After the pavement section is rehabilitated the VSD is returned to zero.

The VSD model for the 60 kN axle load is added onto the pavement section that is partly 'rutted' with previous passes of 40 kN axle loads by subtracting a value of VSD associated with compaction and then adding the existing VSD value obtained by passes of the 40 kN axle. This VSD value associated with compaction is the VSD value obtained after 100,000 passes of the 60 kN axle minus the VSD value obtained after 100,000 passes of the 40 kN axle. Typically, this VSD compaction value was calculated to around 2 mm which is of the correct order compared with results found in the Stage 2 research where the axle load was increased on an already trafficked pavement (Figure 4.10, de Pont et al. 2001).

Another assumption related to initial compaction was applied to the base power model. When determining the progression of VSD for a 60 kN axle on an already 'rutted' pavement as well as taking off a constant, the number of 60 kN axle passes was increased by 39,000. This increase in axle passes was determined as the number of passes of the 60 kN axle needed to obtain the same VSD value obtained after 100,000 for the 40kN axle. It was felt necessary to make this additional assumption to reduce the acceleration of the onset of VSD that is predicted to occur with the base power model in the first few 1000 load cycles for a new pavement. Further, this assumption made very little difference to the final result of determining pavement rehabilitation requirements per year and a summary of the results is given in Table 11.1 (in the main report).

Results of VSD models

The onset in VSD was predicted each year on the imaginary network (Table C1) for the past 40 years and the next 40 years. In the past, traffic volumes were 100,000 passes of a 40 kN axle per year and for the future this changed to 100,000 passes of a 60 kN axle per year. Five VSD models (Table C3) were used and the results are illustrated in Figures C1 to C9. Example deterioration curves are also shown in these figures.
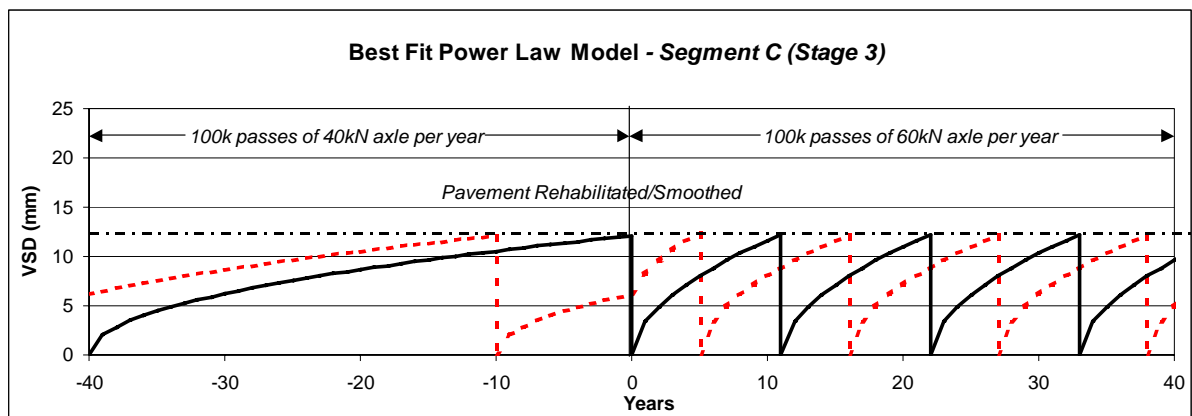

Figure C1   Deterioration of two pavements using base power model for Segment C (Stage 3) pavement type.
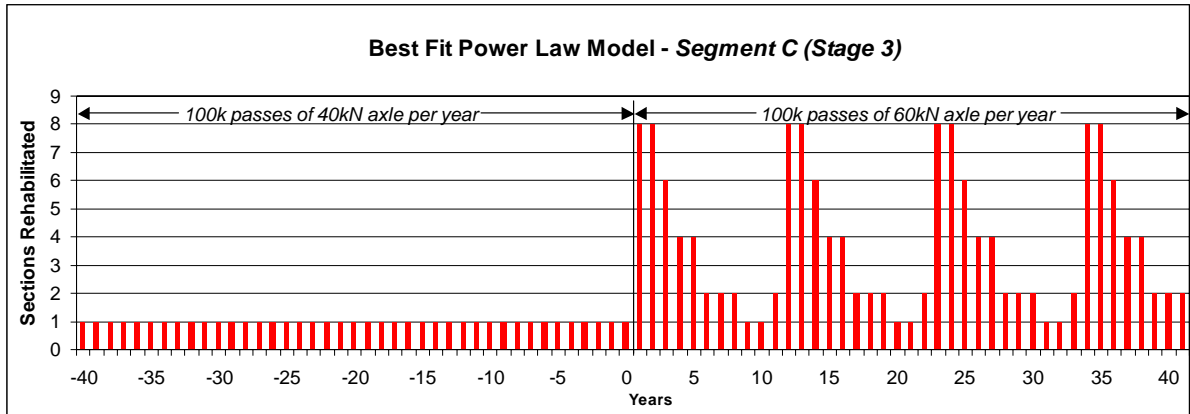
Figure C2   Number of pavement sections rehabilitated per year as predicted using the base power model for Segment C (Stage 3) pavement type.
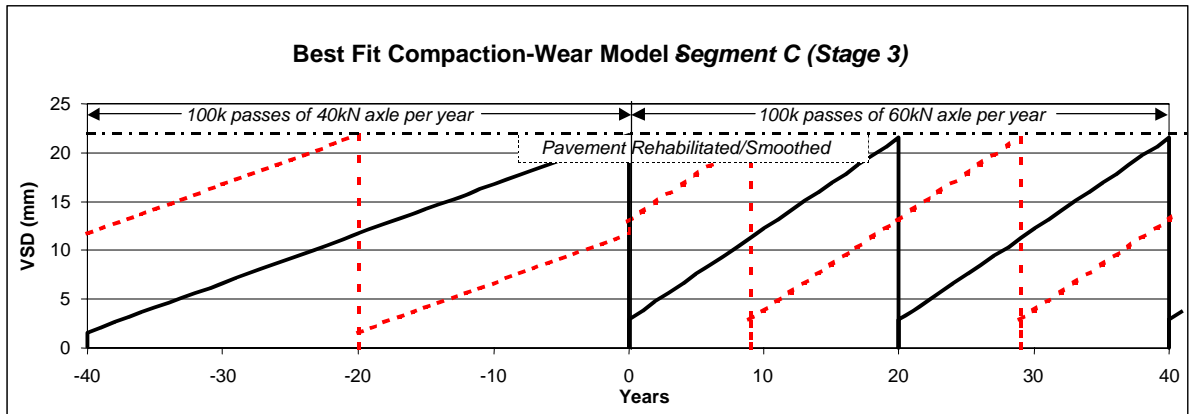

Figure C3   Deterioration of two pavements using best fit compaction-wear model for Segment C (Stage 3) pavement type.
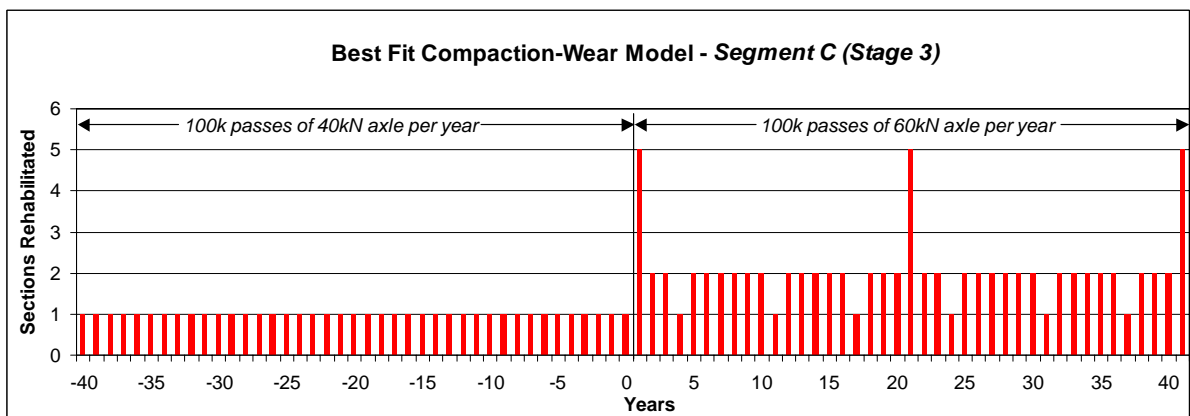

Figure C4   Number of pavement sections rehabilitated per year as predicted using the best fit compaction-wear model for Segment C (Stage 3) pavement type.

Figure C5 Deterioration of two pavements using common coefficients compaction-wear model for Segment C (Stage 3) pavement type.

Figure C6 Number of pavement sections rehabilitated per year as predicted using the common coefficients compaction-wear model for Segment C (Stage 3) pavement type.

Figure C7 Deterioration of two pavements using best fit Wolff and Visser model for Segment C (Stage 3) pavement type.

Figure C8   Number of pavement sections rehabilitated per year as predicted using the best fit Wolff and Visser model for Segment C (Stage 3) pavement type.
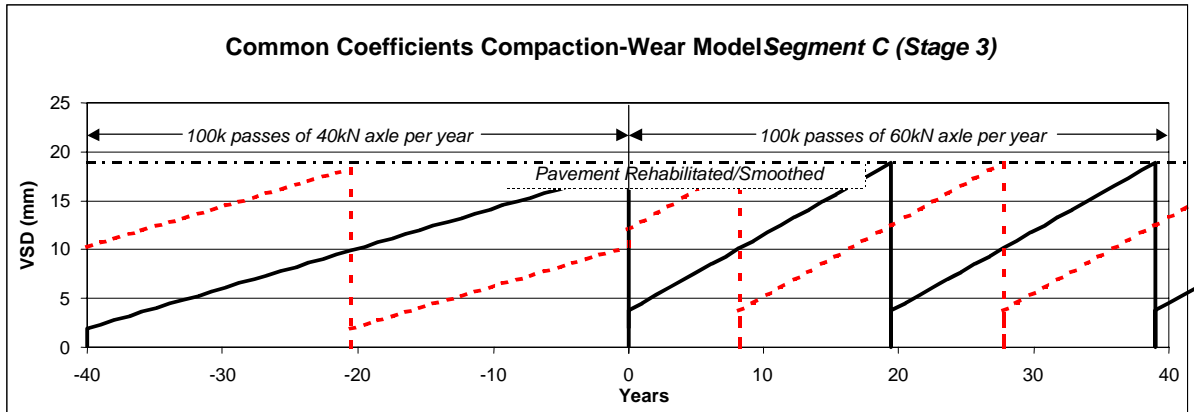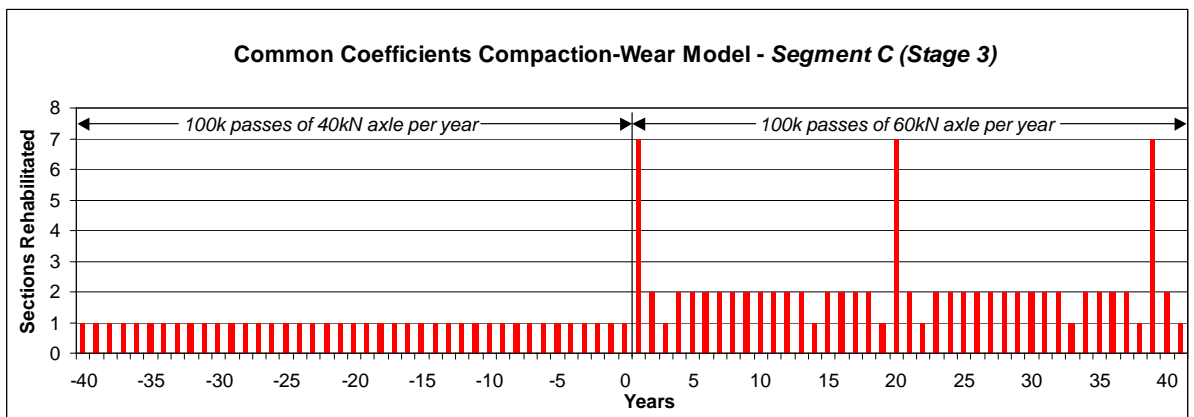

Figure C9   Deterioration of two pavements using common coefficients Wolff and Visser model for Segment C (Stage 3) pavement type.

Figure C10   Number of pavement sections rehabilitated per year as predicted using the common coefficients Wolff and Visser model for Segment C (Stage 3) pavement type.
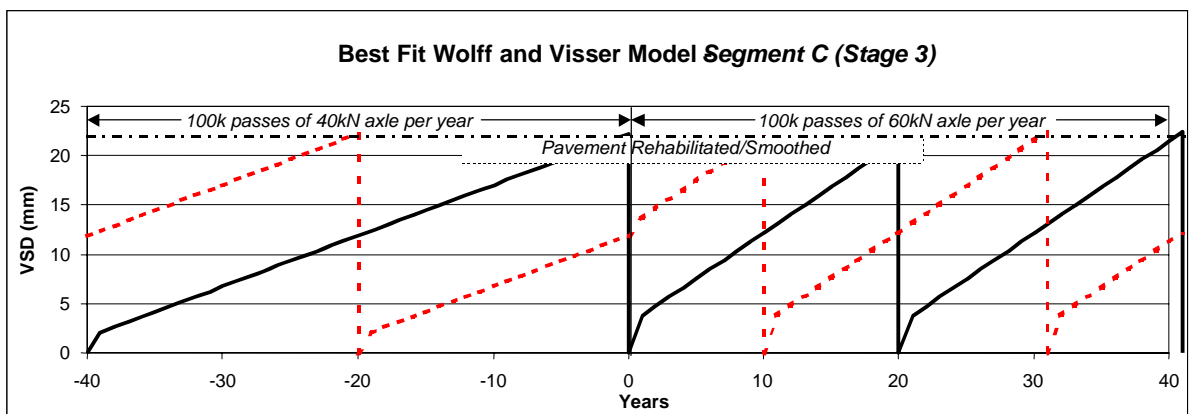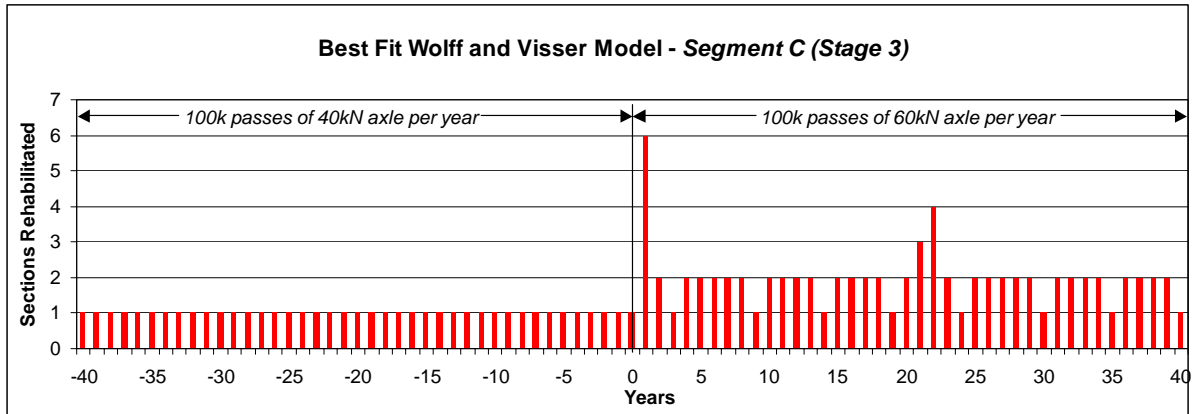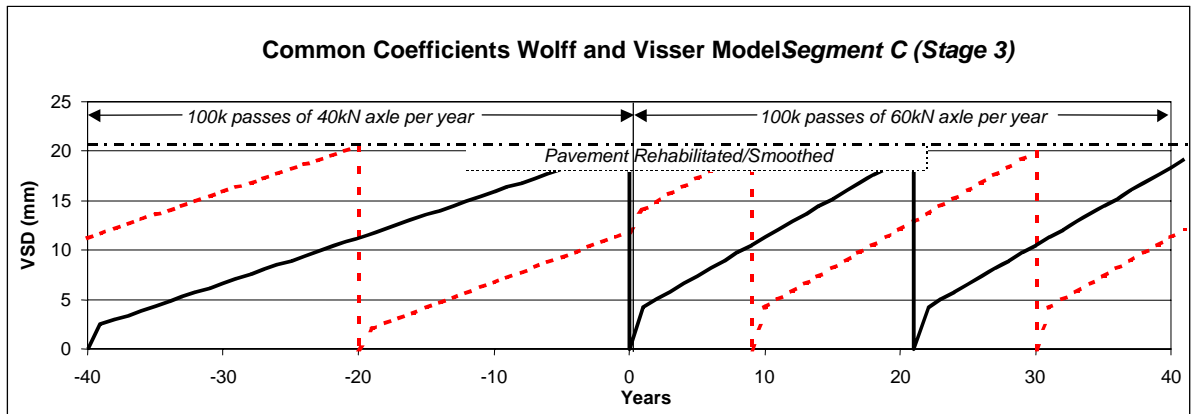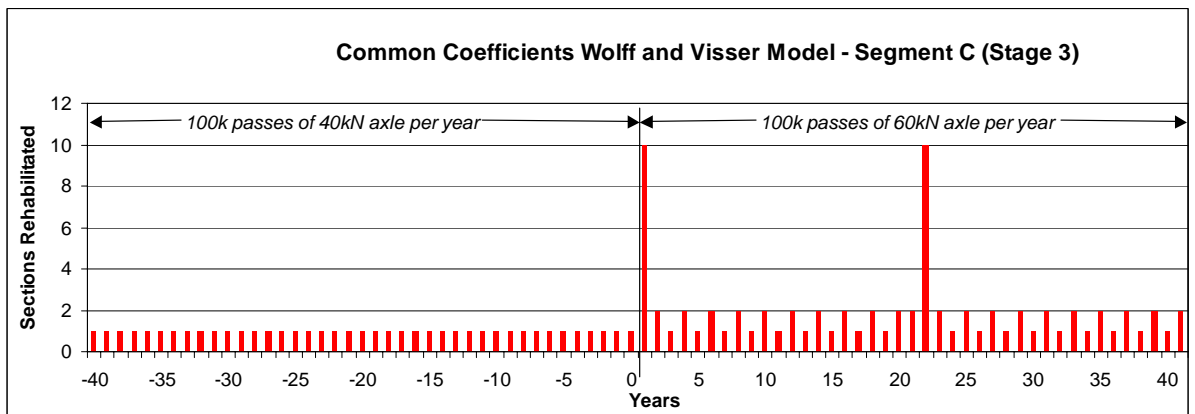
Appendix D: Equivalent axle load calculated from measured strain data for a range of tyre types and loads

Table D1 **Equivalent axle loads calculated from measured strain data for a range of tyre types and loads.**

No.		1	2	3	4	5	6	7	8	9	10	11	12	13
Tyre Type		11 R 22.5	11 R 22.5	11 R 22.5	11 R 22.5	11 R 22.5	11 R 22.5	11 R 22.5	Single	Single	Single	Single	Single	11 R 22.5
Load (kN)		**40**	**40**	**40**	**50**	**50**	**60**	**60**	**40**	**40**	**50**	**50**	**60**	**40**
Pressure (kPa)		650	750	850	750	850	750	850	750	850	750	850	850	650
		Equivalent Axle Load (kN)												
Strain location	***Average:**	41	42	43	48	53	60	64	62	64	62	74	70	37
Depth (mm)	**Layer**	Segment A (stage 1)												
112.5	*BC*	*39*	*39*	*42*	*54*	*45*	*57*	*63*	*185*	*185*	*155*	*179*	*161*	*31*
187.5	*BC*	*36*	*49*	*38*	*44*	*51*	*57*	*59*	*70*	*68*	*59*	*64*	*61*	*40*
262.5	BC	39	47	39	44	50	59	61	59	56	47	59	50	33
337.5	SG	38	40	43	50	51	60	66	75	78	58	84	68	28
412.5	SG	39	41	41	48	49	61	65	62	64	54	71	62	30
487.5	SG	39	42	41	48	49	61	65	56	57	55	65	63	35
562.5	SG	37	41	39	48	49	61	65	52	52	55	61	64	38
Depth (mm)	**Layer**	Segment B (stage 1)												
112.5	*BC*	*49*	*47*	*50*	*54*	*56*	*49*	*54*	*111*	*116*	*108*	*115*	*111*	*45*
187.5	*BC*	*25*	*40*	*25*	*55*	*78*	*55*	*78*	*168*	*175*	*153*	*190*	*175*	*33*
262.5	BC	37	43	37	46	52	61	64	64	66	72	75	78	46
337.5	SG	42	40	44	51	51	60	64	69	70	66	78	73	34
412.5	SG	40	41	41	48	52	61	64	60	61	64	73	73	39
487.5	SG	39	42	39	47	54	61	63	54	54	61	66	70	41
562.5	SG	38	42	39	47	53	61	64	50	52	58	65	67	41
Depth (mm)	**Layer**	Segment C (stage 1)												
112.5	*BC*	*46*	*49*	*44*	*44*	*55*	*57*	*59*	*201*	*205*	*201*	*196*	*205*	*51*
187.5	*BC*	*45*	*45*	*45*	*45*	*60*	*60*	*68*	*124*	*120*	*113*	*124*	*124*	*45*
262.5	BC	65	45	65	45	65	60	70	85	85	90	95	95	40
337.5	SG	49	39	50	53	54	58	62	77	81	66	93	76	30
412.5	SG	39	43	40	46	56	61	64	68	68	65	84	75	33
562.5	SG	40	46	40	45	53	60	61	34	52	60	61	67	44

*   Average excludes values in italics as measurements between the two dual tyres cannot be compared with measurements directly under the super single tyre.